Module 6

Environmental aspects

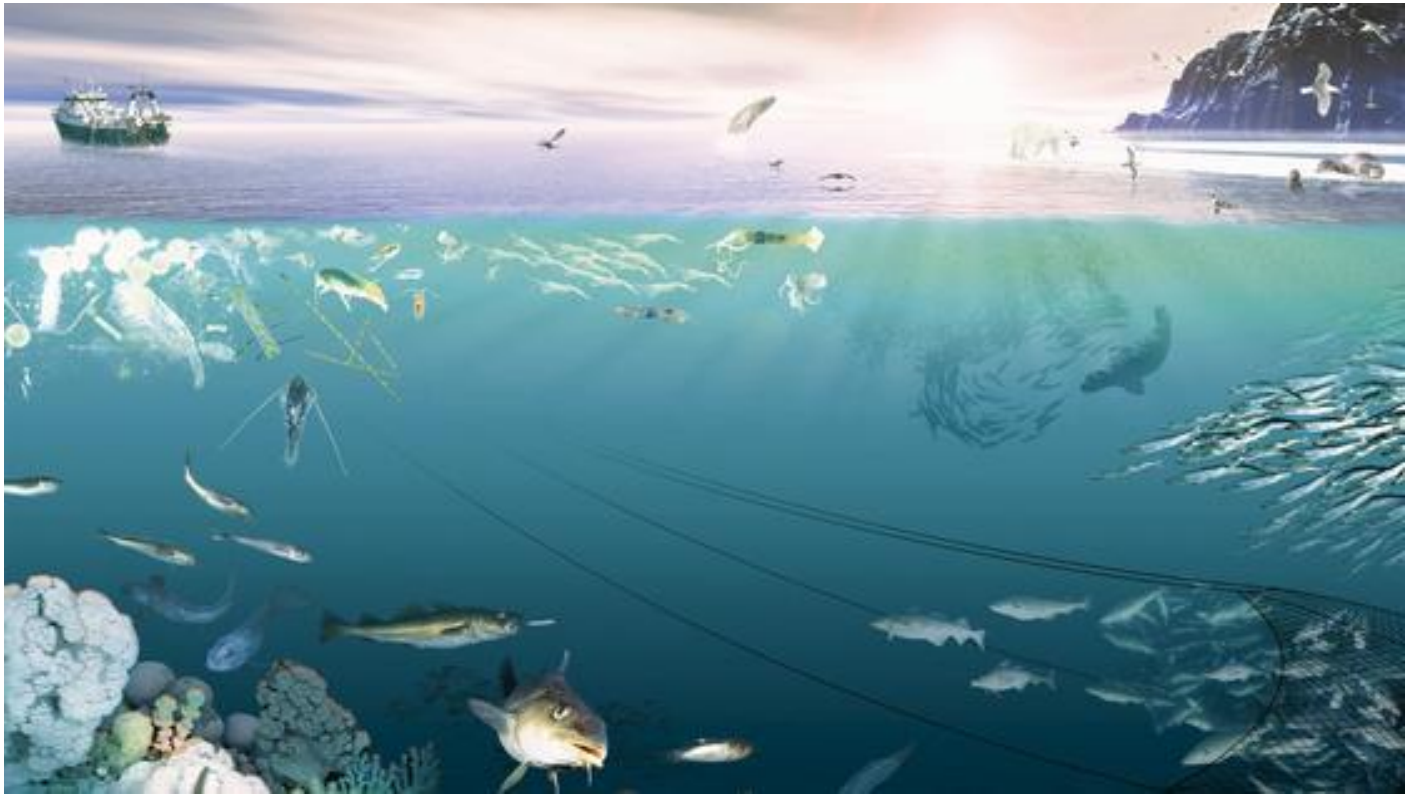

NTNU
Norwegian University of Science and Technology

Martin Landrø and Lasse Amundsen

Seismic shooting and the environment – in the news

23rd April, 2013

NRK Nyheter TV Radio Snarveier

NRK > Nyheter > Distrikt > Troms og Finnmark

Nordnytt

Siste nytt fra NRK i Nord-Norge

Mener lundefuglene kan ha dødd på grunn av seismikkskyting

Død lundefugl (Foto: Kristin Mørch)

Nicolaysen mener trykkbølgene fra seismikkskyting kan ha tatt livet av de 11 lundefuglene i Finnmark. Men førsteamanuensis

There is a need to inform our students and the public opinion about seismic and potential impact on the environment

«If the bird dives and is exposed for seismic shooting – it will not survive», says fisherman Bjørnar Nicolaysen, Andøy; NRK, 23rd April, 2013

Nature's cavity generator: the piston schrimp

The pistol or *snapping shrimp*, 2 cm in size and native to the warmer waters of the Mediterranean, competes with the blue whale in producing loud sounds. The shrimp stuns its prey by snapping its claws together to create a deafening 'crack' - allowing it to move in for the kill. The claw click creates a cavitation bubble that generates acoustic pressures of up to 218 dB at a distance of 4 cm from the claw. The pressure is strong enough to kill small fish. It is equivalent to a zero to peak source level of around 190 dB re 1 µPa @1m. Although pistol shrimps are small, they are responsible for a surprising amount of the noise in the ocean. The snapping has even been known to disrupt the navigation equipment on submarines.

Near field signature S15 water gun

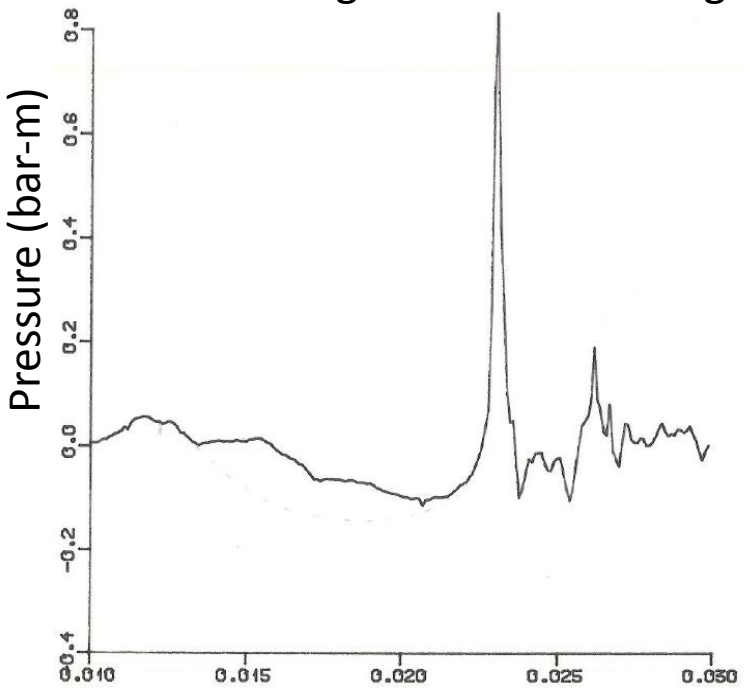

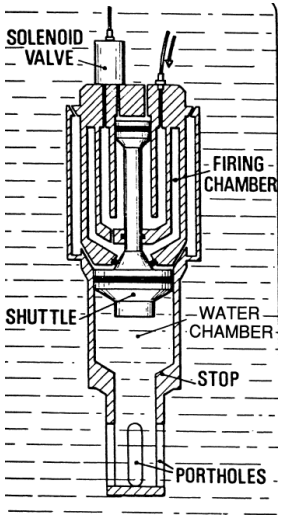

Whale stranding

The King Island, Tasmania, whale stranding in 2009.

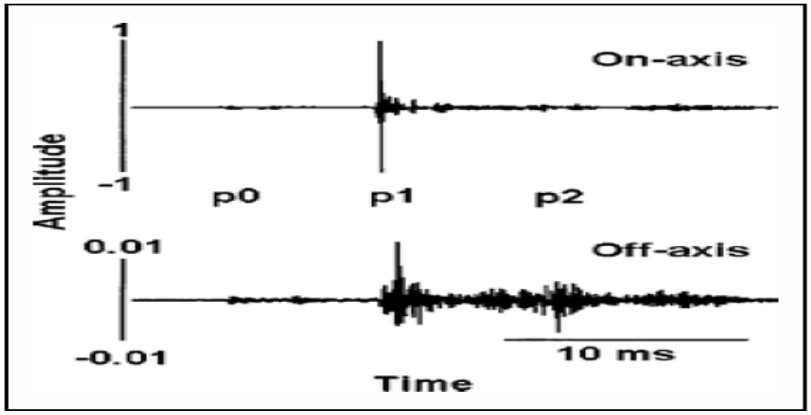

The sperm whale – the most powerful biological sound generator

Photo: Francois Gohier/Science Photo Library

Hearing curves

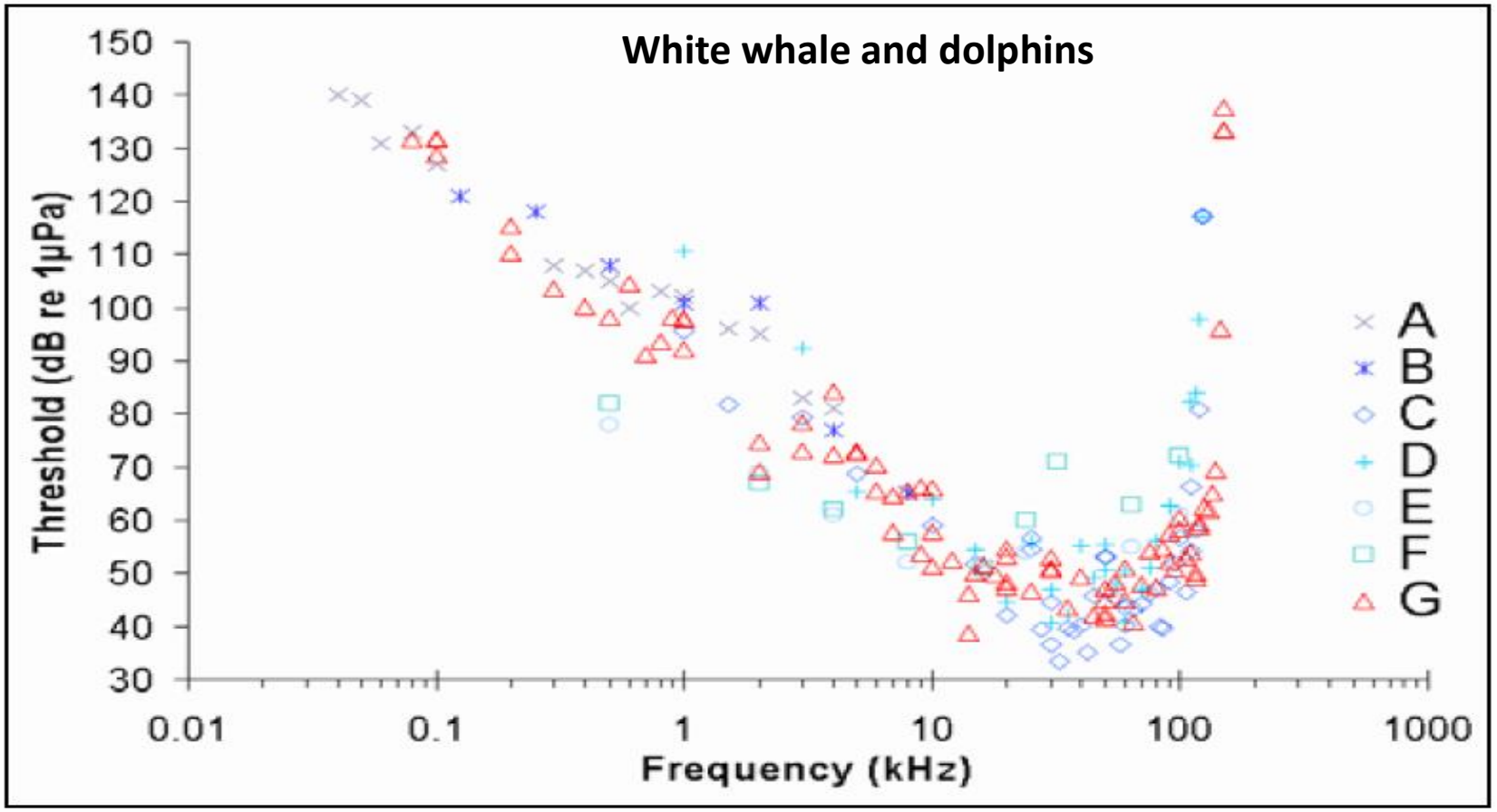

Hearing curves – baleen whales, toothed whales and seals

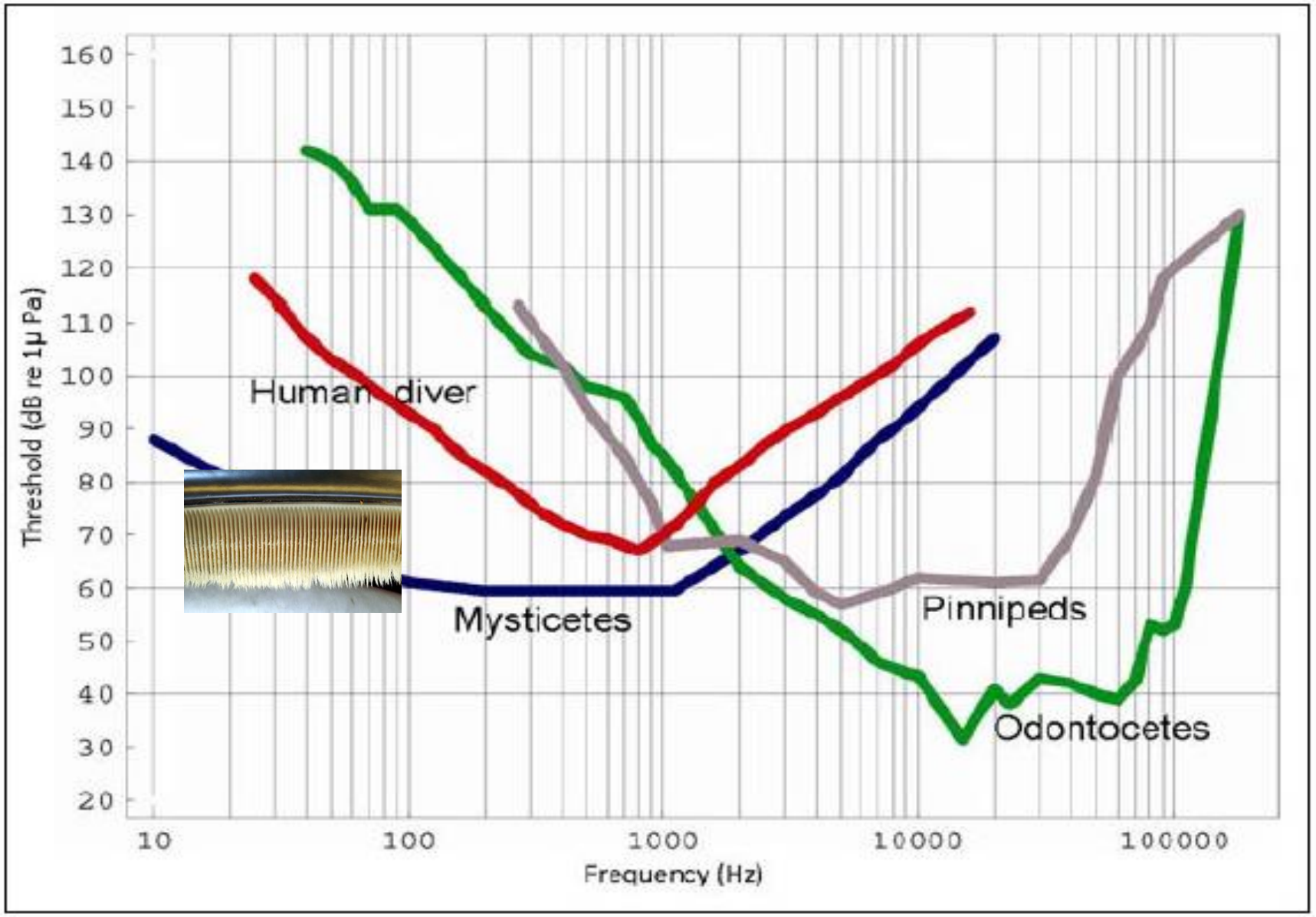

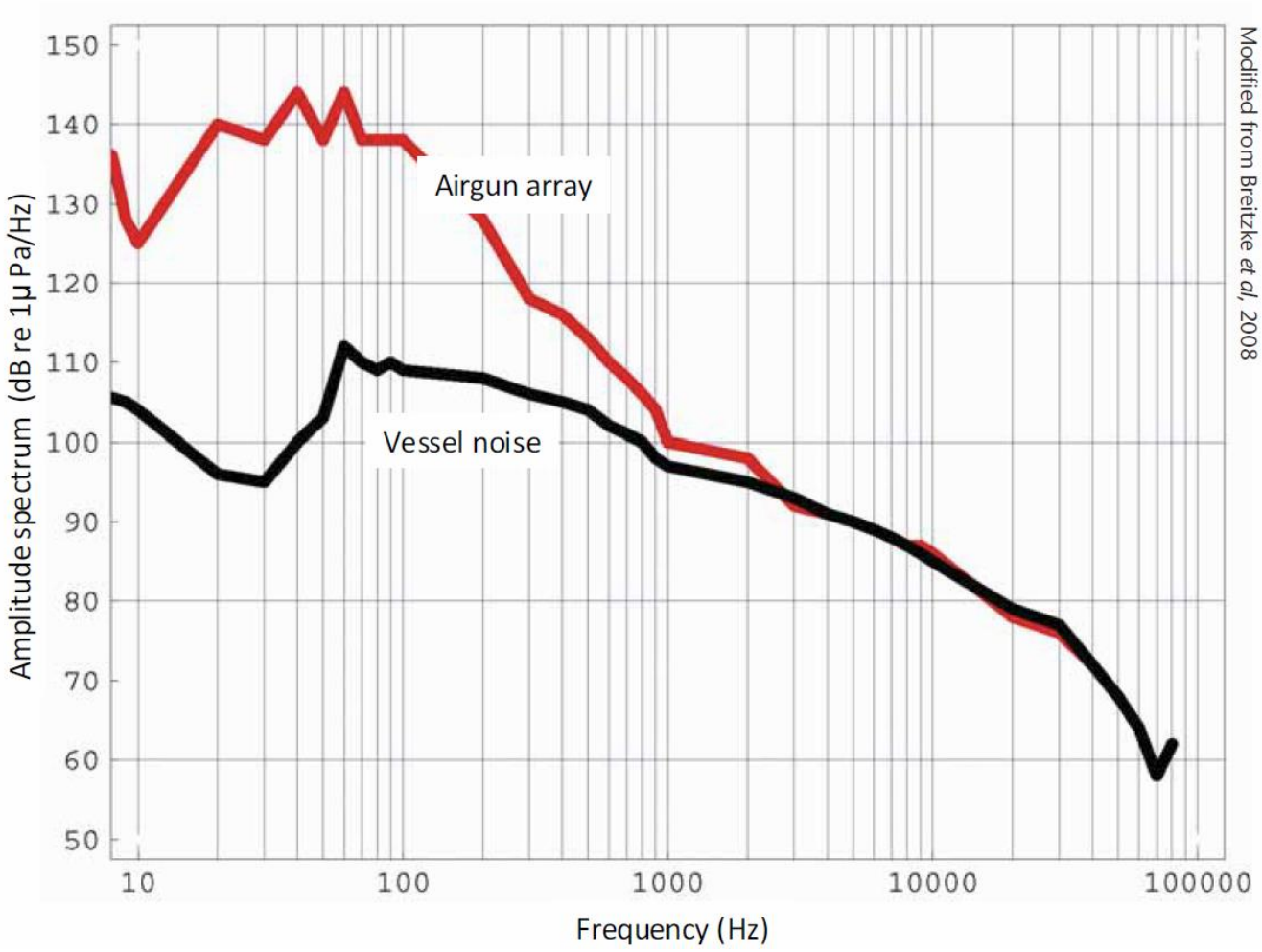

Broad-band smoothed amplitude spectra from 38.2 litre-gun array at 550m range, received by a hydrophone at 35m depth, compared to noise generated by the seismic vessel. Below 1 kHz the amplitude spectrum of the air-gun signal differs significantly from the vessel's noise spectrum due to the low-frequency energy emitted by the air-gun, while above 1 kHz the amplitude spectrum of the air-gun signal coincides with the vessel's noise almost completely. This indicates that the slow spectral level decay is mainly caused by ship-generated noise.

Sound from killer whales

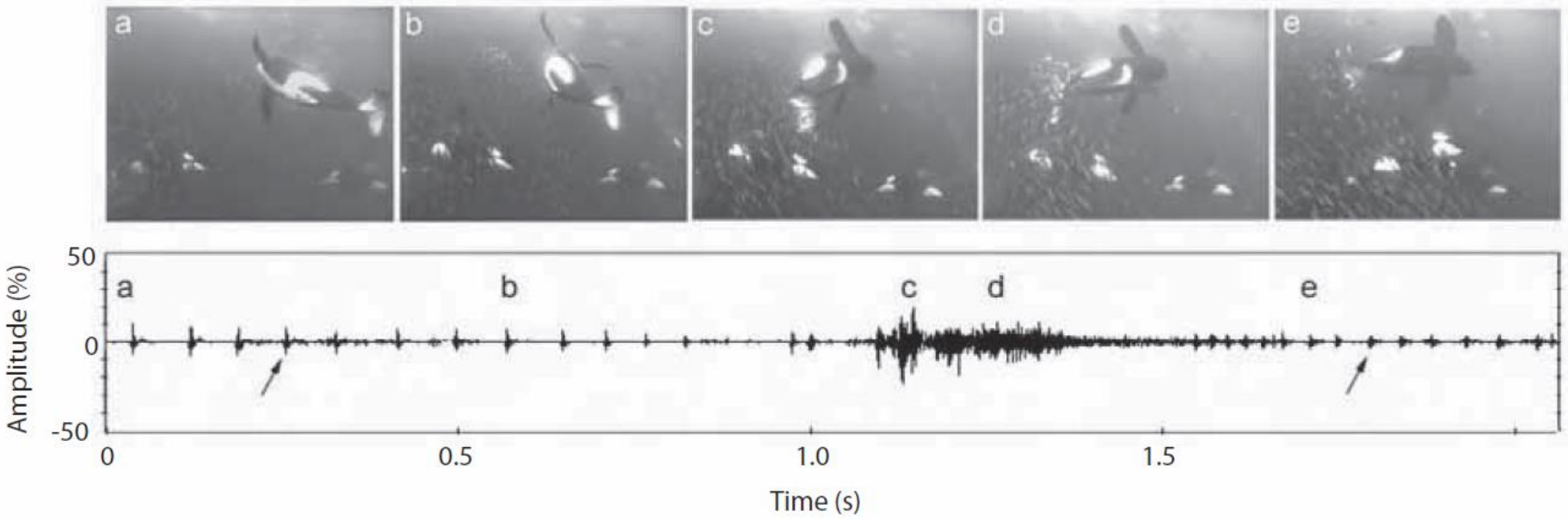

The C-start response

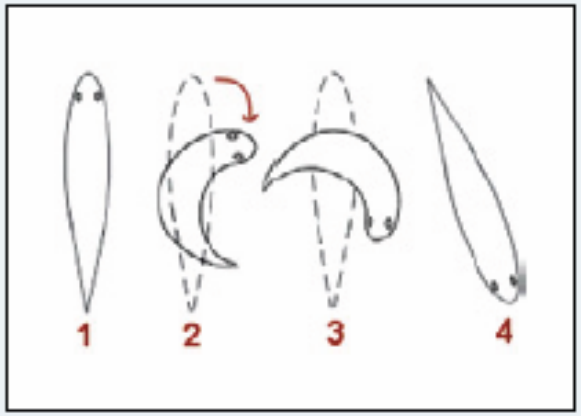

When a fish receives a strong sound stimulus, or is attacked, an alarm reaction or an escape reaction is triggered. The reaction is known among scientists as the "C-start" response, and it is perhaps one the best-studied fish behavior patterns. The "C-Start" has its name from the shape the fish makes as it rapidly starts its escape from danger. The drawing shows that a threatened fish will perform two distinct movements to change direction and speed away from the threat. First, it will curve its body into the shape of a "C" away from the source of sound. Second, it will then straighten its body from the curved position. The straightening motion allows the fish to push water off the full broadside of its body to quickly swim away from its attacker.

Field experiments have demonstrated that sound energy transmitted from air guns initiates this type of response on various fish species. In particular, intense infrasound results in escape reactions.

Images from video tape of three 30–40 cm saithe swimming towards the airgun at 16m range and about 4m from the sea bed and 10m from the surface. When the gun fires they show the typical C-start, veer off course and then continue swimming in the direction of the gun. All three saithe show the reaction in the same TV frame (Frame 2). Note the sound pulse, lasting 6ms, travels 30m during one TV frame of 20ms and the visual range is about 6m. The first three images are 20ms apart, the fourth frame is 5s later.

Fish behaviour and air gun signals – the C-start

Auditory and startle thresholds for codfish, which are hearing generalists with medium hearing ability. The audiogram (black curve) gives the faintest sounds that can be heard at each frequency. The startle response level (red curve) is assumed to be around 80 dB above the known hearing threshold. The red curve is displayed as a smoothed version of the black curve, added around 80 dB. Fish species react very differently to sound. Therefore, any generalisation about the effects of sound on fish should be made with care. The reactions of fish to anthropogenic sound are expected to depend on the sound spectrum and level, as well as the context (e.g. location, temperature, physiological state, age, body size, etc.)

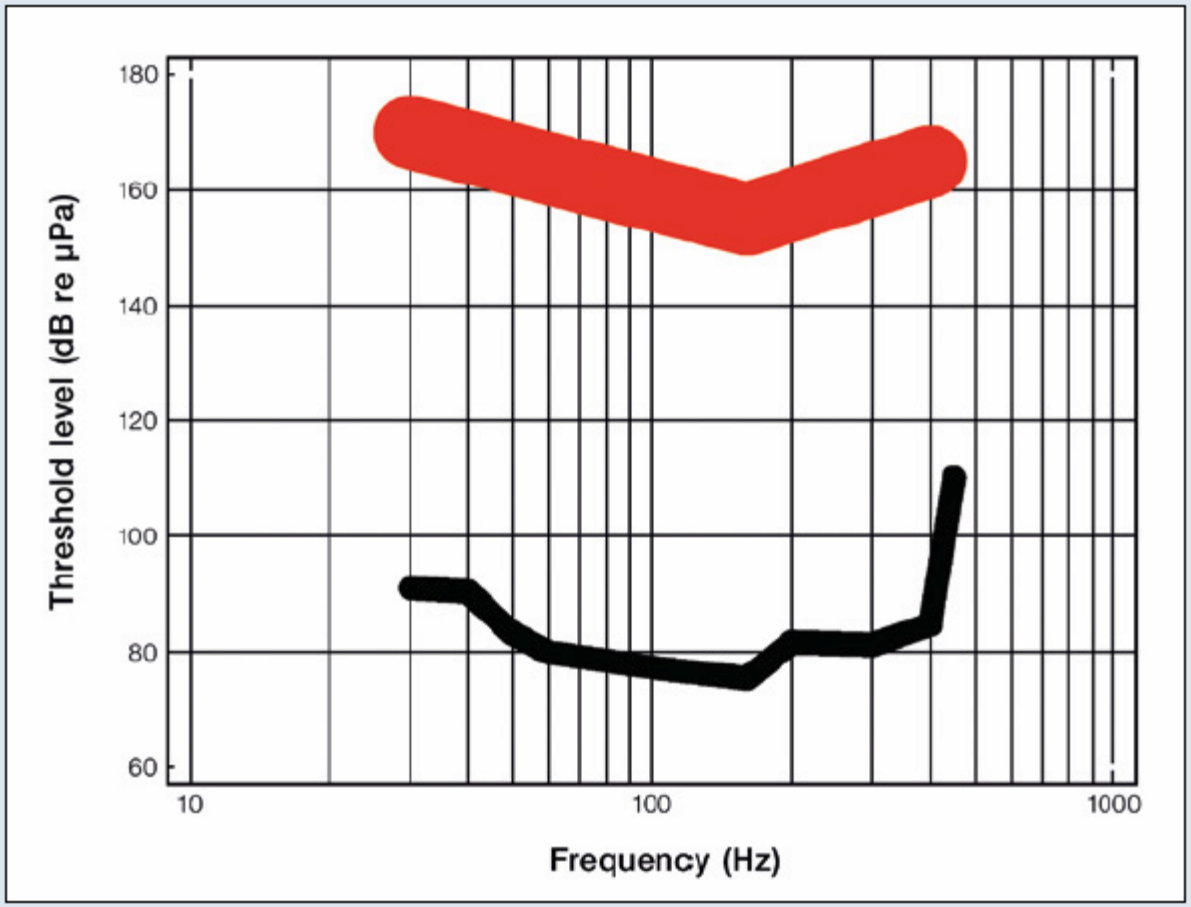

Marine Seismic Sources

PART VIII: FISH HEAR A GREAT DEAL

To understand how human-generated sounds affect fish it is necessary to understand how and what fish can hear, and how they respond to different types of sounds.

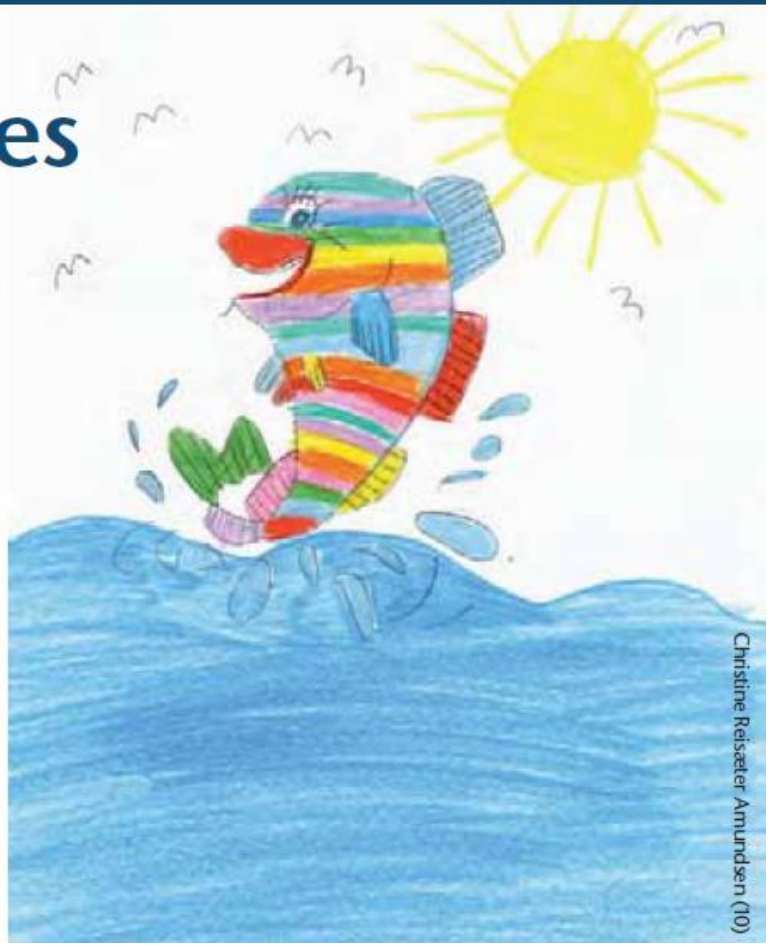

Christine Reisæter Amundsen (10)

The Lofoten and Vesterålen Survey - 2009

- 3D survey covering 15x85 km2, 3500 cubic inch air gun array
- Investigated behaviour of various fish species
- Study performed by Institute of Marine Research (IMR)
- 12 days before, 38 days shooting and 25 days after the survey
- At 30 km distance: 140 dB (above the hearing threshold for cod) but below their threshold for behavioural change

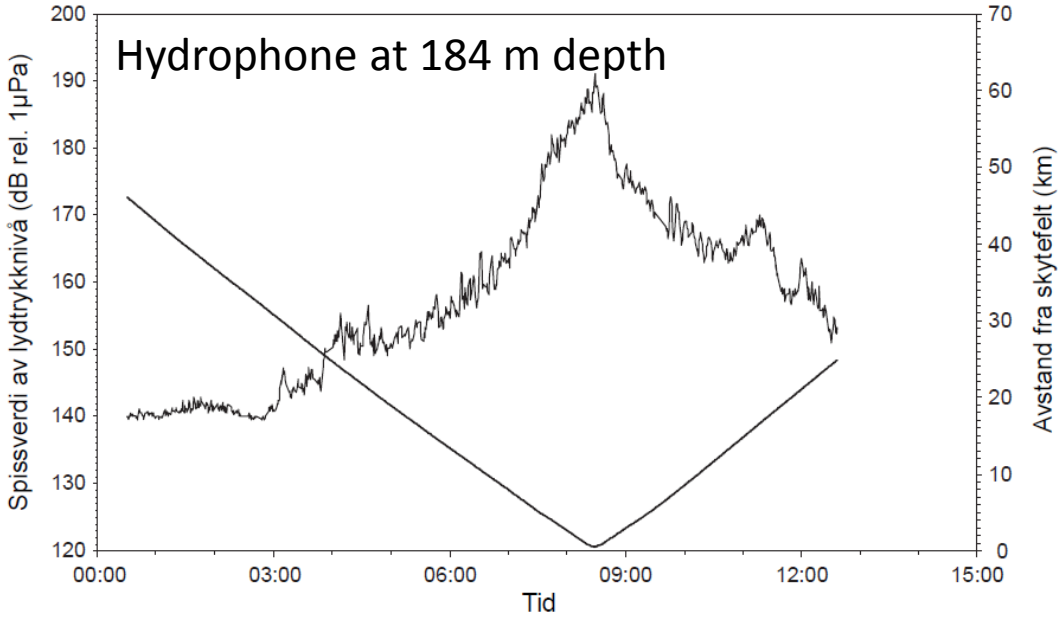

Conclusions from the survey

- Fish react to the sound from air guns by changed behaviour
- Increased catches for some species and smaller catches for others – probably caused by increased stress level
- Pollack and saithe migrated out of the area
- No change in fish stomach content during the survey
- No changes in plankton distribution
- Many streamers => fewer shots per square kilometer

- Overall this study shows few negative effects of air guns on fish

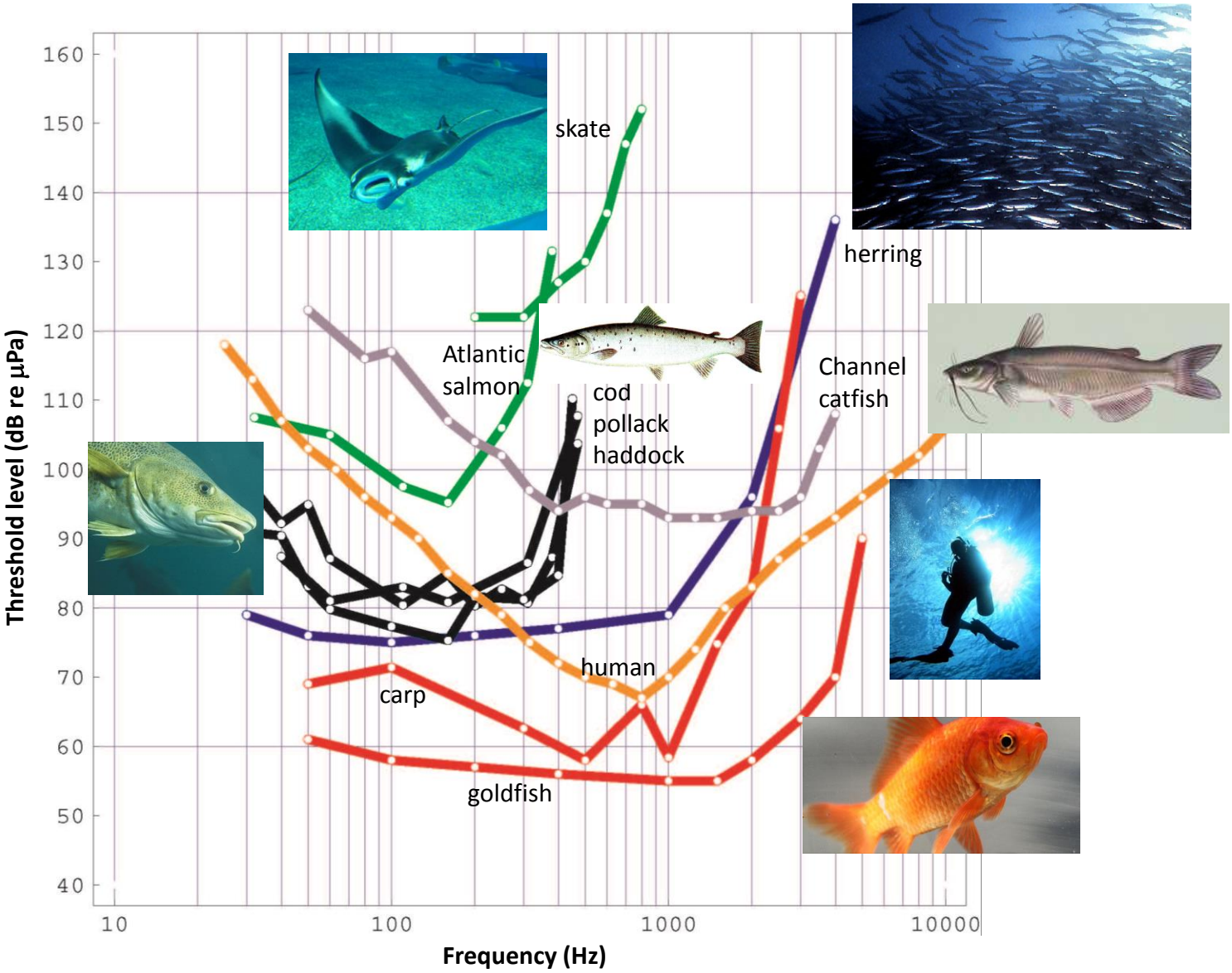
skate
herring
Atlantic
salmon
cod
pollack
haddock
Channel
catfish
human
carp
goldfish
Threshold level (dB re µPa)
Frequency (Hz)
160
150
140
130
120
110
100
90
80
70
60
50
40
10
100
1000
10000

semi-
lith or-
rough

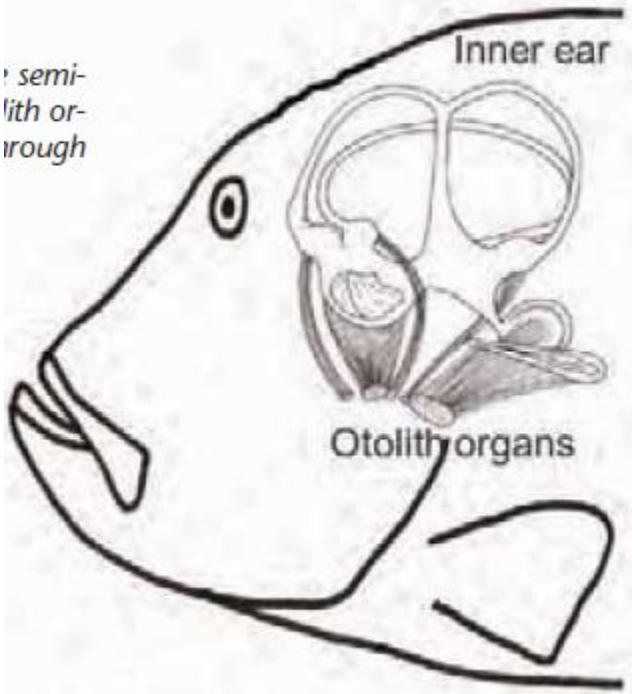

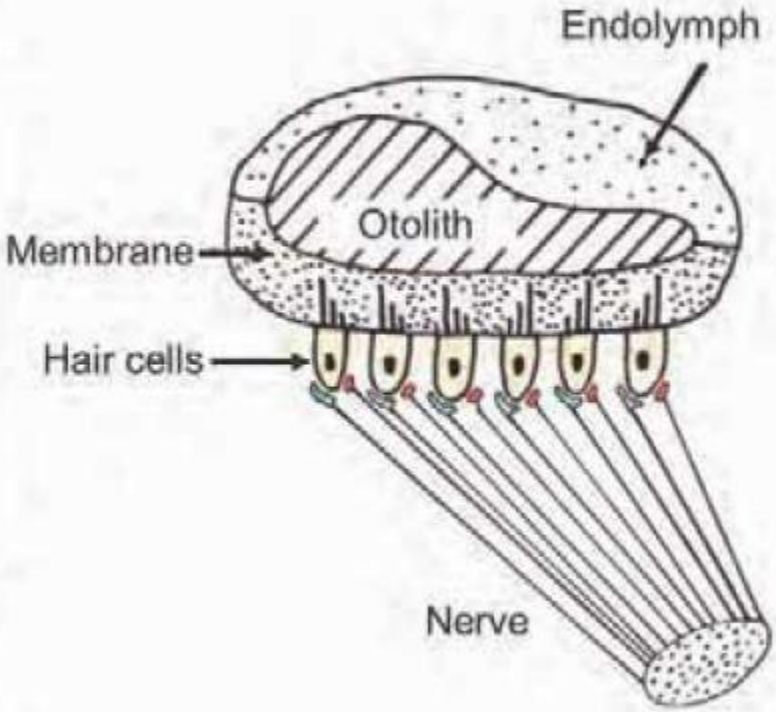

Fish species with either no swim bladder (e.g. elasmobranchs, the collective name for sharks, skates and rays) or a much reduced one (many benthic species living on, in, or near the seabed like flatfish) tend to have relatively low auditory sensitivity, and generally cannot hear sounds at frequencies above 1 kHz. The sound pressure threshold can be as high as 120 dB re 1 μPa (hereafter dB) at the best frequency. Such fishes are therefore "hearing generalist" species. Fish without swim bladders are only sensitive to the particle motion component of the sound field.

Fish having a fully functional swim bladder have increased hearing sensitivity, especially when there is some form of close coupling between the swim bladder and the inner ear. These transmit oscillations of the swimming bladder wall in the pressure field to the inner ear. With the ability to perceive also the pressure component of sound these fish are referred to as "hearing specialists".

In the clupeids, (common food fish like herrings, shads, sardines and anchovies), the coupling takes the form of a gas-containing sphere (prootic bulla) connecting the swim bladder to the hearing system. This considerably lowers their hearing thresholds and extends the hearing bandwidth to higher frequencies up to several kHz.

In otophysan fish (e.g., the carps, minnows, channel catfishes, and characins; the majority of freshwater fish worldwide), a bony coupling is formed by the Weberian ossicles. These bones allow them to use their swim bladder as a sort of drum to detect a greater range of sounds, and create a superleague of hearing-sensitive fish.

Examples with distance	Sound Pressure Level (dB re 20 µPa)
1883 Krakatoa eruption	310 (N)
1908 Tunguska comet explosion	300 (N)
Threshold of irreparable damage; Jet 50 m away	140
Threshold of pain	130-140
Threshold of discomfort; Rock concert	120
Disco, 1 m from speaker; Power lawnmower at 1 m	100
Hearing damage from long-term exposure	90
Diesel truck, 10 m away	
Kerbside of busy road, 5 m	80
Office environment	60
Average home	50
Quiet bedroom at night	30

Source: Wiki

An 1888 lithograph of the 1883 eruption of Krakatoa, which is thought to have produced one of the loudest sounds ever heard by man.

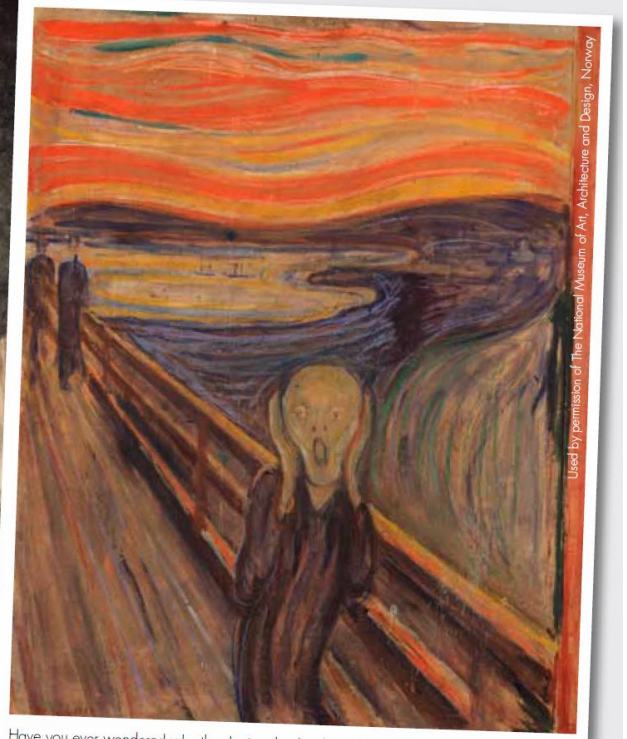

Used by permission of The National Museum of Art, Architecture and Design, Norway

Have you ever wondered why the sky is a lurid red in "The Scream", Edvard Munch's 1893 painting of modern angst? Astronomers suggest that Munch drew his inspiration from the vivid red Krakatoa volcanic twilights seen in Europe from November 1883 to February

Similarity between water guns and pistol shrimp: Cavitation

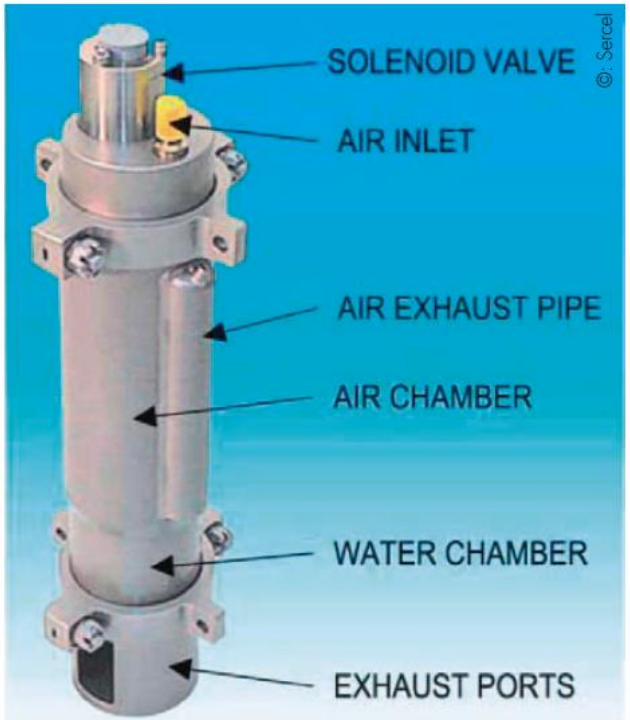

S15 water gun.

Loudest animals in the sea

The tiny pistol shrimp is remarkably loud.

The *Sperm whale*, with the largest brain of any animal, makes the loudest sounds by any living source. Its clicks, used for both echolocation and communication, can have extremely intense source levels up to 236 dB re 1 µPa (rms), at the standard reference distance of 1m, with dominant frequency at 15 kHz. In the next issue of *GEO Expro*, we will report on studies of sperm whales in relation to seismic surveys. The *Blue whale*, the largest living animal, is also loud. Its low-frequency calls have been measured at 190 dB and can travel in deep-

Photograph of a transient cloud of cavitation bubbles generated acoustically.

Picture of bubble (top) and propeller cavitation.

Marine Seismic Sources

PART XI: EFFECT OF SEISMIC ON CRABS

The Atlantic Ghost Cra
quadrata) is a very com
on the beaches of north
where it lives in burrow
the high tide line. Altho
itself is seldom seen du
hours, the round shap
to its burrows and the tr
in the sand are quite co

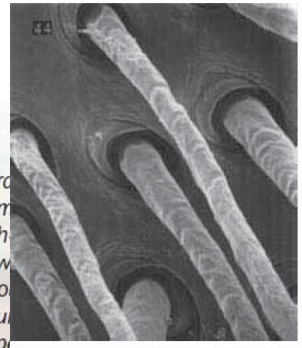

Scanning microscope photo of crab hearing hairs (Christian et al, 2003). Typical length of these hairs is 300 micrometers. These hairs are similar to seismic streamer cables, although the dimensions are 'slightly different' – 300 micrometers versus 6 km. Another similarity with seismic acquisition is the use of several streamers: while seismic contractors can tow up to 20 streamers, the snow crab is equipped with even more receptors!

"You cannot teach a crab to walk straight"

Aristophanes, 446-386 BC, the 'father of old comedy'

Hearing curves for crabs

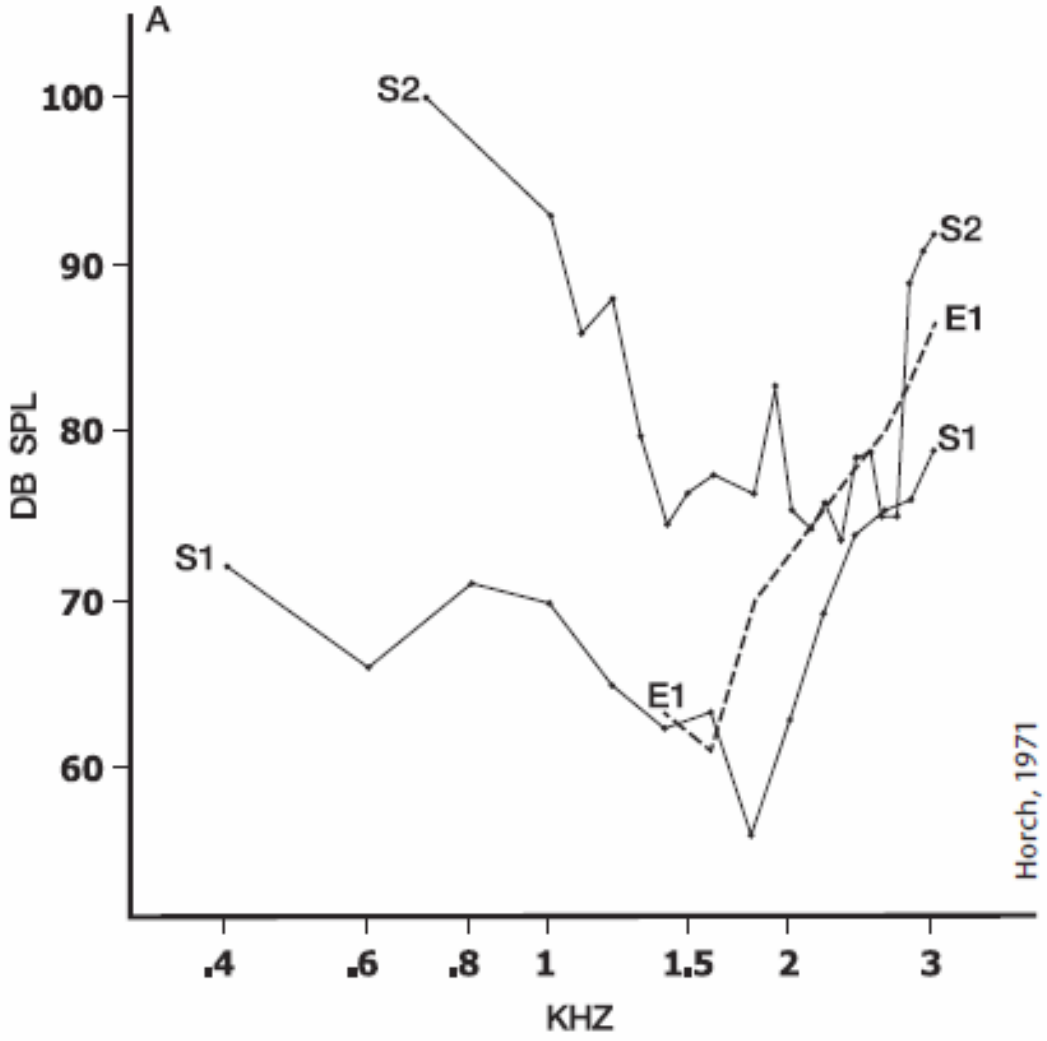

Hearing curves for two ocypodes. Thresholds determined electrophysiologically with recordings made from electrodes implanted in the brains of animals suspended in air. Tones presented by loudspeaker (S) or to individual walking legs with a small earphone (E). DB SPL: sound pressure relative to 0.0002 microbar.

Photo (from Christian et al., report 2003) of sensory hairs in the snow crab statocyst. The crab is equipped with at least three various hair types. One detects vibration or direct contact, another is sensitive to chemicals and the third is designed to detect pressure changes in the water. These hairs are similar to seismic hydrophones used to record seismic signals. Experiments show that crabs do not respond to sound signals like music; however, they react instantly if you jump close to them.

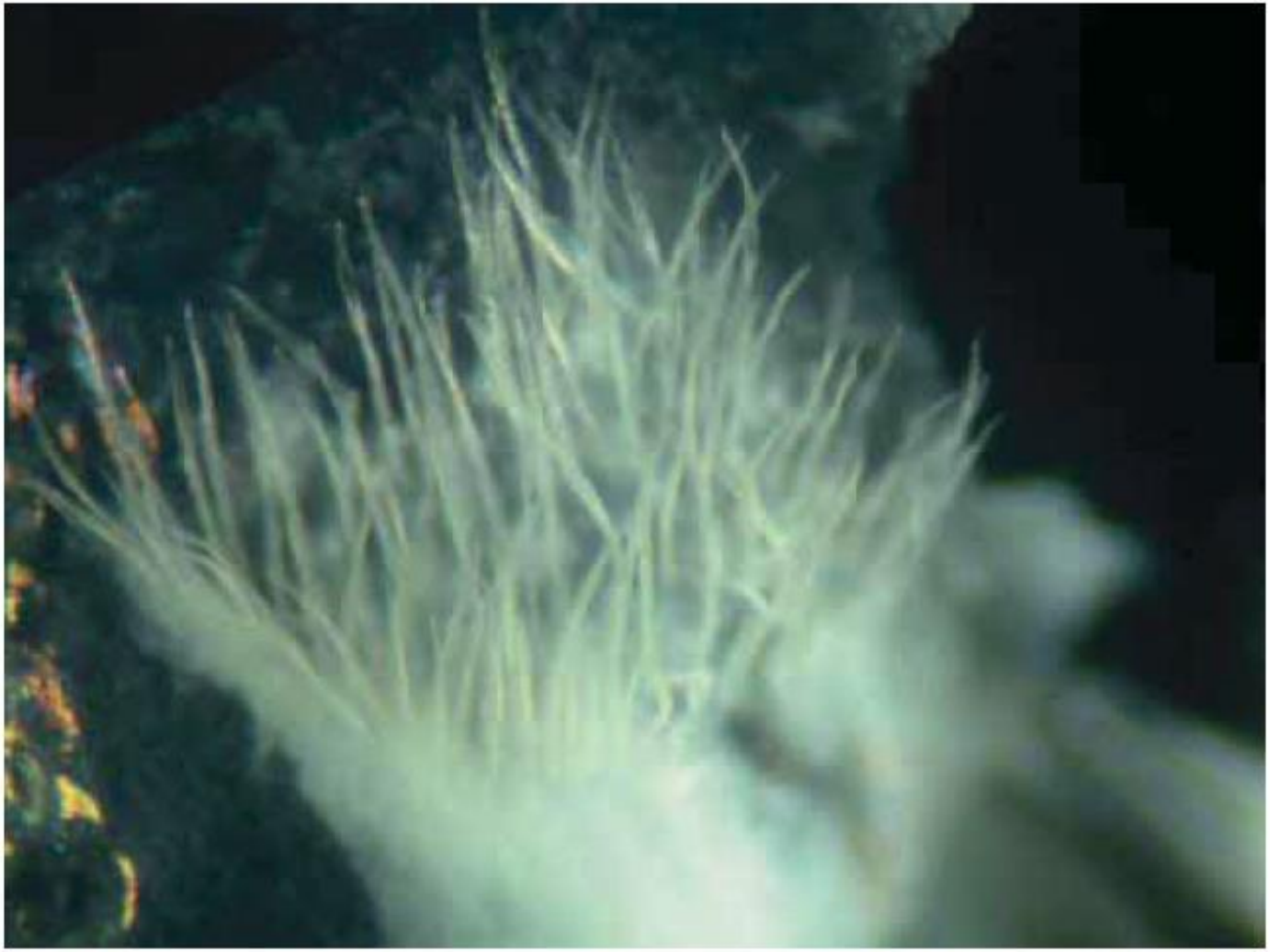

Source: Wikipedia

Using seismic waves for communication

A golden mole ensures **good coupling** to the ground to detect seismic waves

The middle east blind mole rat – first mammal where vibrational communication was documented – banging their head against the tunnel wall to communicate with neigbouring mole rats

Footdrumming is used widely as a predator warning or defensive action used by skunks, rabbits, deers, elephants, kangaroo rats, …

Seismic properties of Asian elephant (*Elephas maximus*) vocalizations and locomotion

C. E. O'Connell-Rodwell[a)]
Center for Conservation Biology, Department of Biological Sciences, Stanford University, Stanford, California 94305-5020

B. T. Arnason
Tezar Inc., P.O. Box 26235, Austin, Texas 78755-0235

L. A. Hart[b)]
Department of Population Health and Reproduction, University of California, Davis, California 95616

J. Acoust. Soc. Am. **108** (6), December 2000

- Elephants generate Rayleigh waves in the ground
- Rayleigh velocity is around 250 m/s => shorter wavelength than airbourne sound
- Distance between legs larger than between airs (2-2.5 m compared to 0.5 m) => better directivity for the Rayleigh signals

Reuter *et al.* (1998) suggest that detection of seismic signals in elephants may be possible via bone conduction, due to the size of their middle ear ossicles. Somatosensory reception in the feet may also play a role in seismic reception and would be a more direct mechanism to detect vibrations without the problem of attenuation between the foot and the ear (O'Connell *et al.*, 1999). Such somatosensory receptors

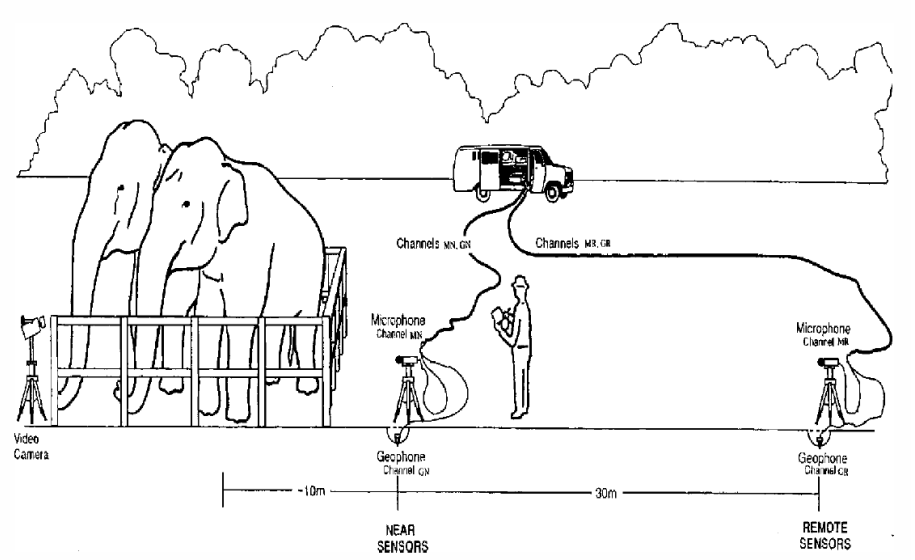

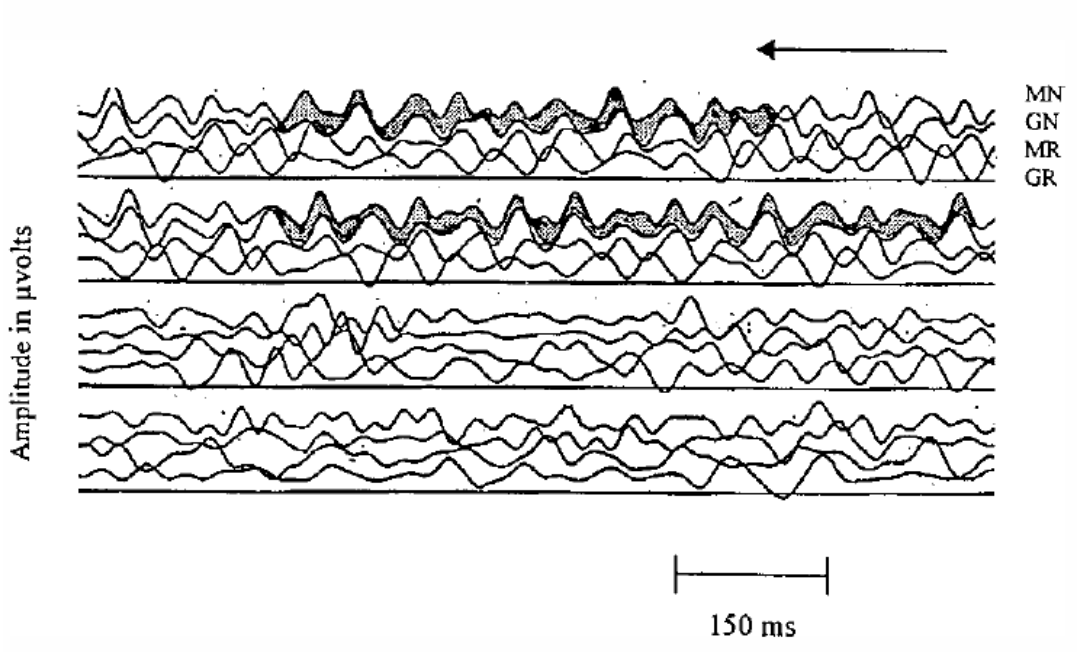

Rodwell et al., J. Acoust. Sos. Am., 2000,

Fig. 3. Acoustic and seismic spectrogram of an African elephant vocalization.

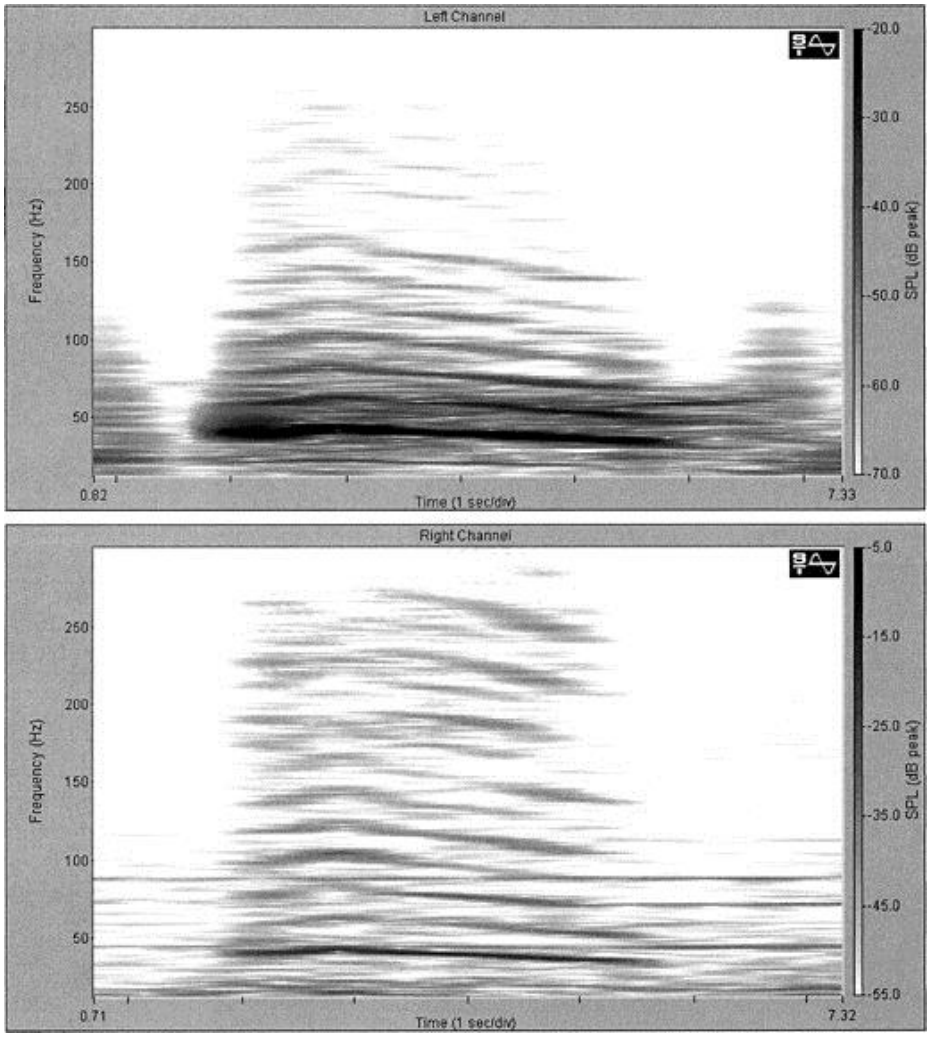

O'Connell-Rodwell C E et al. Amer. Zool. 2001;41:1157-1170

Where does the sound go?

Source directivity: Ghost effect and length of array

$$\left|H(f)\right| = \left|2\sin\frac{2\pi f z_g \cos\theta}{c}\right|$$

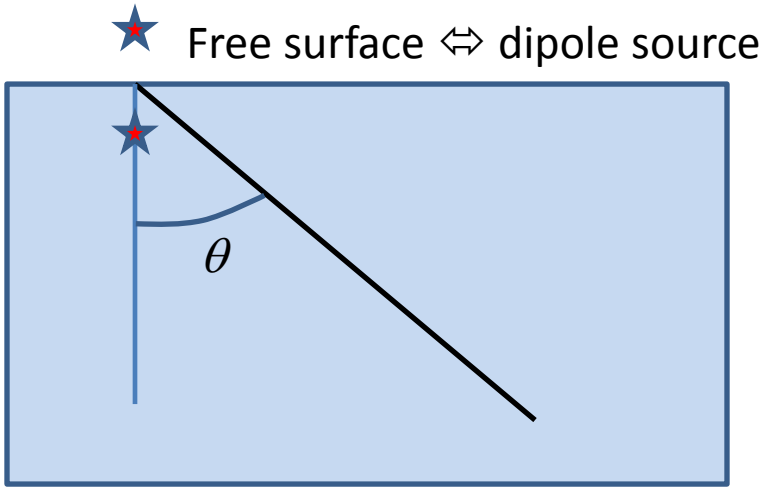

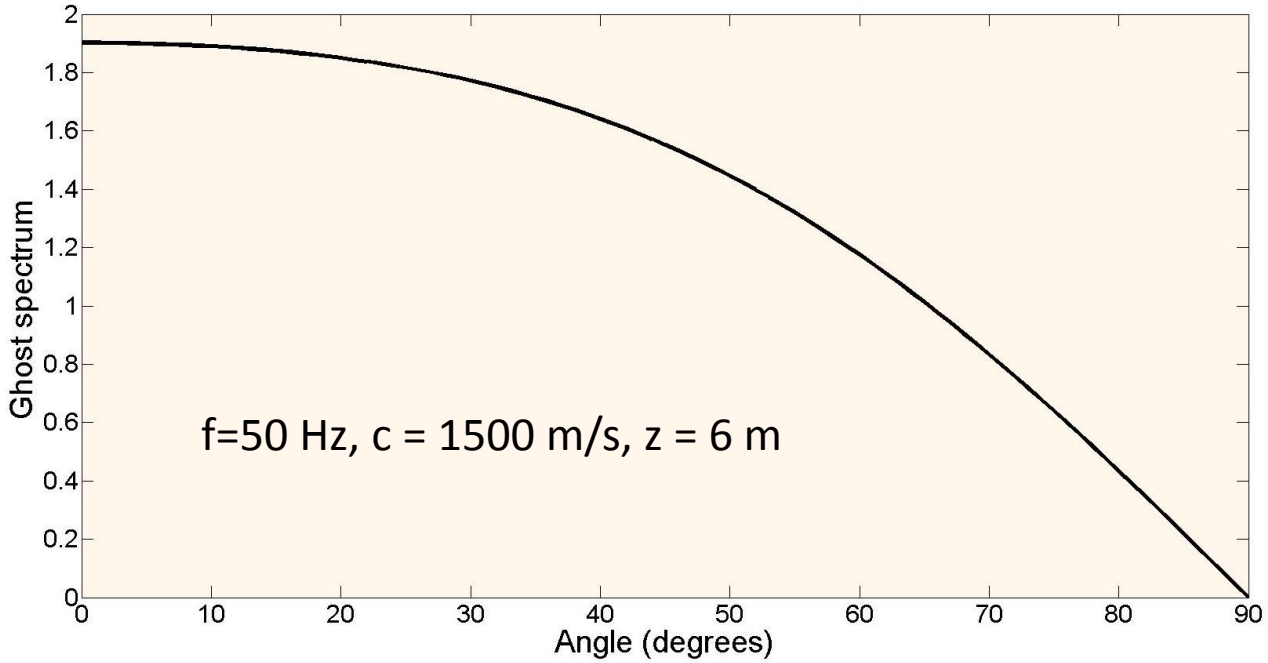

Vertical and directional far-field signatures & spectra

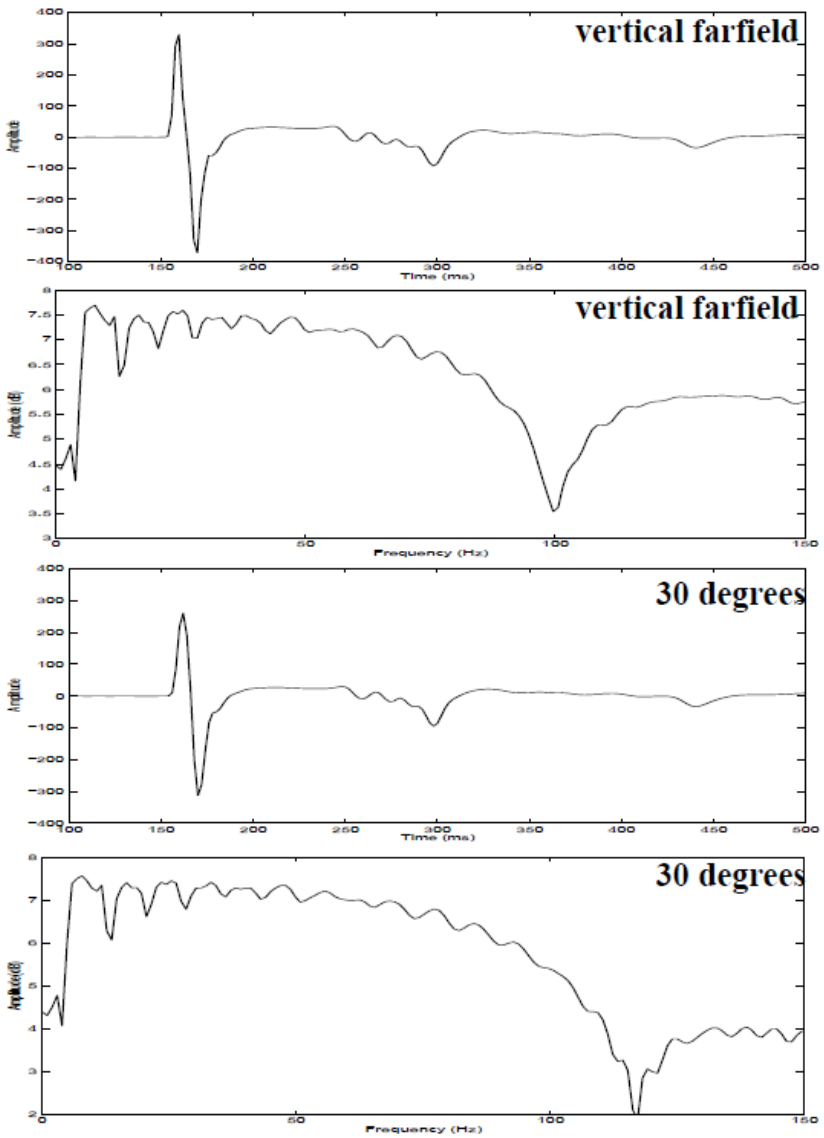

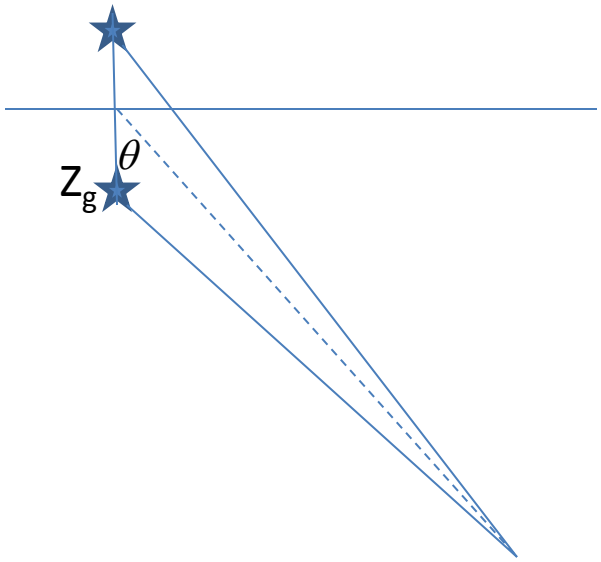

$$f_N = \frac{c}{2z_g \cos\theta}$$

Notch fequency increases with observation angle

Where does the sound go?

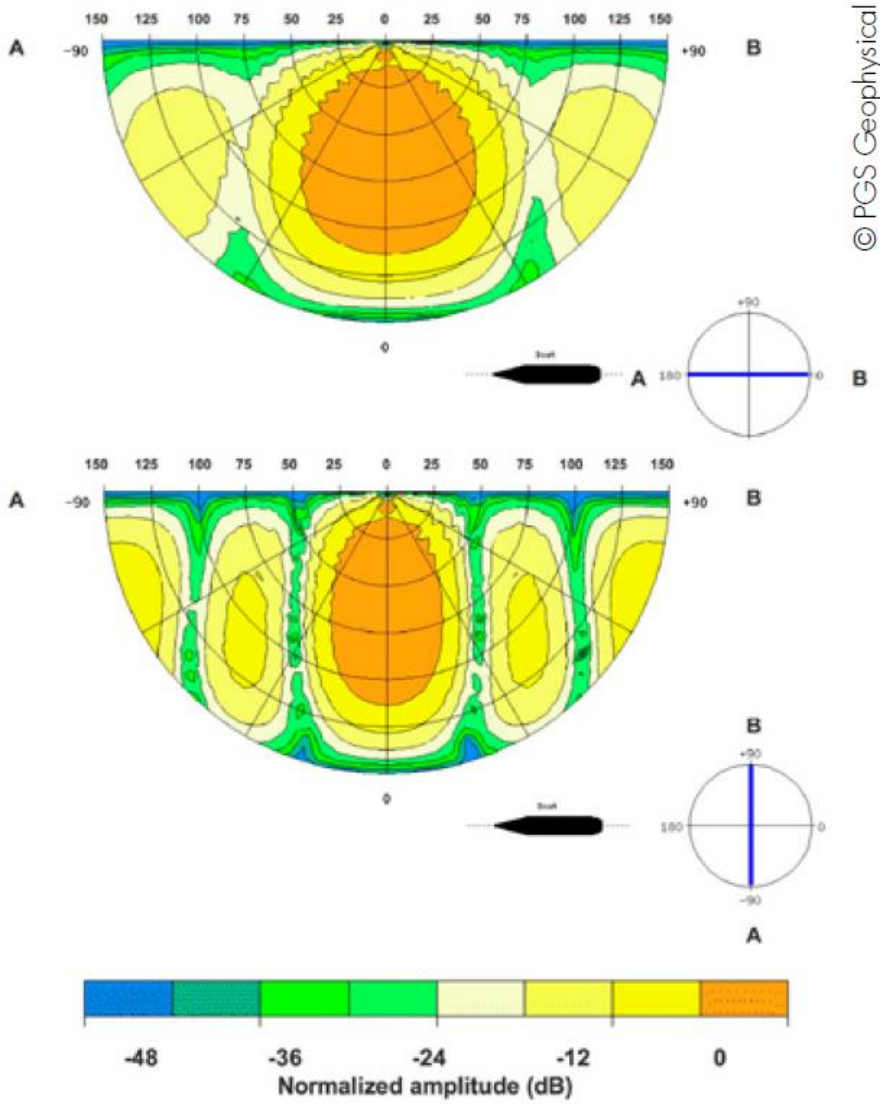

Vertical cone 0-40 degrees

High frequency noise from air guns

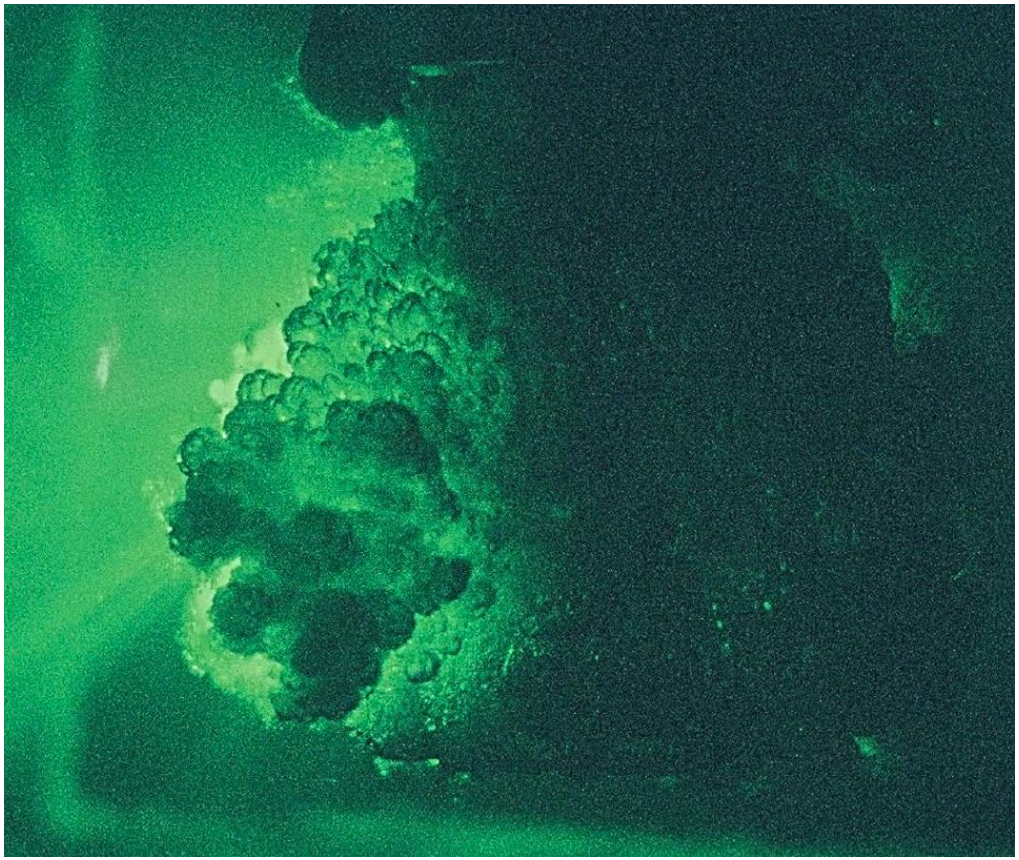

High frequency signals from air guns

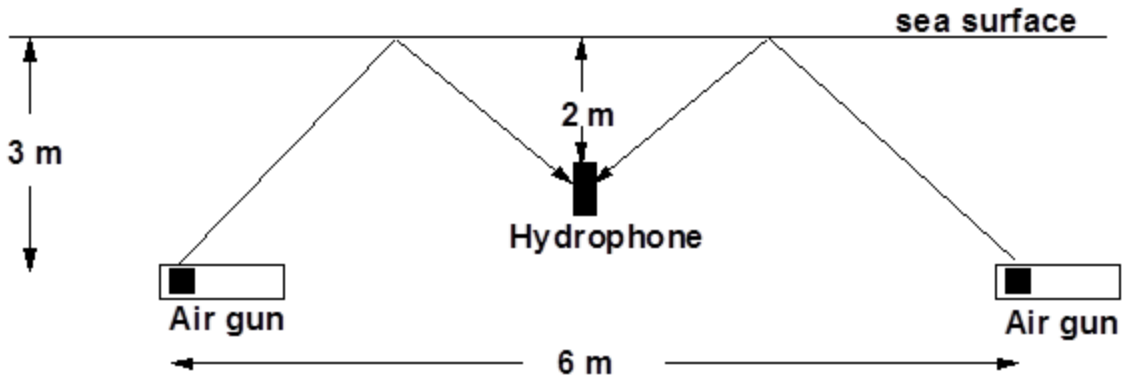

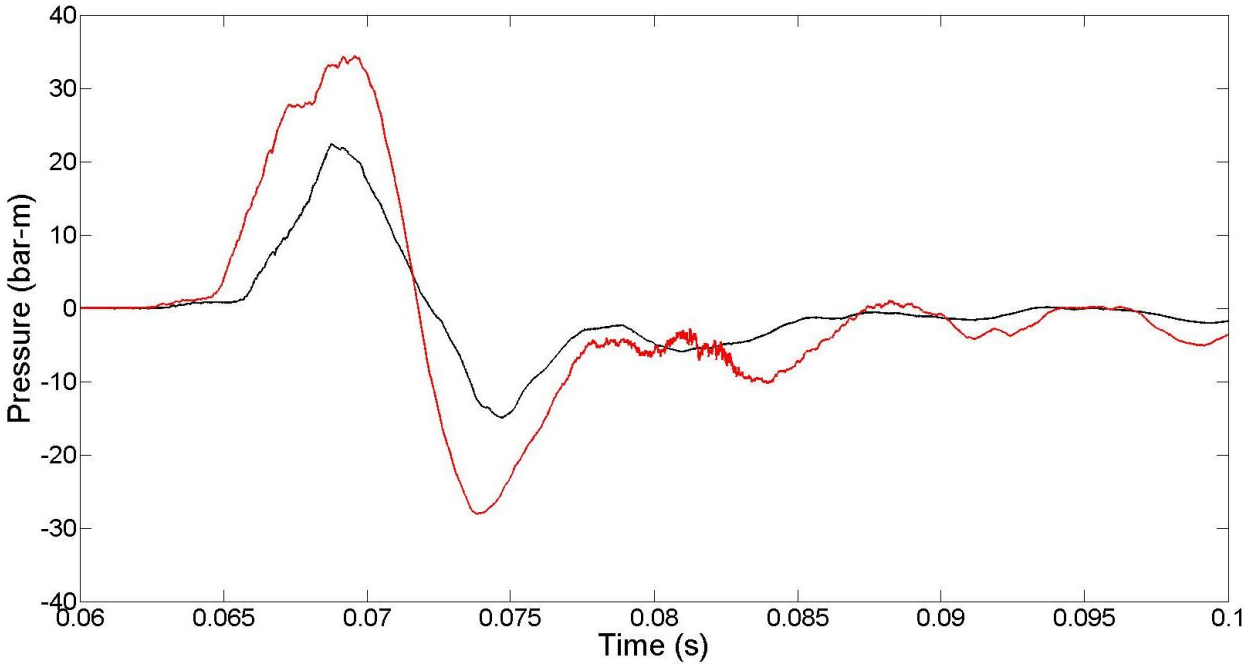

Detailed comparison

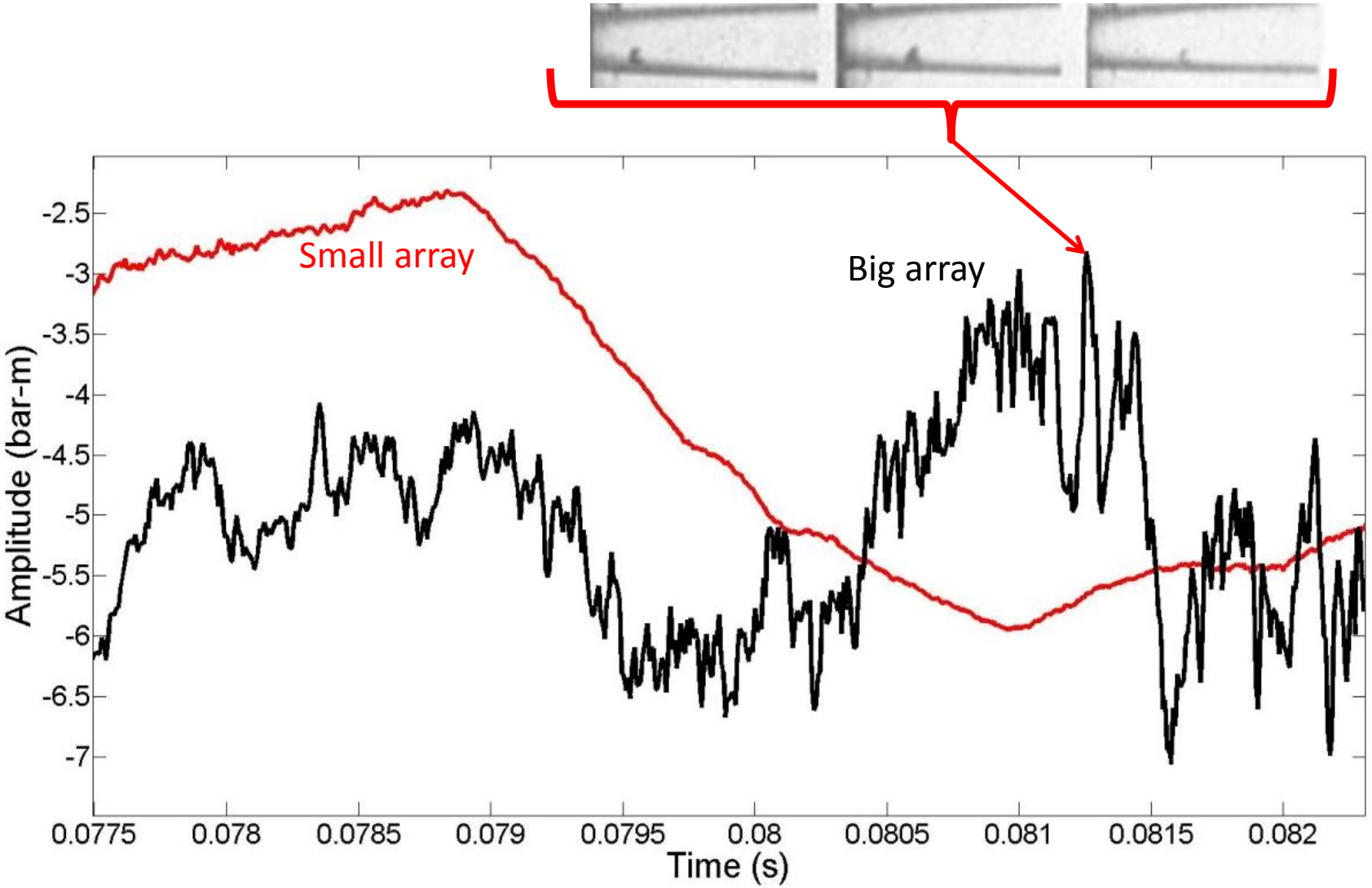

Multiple cavity collapses?

1 kHz high pass filter

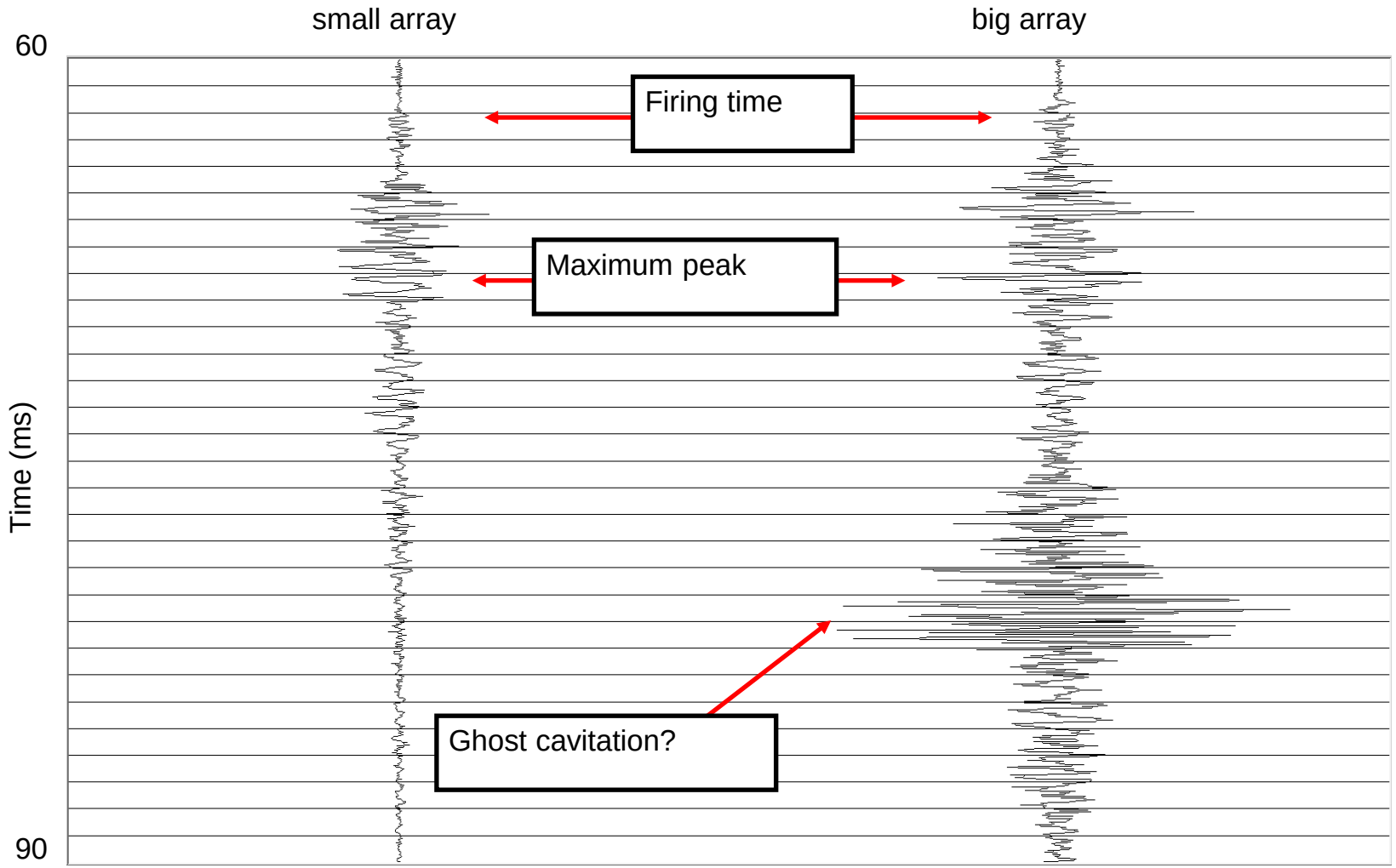

High-frequency signals from air-gun arrays

GEOPHYSICS, VOL. 76, NO. 4 (JULY-AUGUST 2011)

M. Landrø[1], L. Amundsen[2], and D. Barker[1]

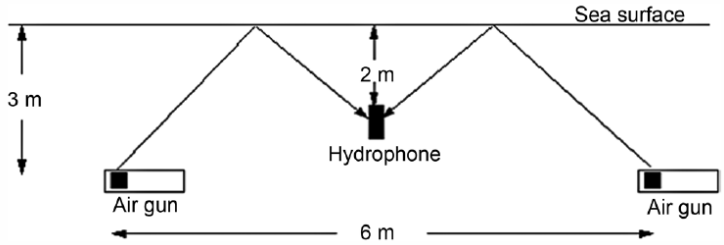

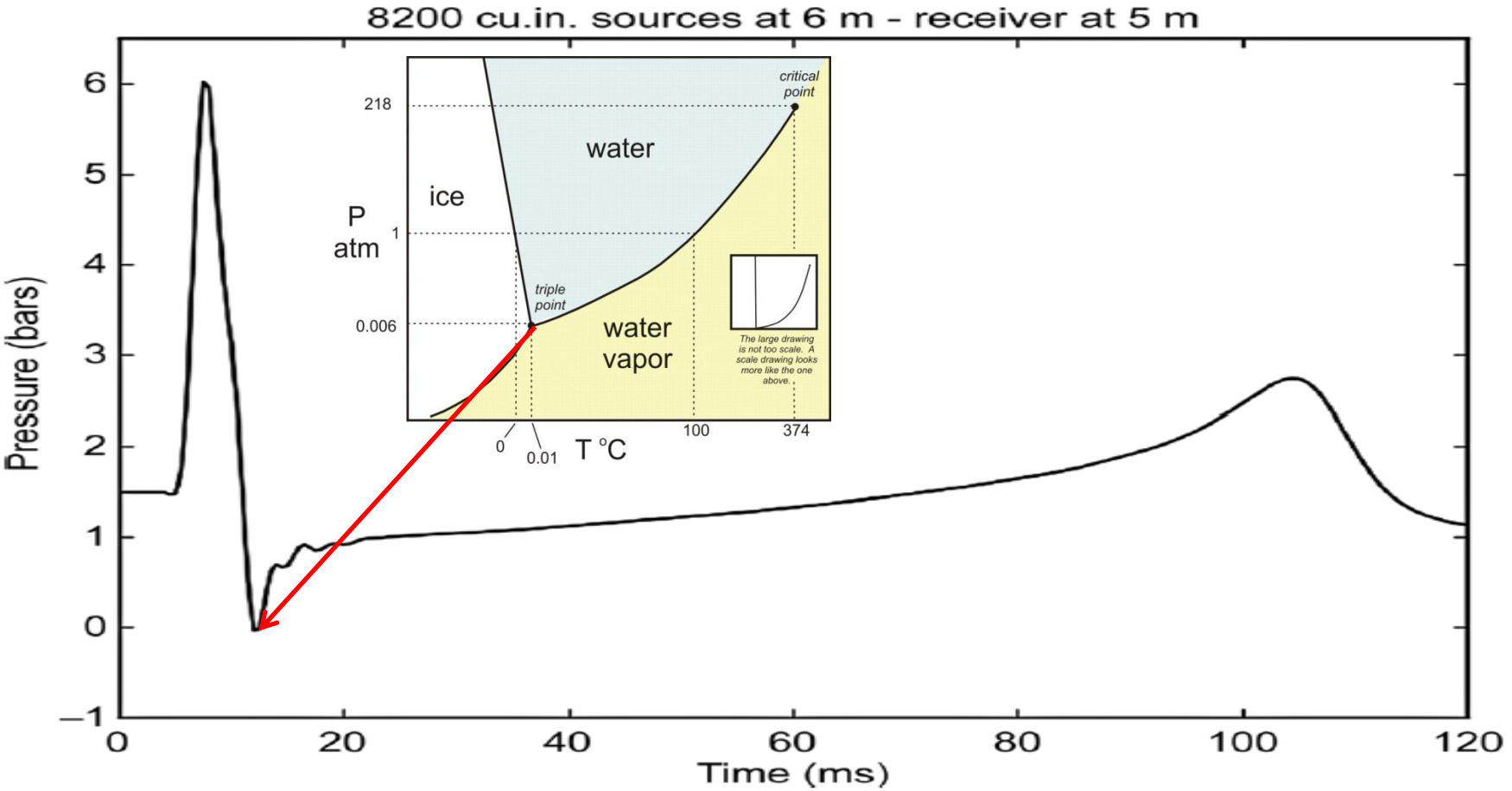

THE JOURNAL OF THE ACOUSTICAL SOCIETY OF AMERICA VOLUME 24, NUMBER 6 NOVEMBER, 1952

An Experimental Study of Single Bubble Cavitation Noise*

MARK HARRISON
David Taylor Model Basin, Department of the Navy, Washington 7, D. C.
(Received May 23, 1952)

An experimental study of the noise produced by a single cavitation bubble has been made. The noise consists principally of a transient pressure pulse associated with the collapse of the bubble. The motion of the bubble has been photographed simultaneously with the measurement of the pressure pulse.

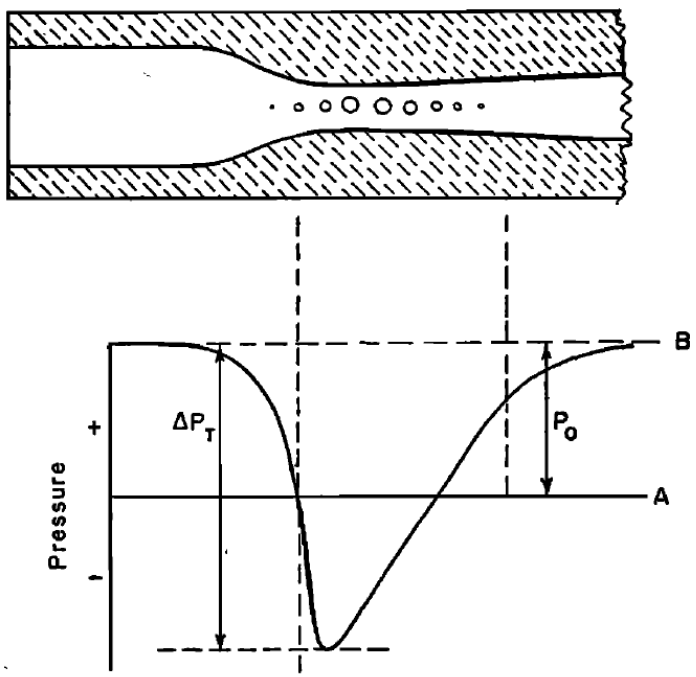

FIG. 3. Sketch of the pressure in the venturi nozzle; the history of a single bubble is illustrated.

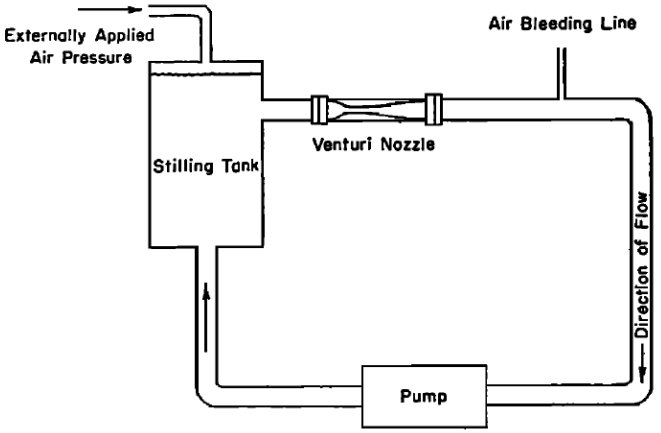

Cavities formed close to air bubbles injected into the water – for small air bubbles (not visible) the vapor cavity collapsed completely =>

Observed cavity and comparison with the Rayleigh formula

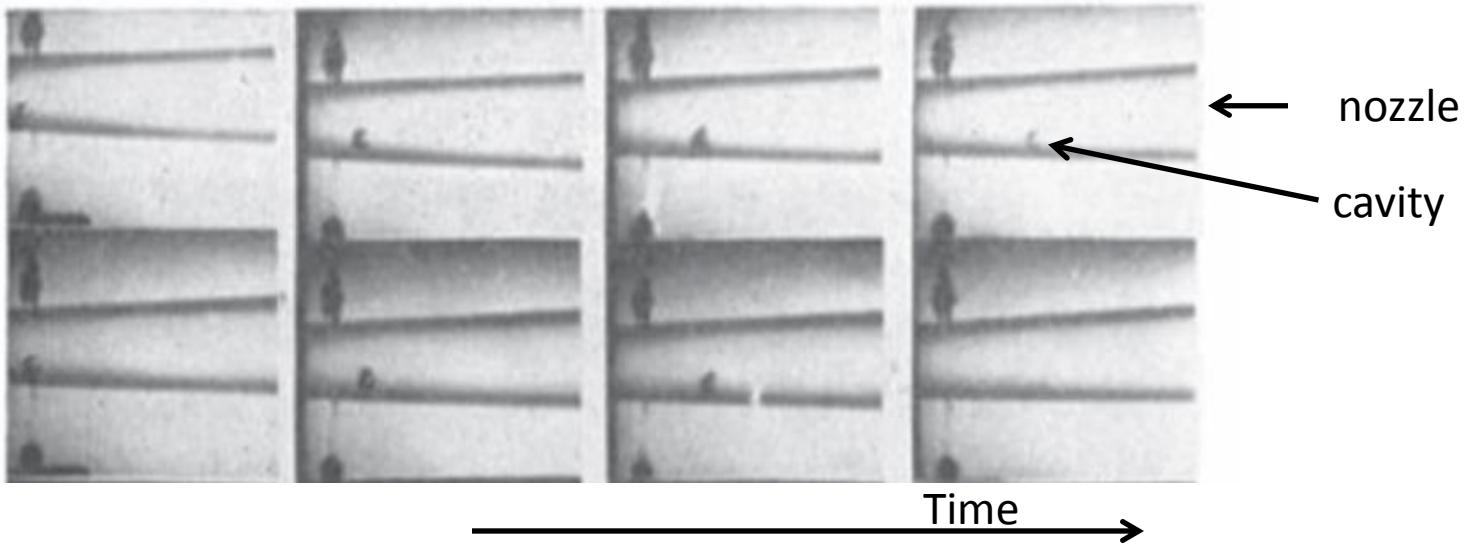

$$t = \sqrt{\left(\frac{3\rho}{2P}\right)} \cdot \int_{R}^{R_0} \frac{R^{3/2} dR}{(R_0^3 - R^3)^{\frac{1}{2}}} = R_0 \sqrt{\left(\frac{3\rho}{2P}\right)} \cdot \int_{\beta}^{1} \frac{\beta^{3/2} d\beta}{(1-\beta^3)^{\frac{1}{2}}}$$

Rayleigh's collapse time formula fits the experimental data

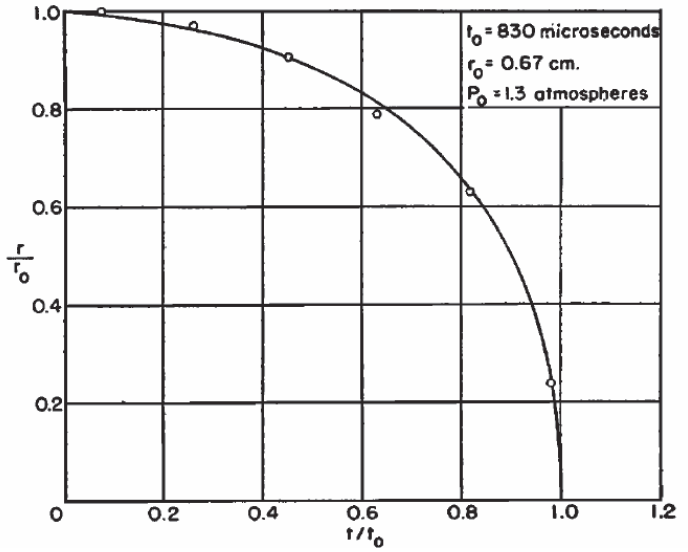

High frequency recorded farfield signatures (seabed hydrophone at 60 m)

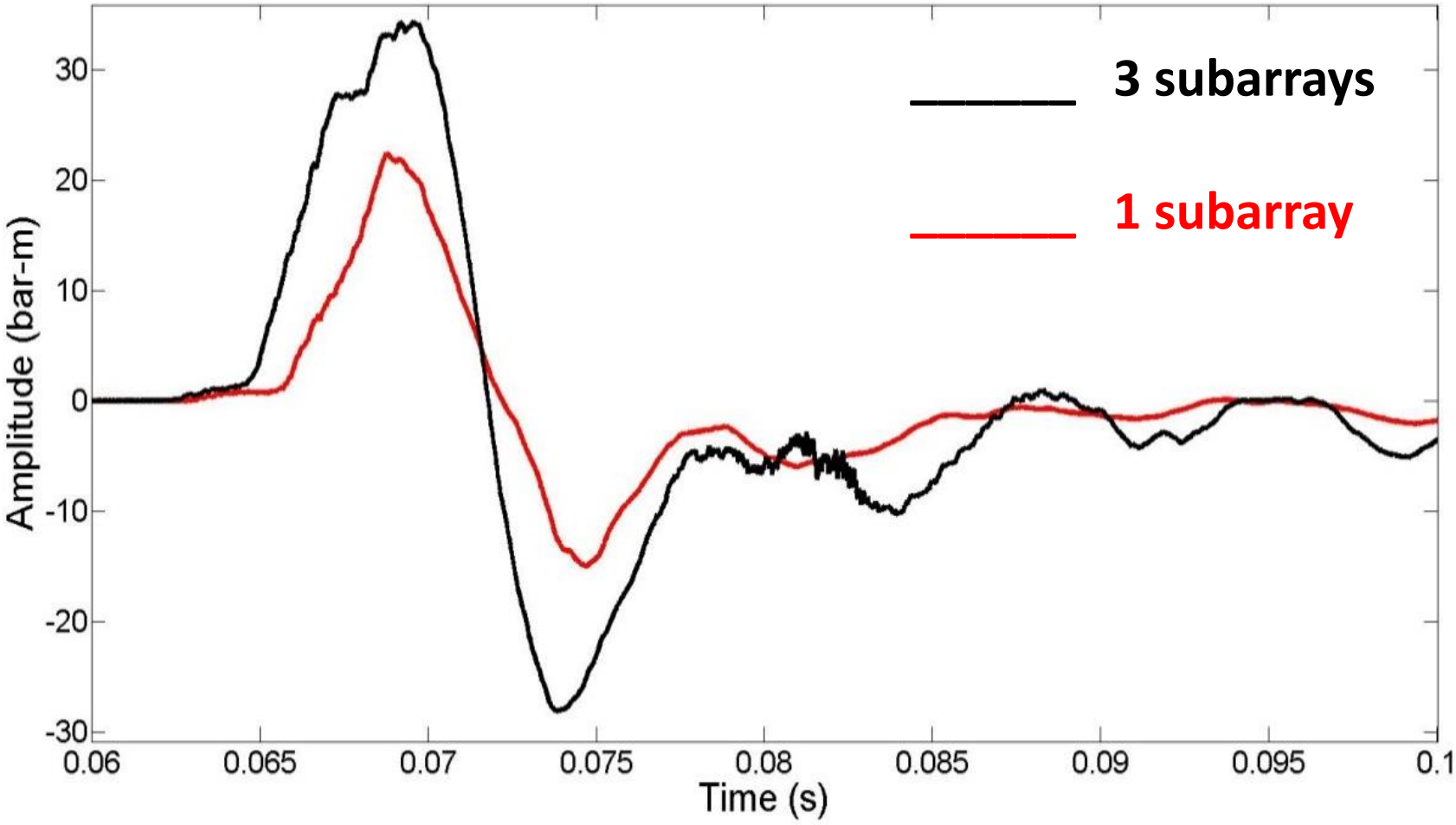

1 kHz High pass filter of data

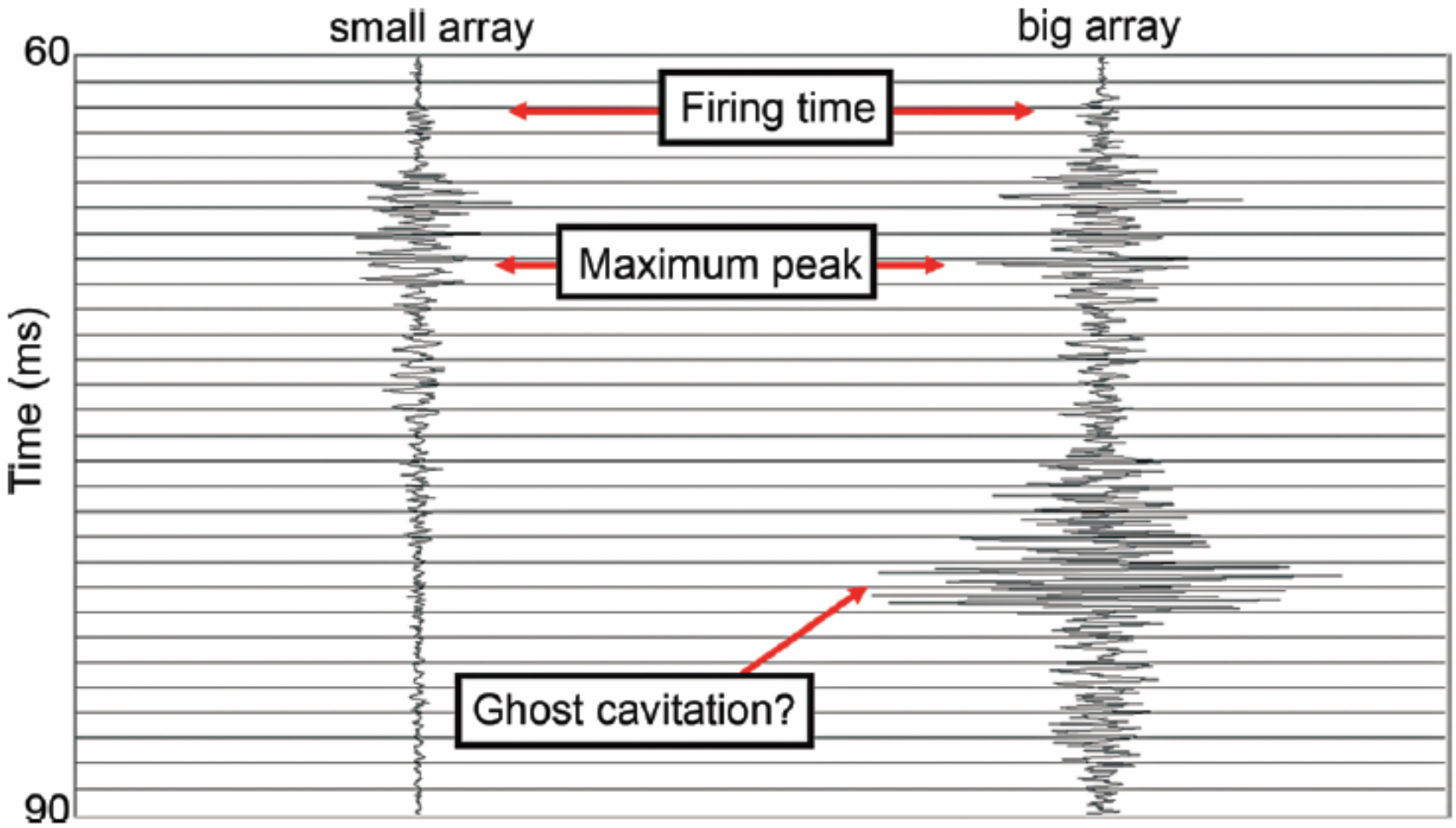

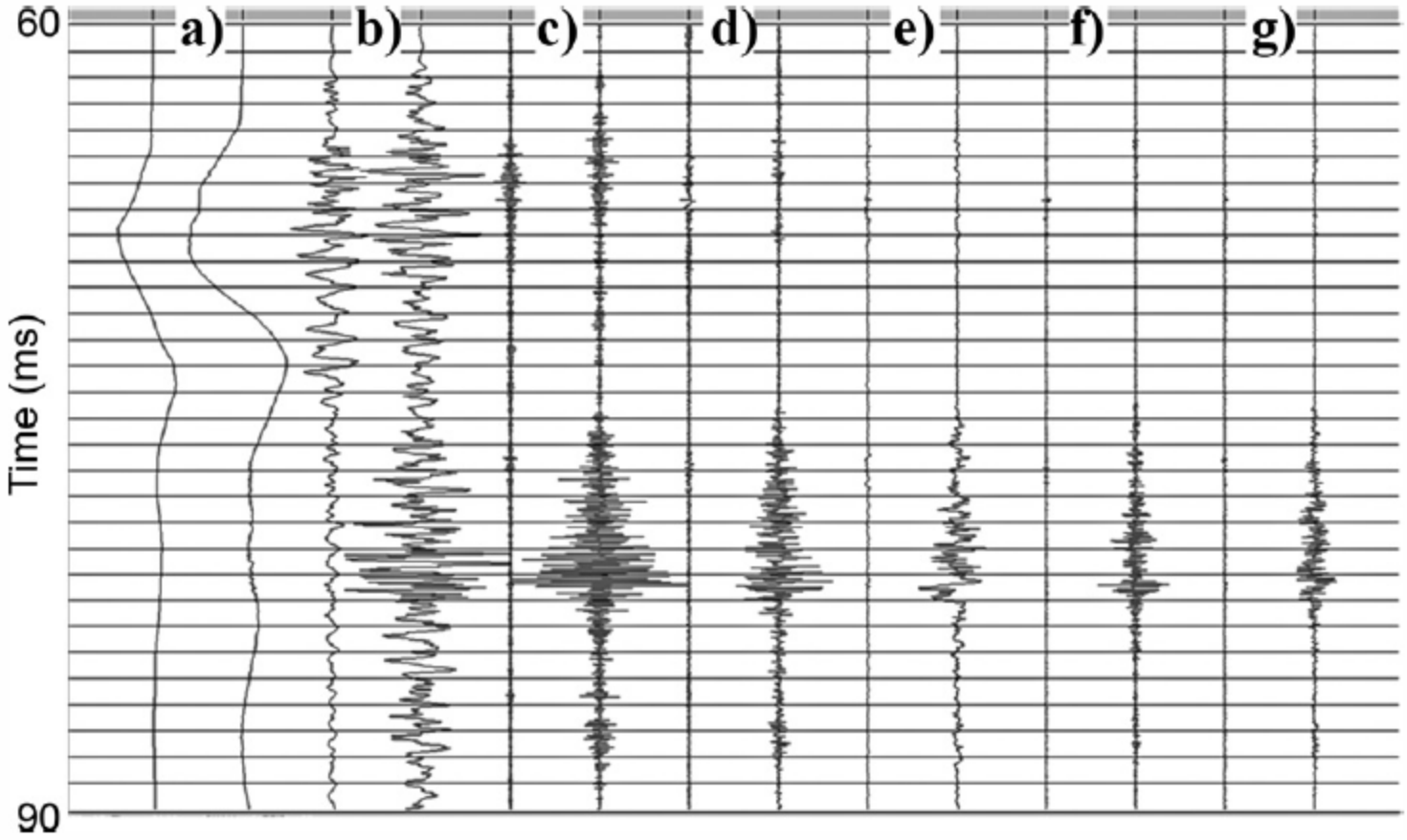

Figure 9. Pairs of small-array and big-array signatures with various filters: a, no filter; b, 1–10 kHz; c, 10–20 kHz; d, 20–30 kHz; e, 30–40 kHz; f, 40–50 kHz; g, 50–60 kHz. Pair a has been scaled by 0.01, and pair b has been scaled by 0.5 relative to the other

Frequency comparison

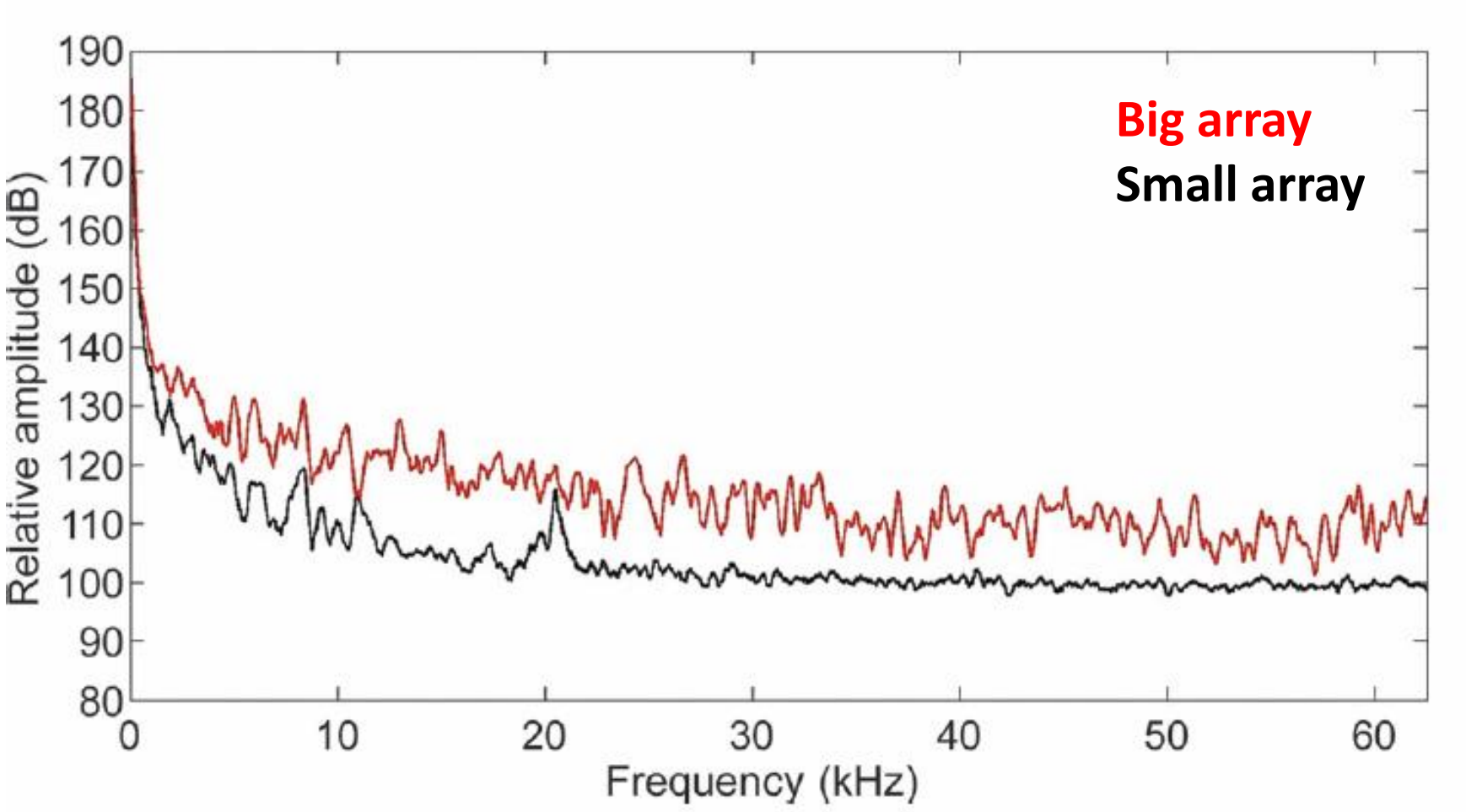

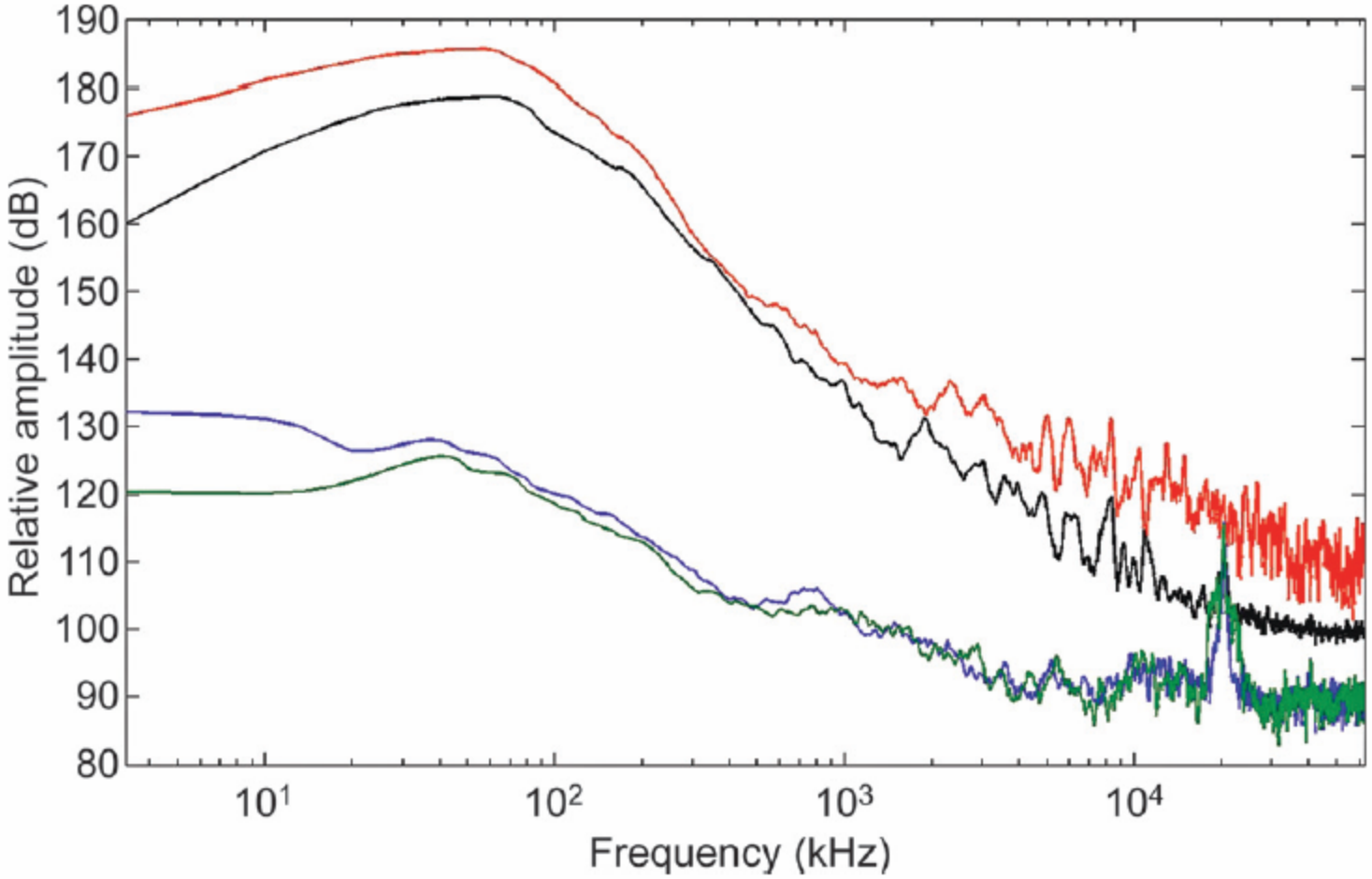

Figure 17. Comparison of two ambient-noise records (blue and green lines) and the air-gun array signals (red line: big array; black line: small array). The ambient-noise spectra were computed from the data window prior to firing the source array, that is, from 0 to 0.05 s (see Figure 7). All curves have been smoothed.

Is this high frequency signal repeatable?

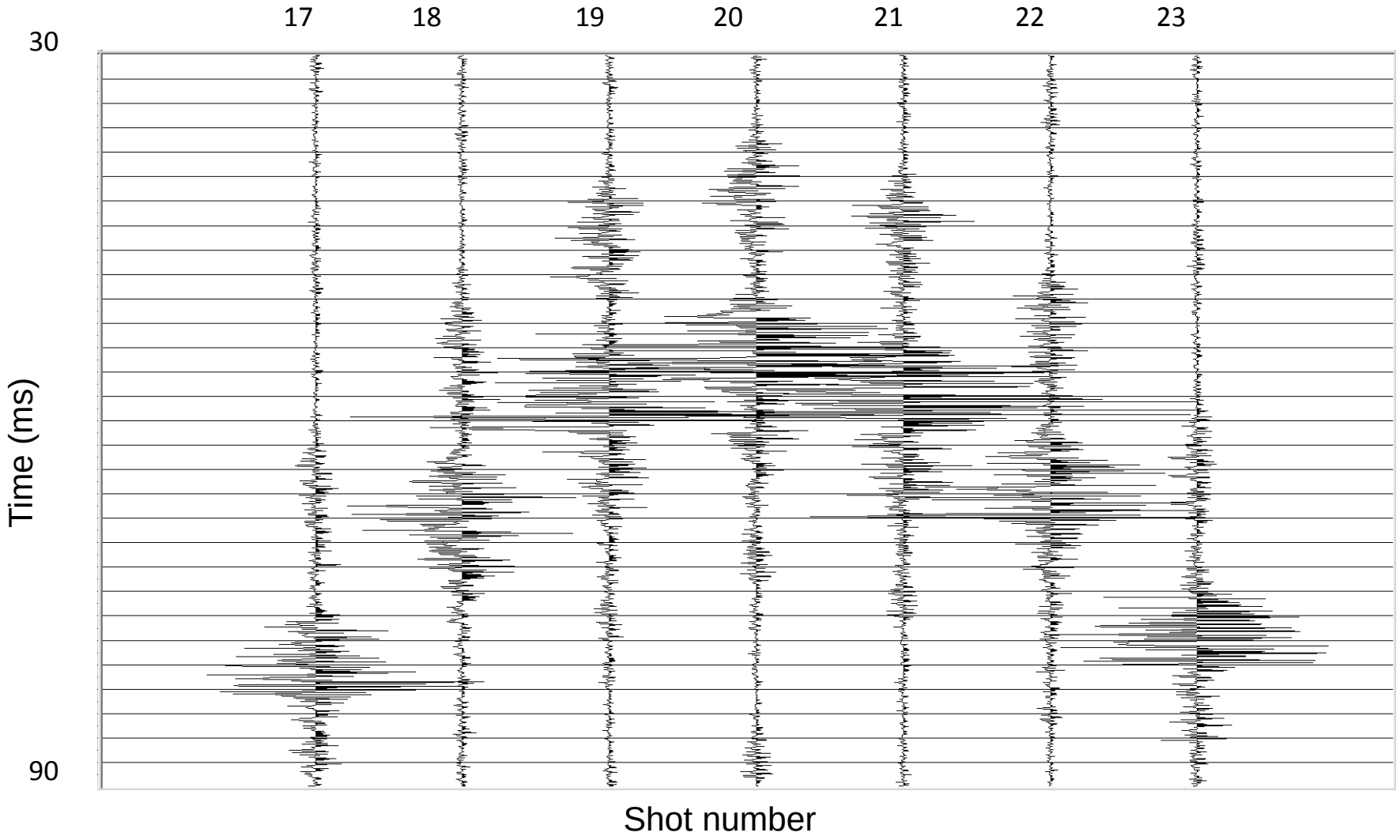

Absolute value of signal + a mean smoother + flattening

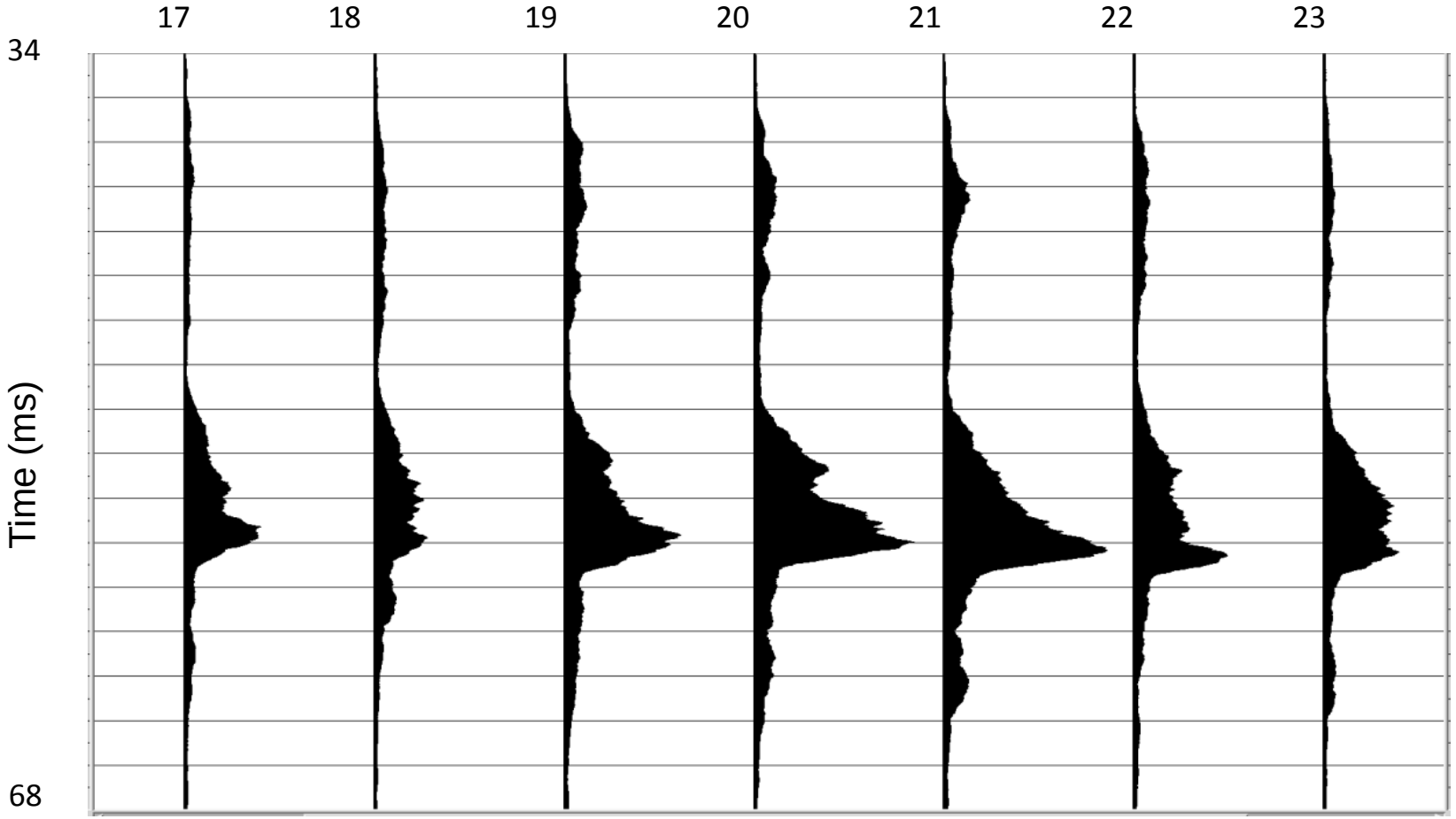

Modeled dynamic pressure at 2 m depth varying the sea surface reflection coefficient

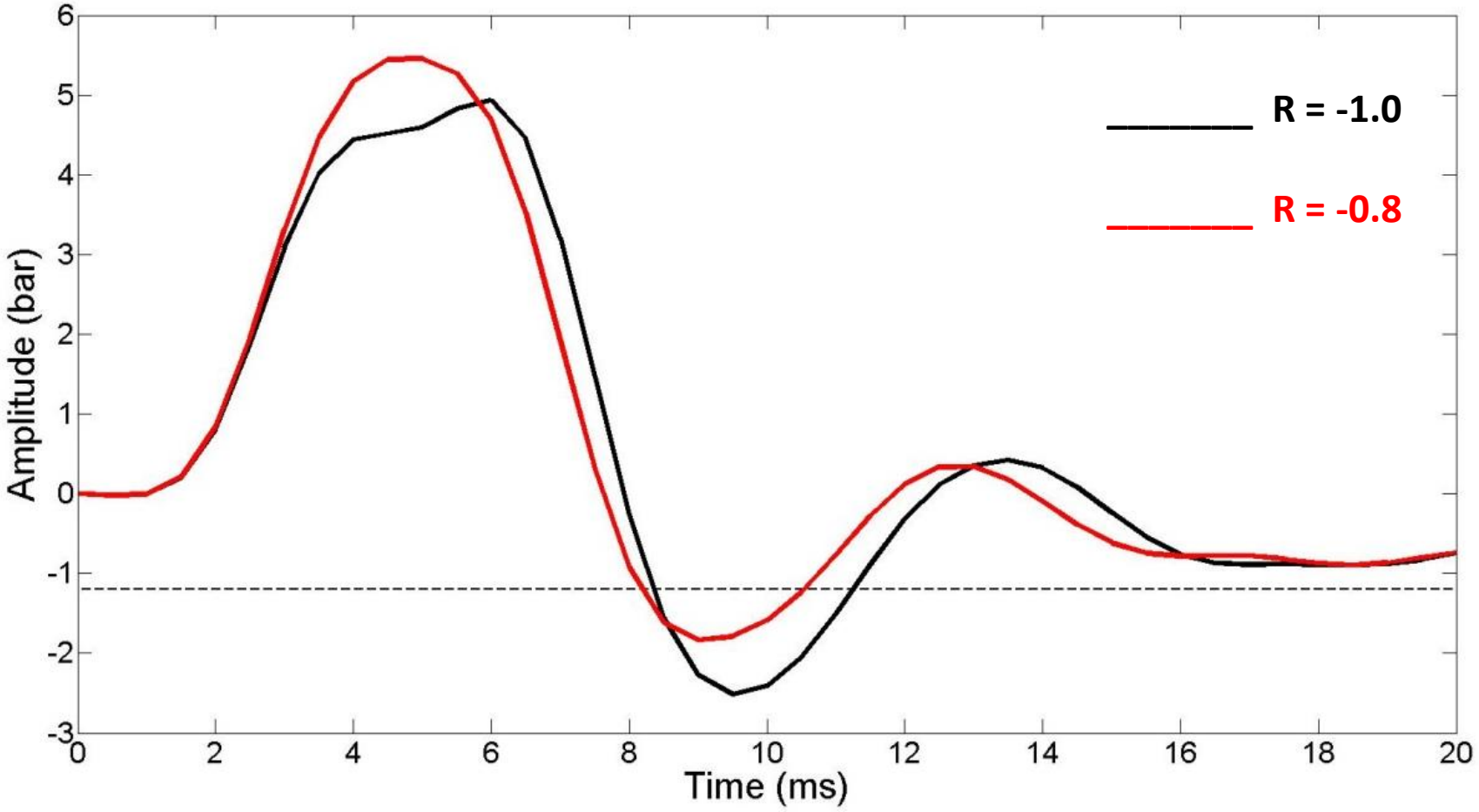

Less cavitation for weaker sea surface reflection coefficient

The effect of increasing the distance between the subarrays from 6 to 10 m

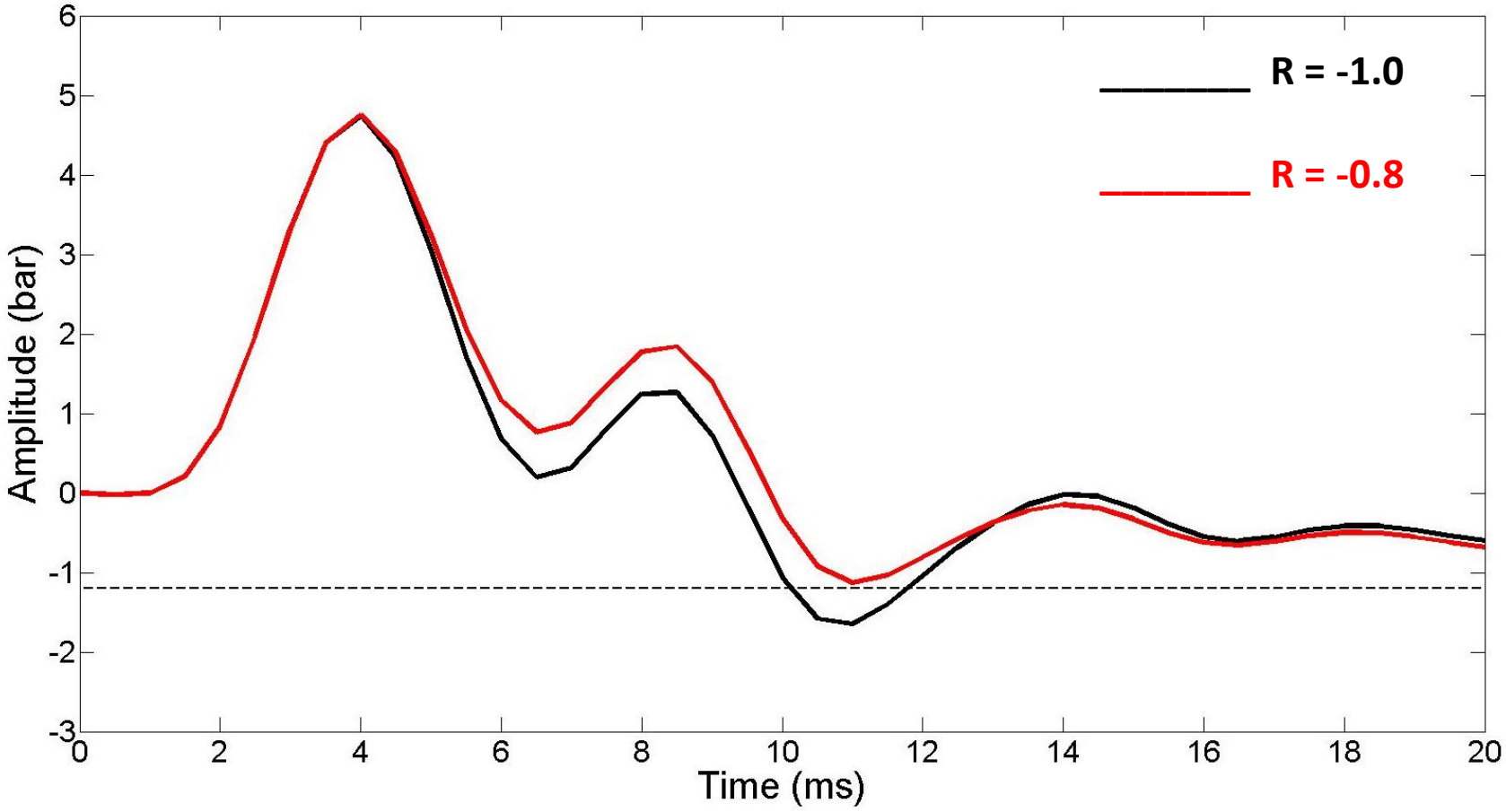

Less cavitation for increased distance between the subarrays

Searching the ghost of the high frequency signal

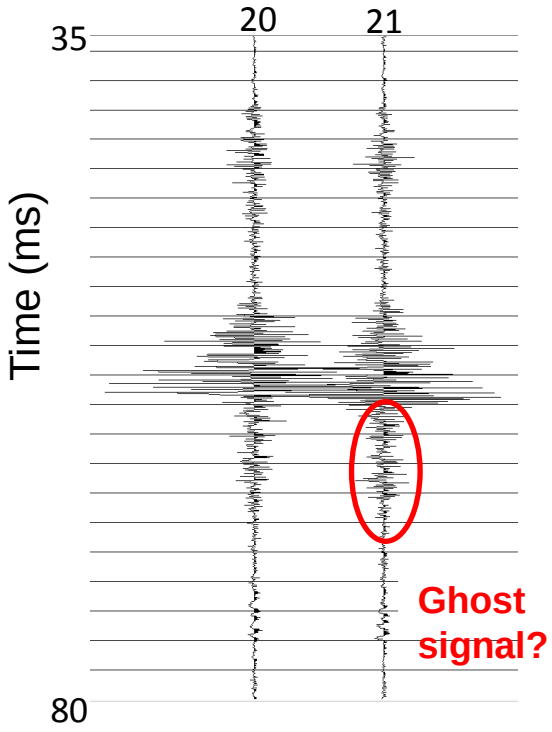

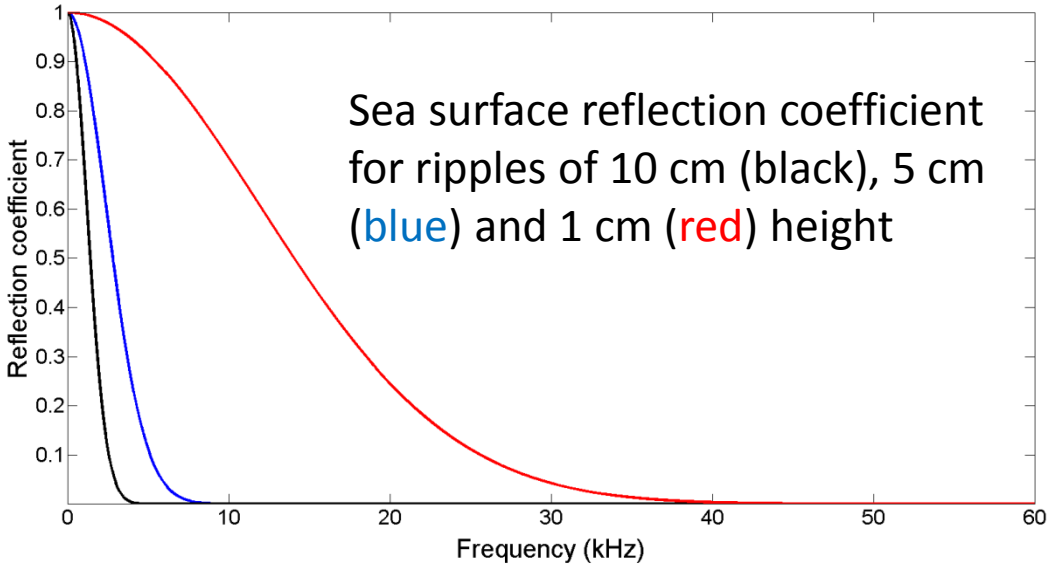

Sea surface reflection coefficient for ripples of 10 cm (black), 5 cm (blue) and 1 cm (red) height

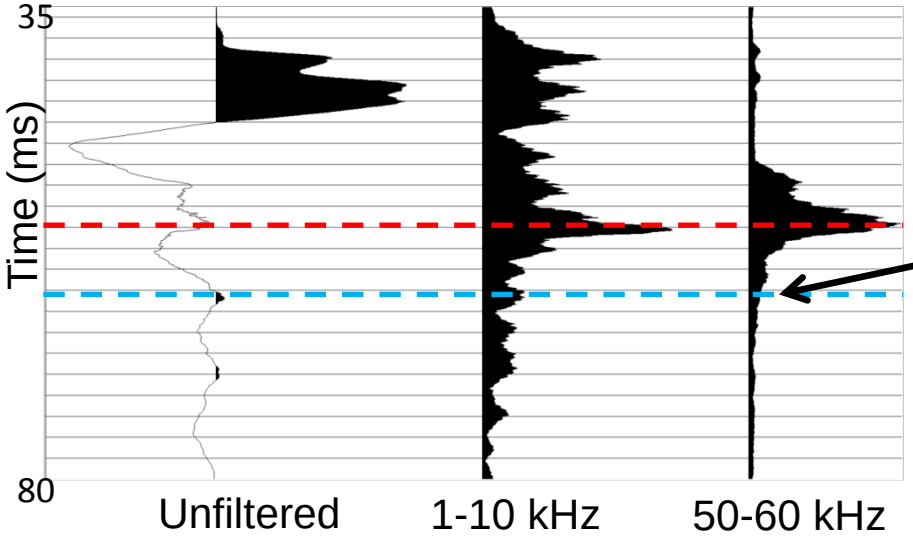

Less high frequency ghost signal may be caused by weaker reflection coefficient

Mammal detection

Detecting whales

Grønaas, Frivik, Melboe and Svendsen, EAGE, 2011

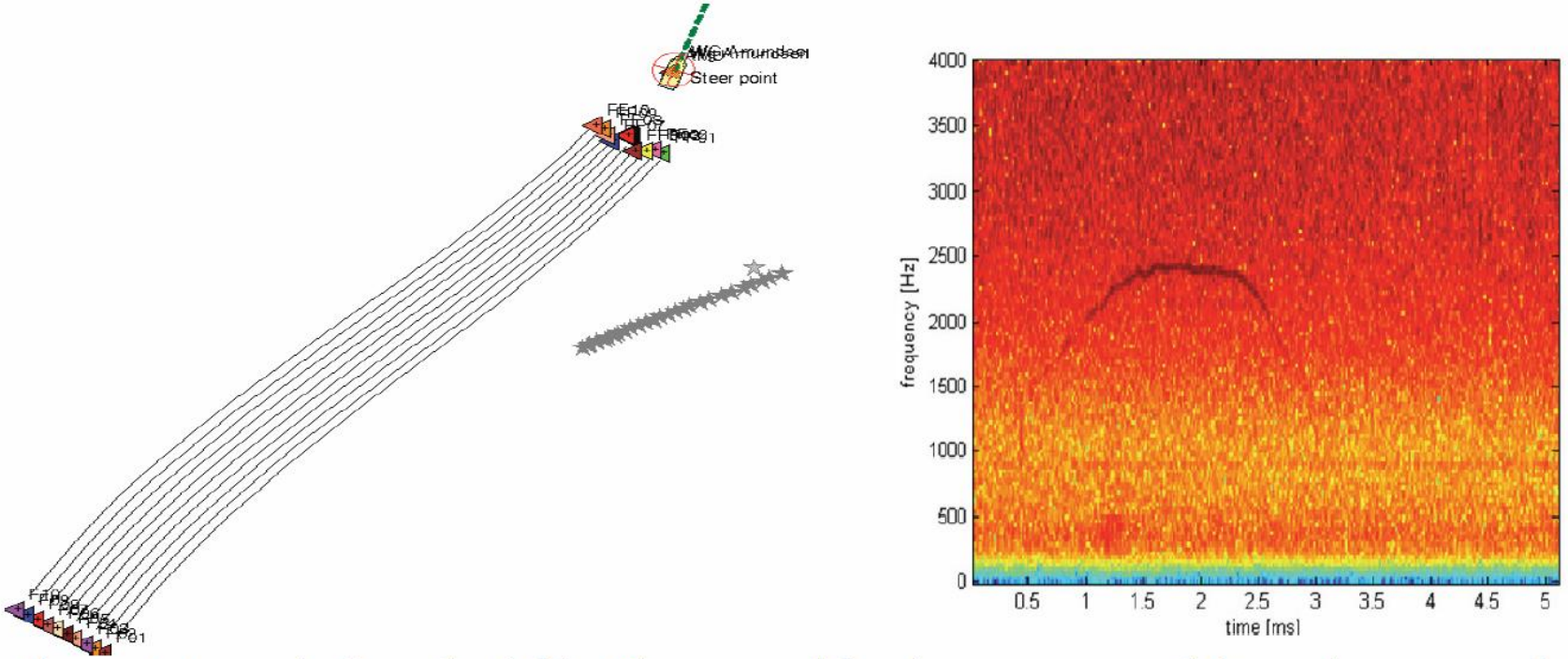

Figure 1. *Example from the field: The mammal localization system (left) tracking a sound source. The grey colour indicates detections. The plot on the right shows the spectrogram of a whistle sound recorded by the system in the Indian Ocean using seismic streamer positioning hydrophones. The signal-to-noise ratio is adequate to get a proper detection.*

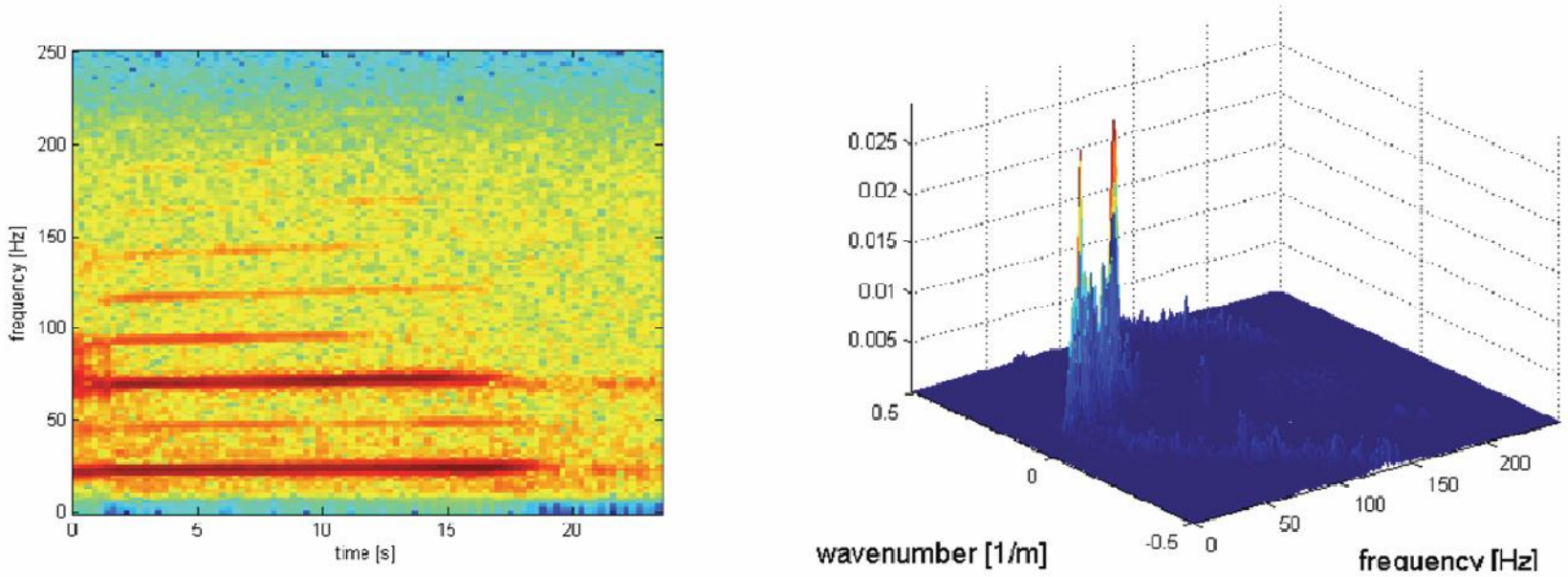

Figure 4 *Low frequency data processing. Left: Pygmy whale call with two main harmonics at 23 Hz and 70Hz. Right: f-k spectrum from simulation of a subsection receiving the call of a pygmy whale. The peaks in the f-k spectrum match the frequencies in the call.*

Grønaas et al., EAGE 2011

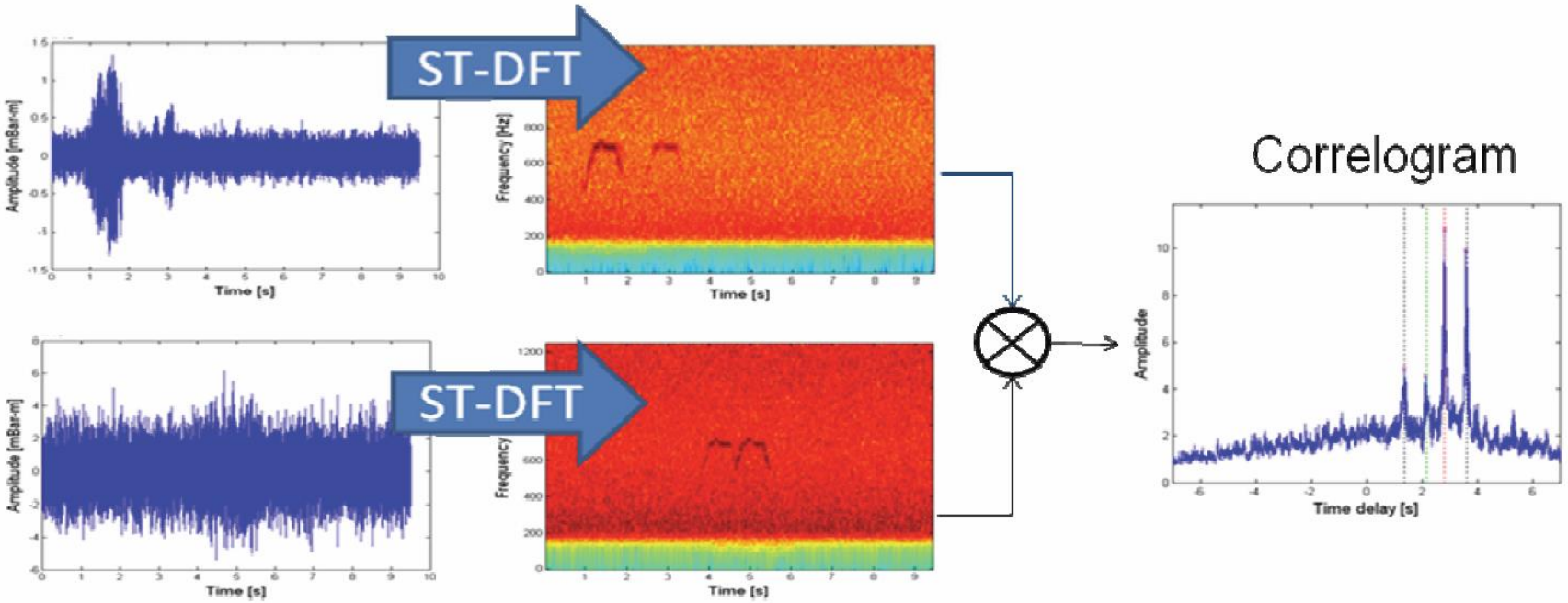

Figure 5 *High-frequency data processing. Two simulated traces with humpback whale calls (left) are transformed to spectrograms (middle) using short-term Fourier transforms. The spectrograms are correlated to produces a correlogram (right), from which time differences of arrivals can be estimated*

Grønaas et al., EAGE 2011

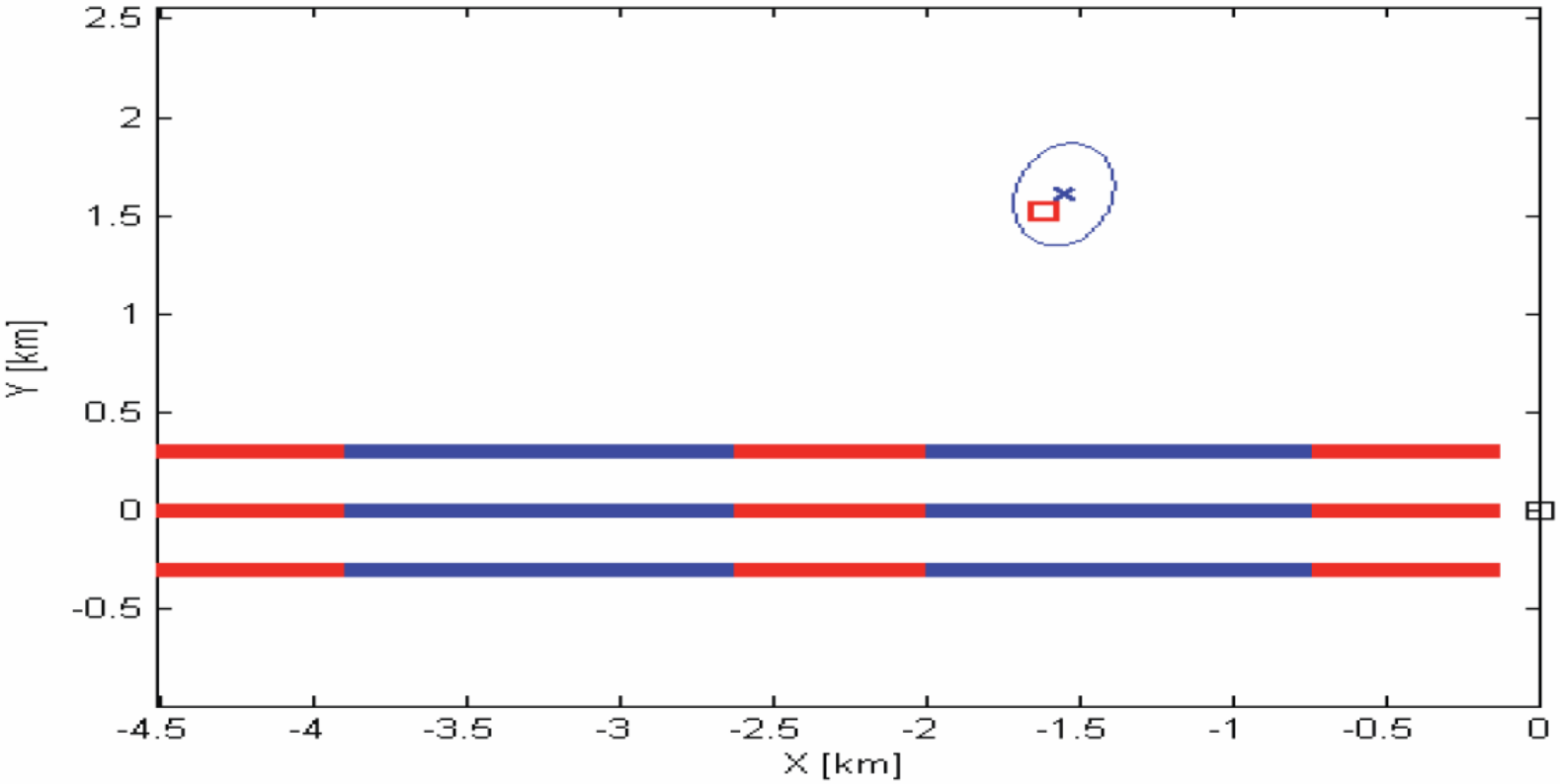

Figure 6 *Simulation of a whale location using the seismic hydrophones. The red square is the true location and the blue cross is the estimated location. The error ellipse is blue. The horizontal lines indicate the seismic streamers. The location and extension of the subsections used for beamforming are indicated by red lines. The detection array consists of subsections on the two outer streamers together with a single center streamer. The full seismic array consists of ten streamers, and is not shown here.*

Normal modes and the signal at large distances

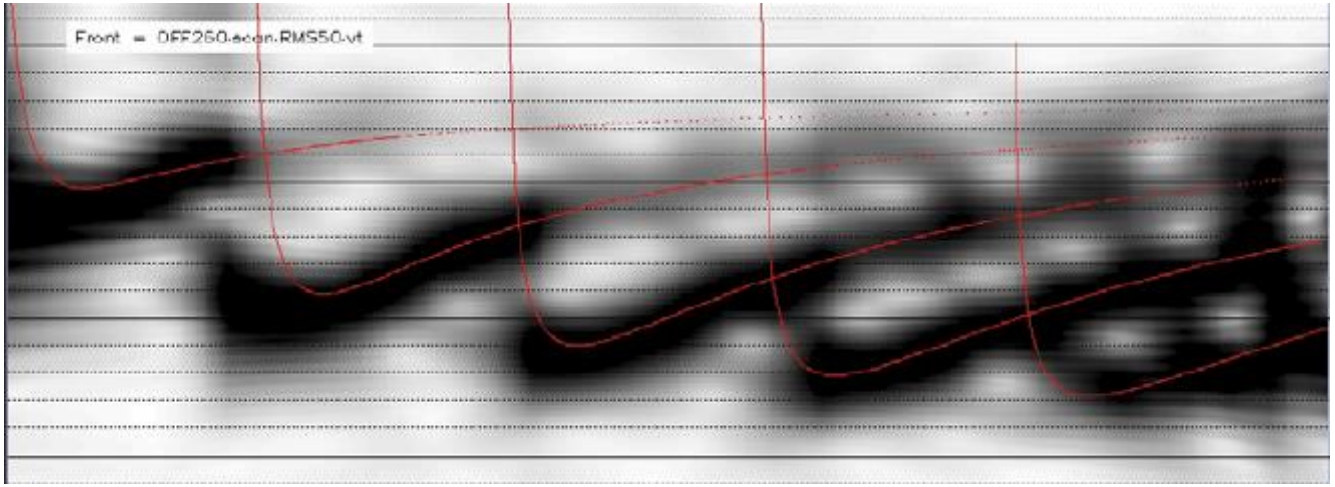

Definitions used by Pekeris

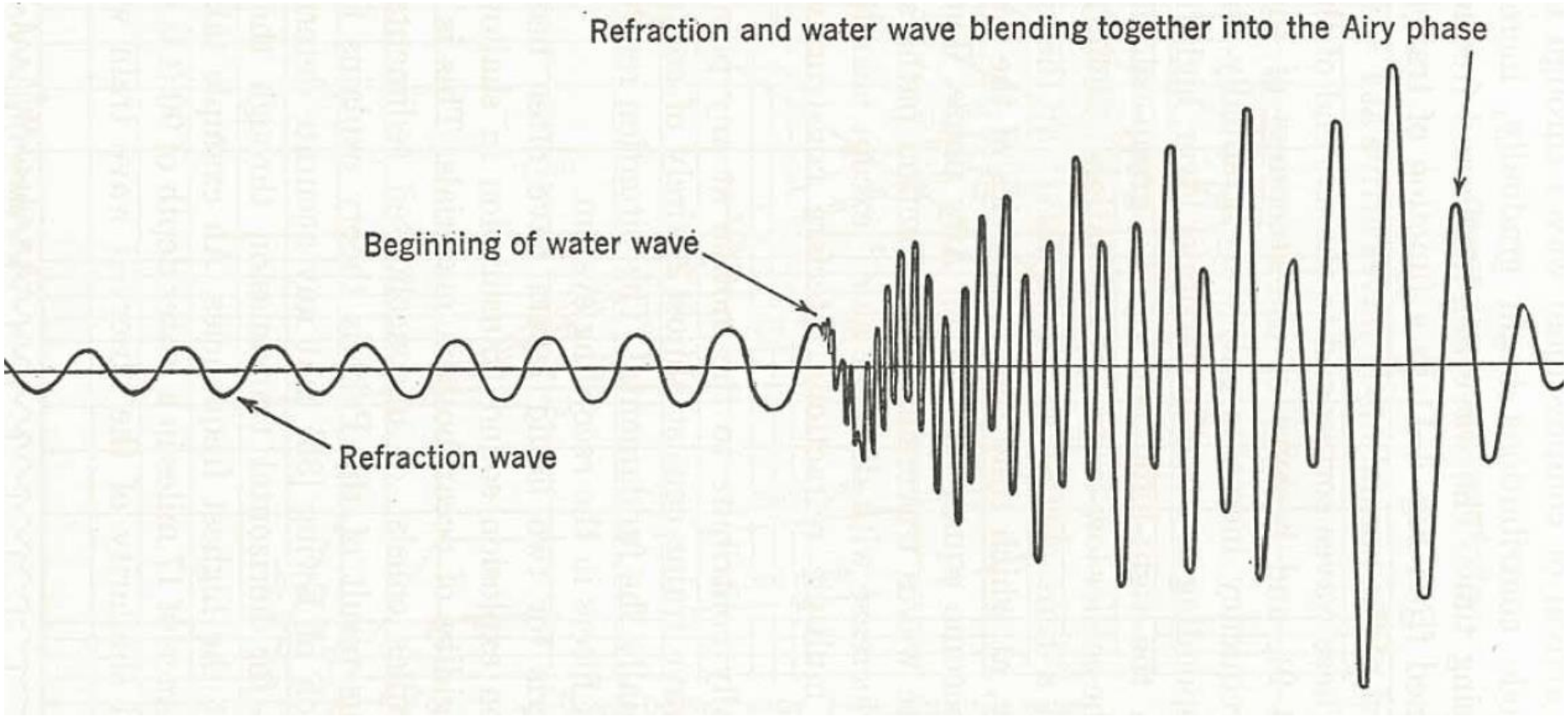

REFRACTION WAVE **WATER WAVE**

The refracted wave

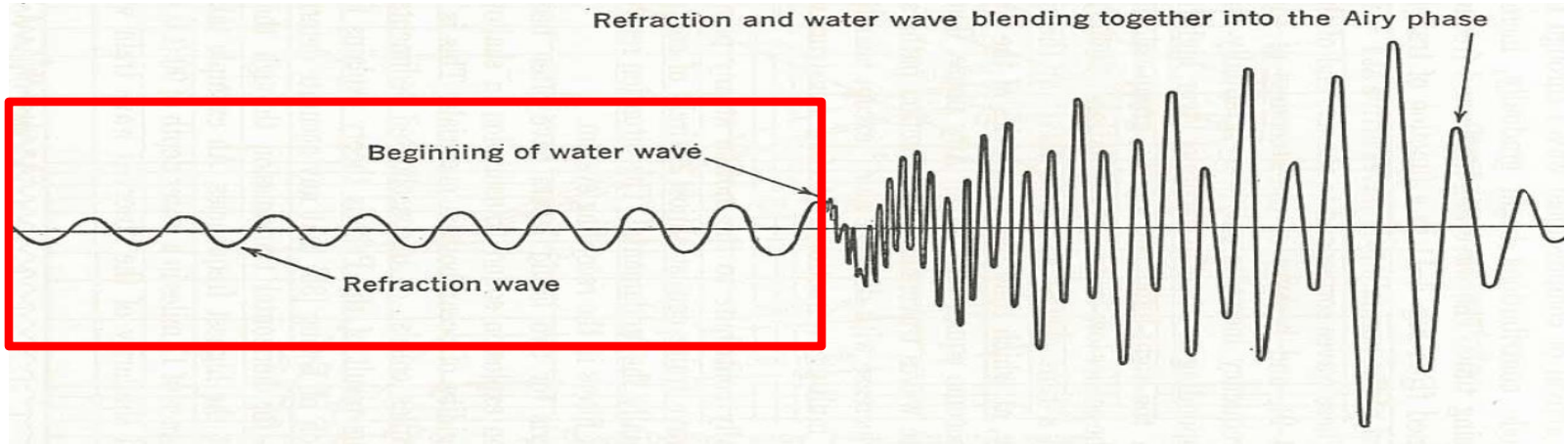

This wave is close to monochromatic – can we estimate the frequency?

Assuming a phase velocity close to that of the second layer, we find from the period equation:

$$k_n H \approx (2n-1)\frac{\pi}{2\sqrt{\frac{\alpha_2^2}{\alpha_1^2}-1}}$$

=>

$$f_n = \frac{(2n-1)\alpha_1\alpha_2}{4H\sqrt{\alpha_2^2-\alpha_1^2}}$$

THEORY

(Ewing et al, 1957)

Acoustic case: Water layer over an infinite half-space:

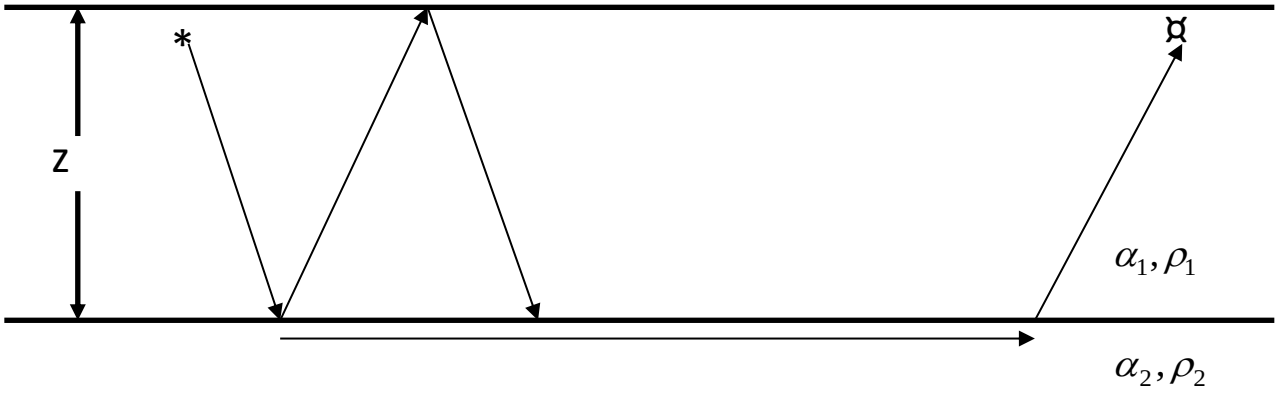

The periodic equation:

$$\tan kH\sqrt{\frac{c^2}{\alpha_1^2}-1}=-\frac{\rho_2}{\rho_1}\frac{\sqrt{\frac{c^2}{\alpha_1^2}-1}}{\sqrt{1-\frac{c^2}{\alpha_2^2}}}$$

=>

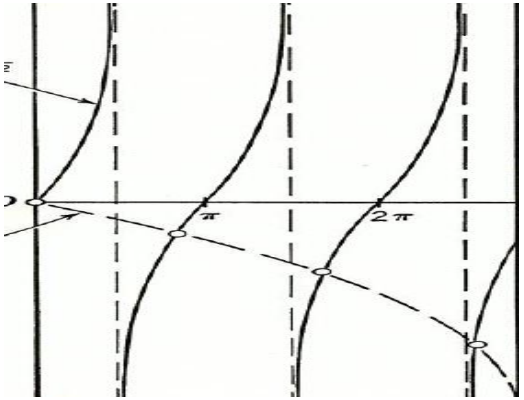

C = phase velocity of normal mode

Solutions corresponding to different modes of propagation

Estimating subtle changes in water layer velocities

Analysis of Guided Waves Recorded on Permanent Ocean Bottom Cables

P.J. Hatchell* (Shell International Exploration & Production BV), P.B. Wills (Shell International Exploration & Production BV) & M. Landro (NTNU)

EAGE, London, 2007

Variation of NMO velocity between various surveys at Valhall is used to estimate subtle changes in water velocity: ~ 1.3 %! Such changes are important for accurate 4D time shift analysis.

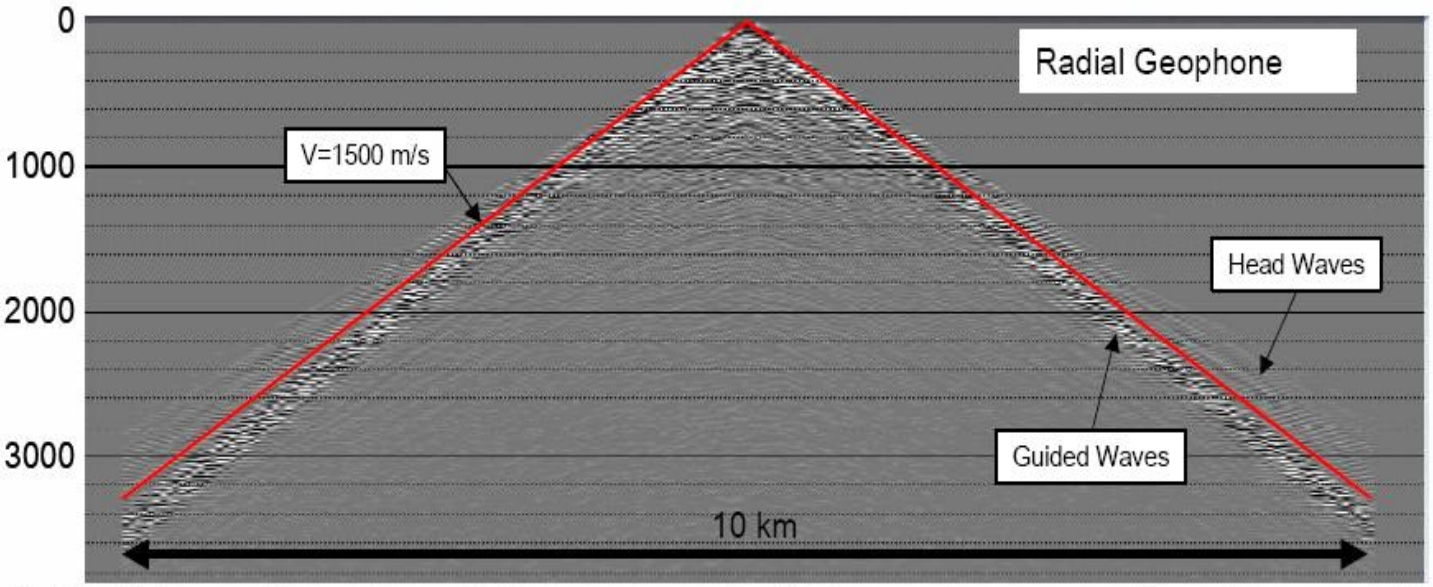

Figure 1: Radial geophone records from an array of airgun shots extending 5 km on either side of the geophone location. The shot spacing is 50m.

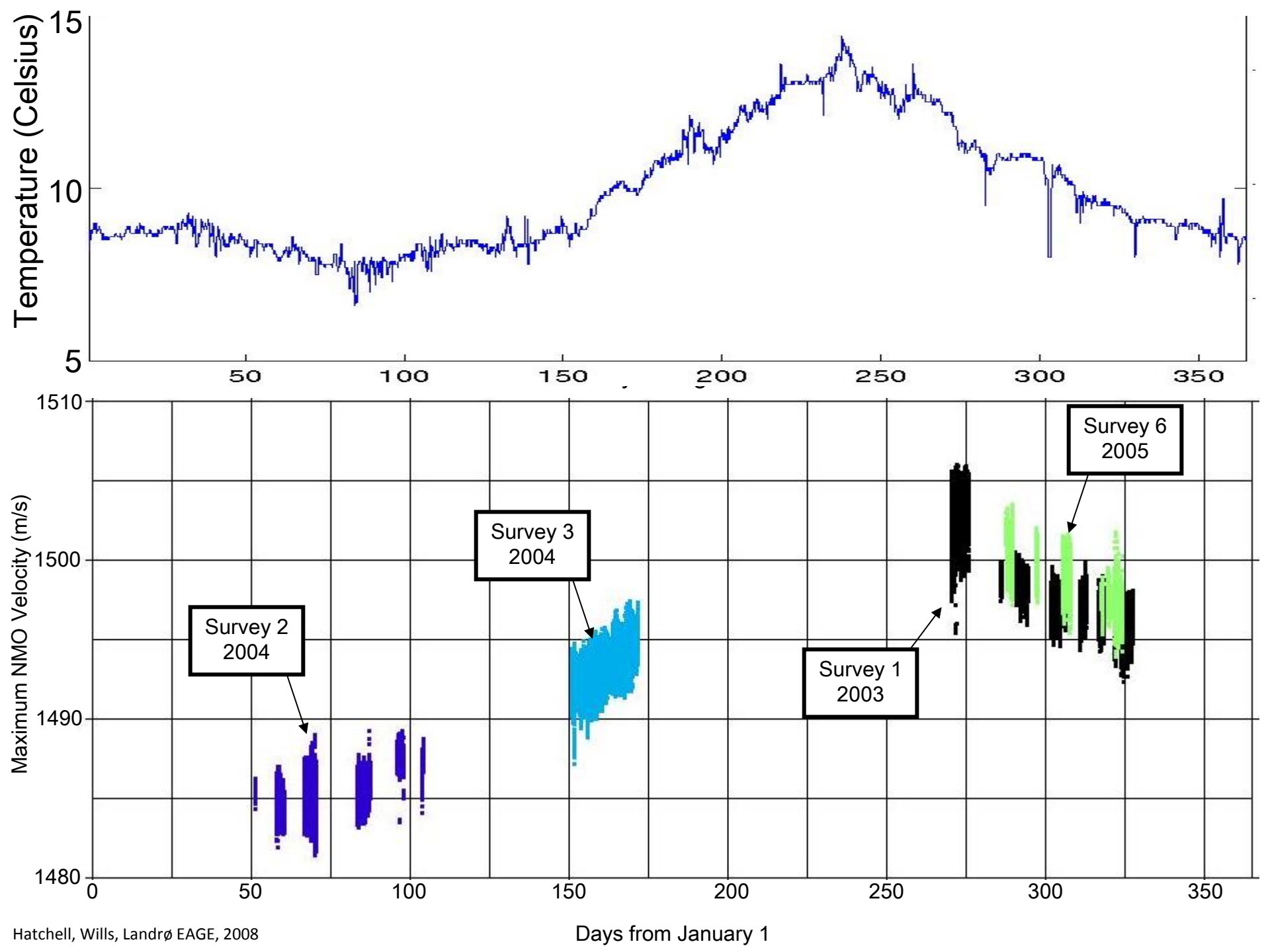

Hatchell, Wills, Landrø EAGE, 2008

Impact of water velocities/multiples on time-lapse time-shifts

Top reservoir timeshifts

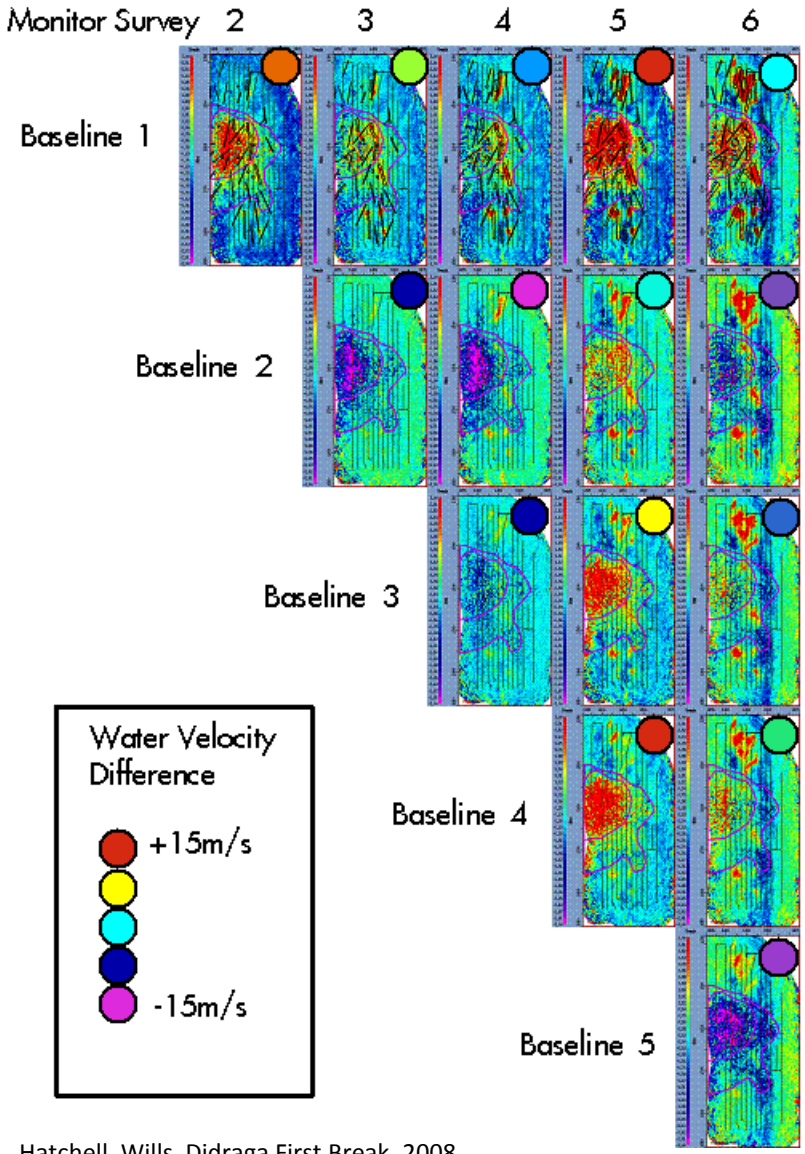

After data adaptive removal

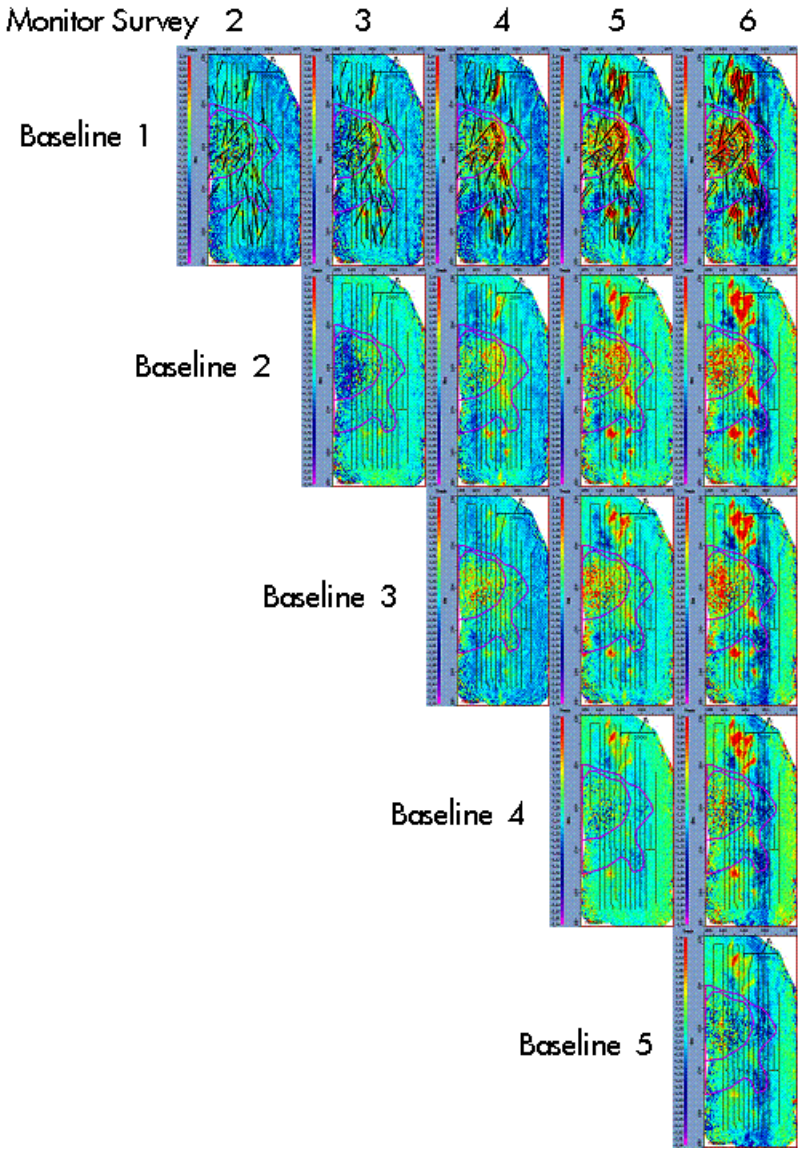

Hatchell, Wills, Didraga First Break, 2008

Modeled normal modes (4 modes)

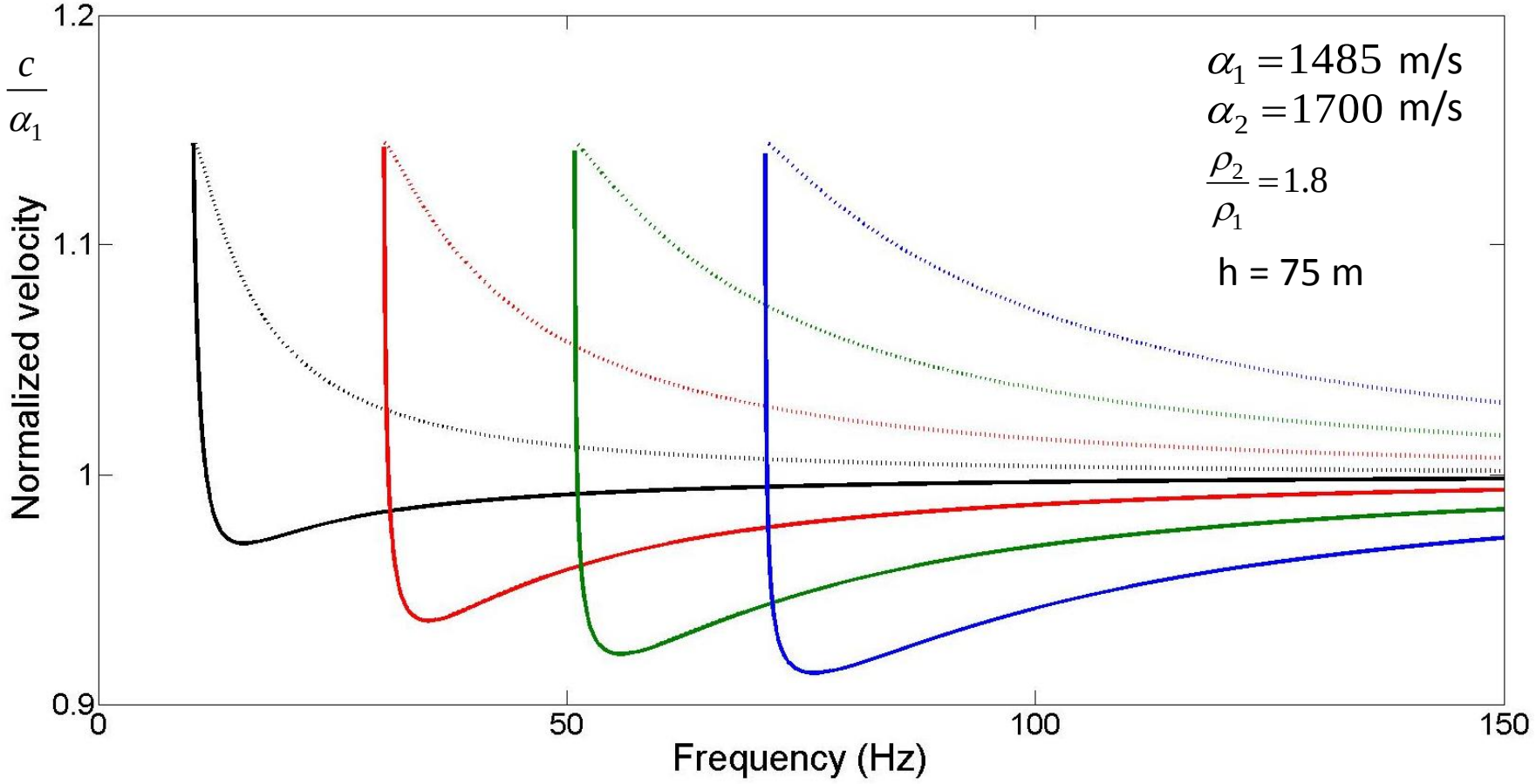

-Maximum phase and group velocity equal to velocity of second layer
-Minimum phase velocity equal to water velocity
-Minimum group velocity decreases with increasing mode number

Fluid-solid interface (Press and Ewing, 1950)

$$\tan kH\sqrt{\frac{c^2}{\alpha_1^2}-1}=\frac{\rho_2\beta_2^4}{\rho_1 c^4}\frac{\sqrt{\frac{c^2}{\alpha_1^2}-1}}{\sqrt{1-\frac{c^2}{\alpha_2^2}}}\left[4\sqrt{1-\frac{c^2}{\alpha_2^2}}\sqrt{1-\frac{c^2}{\beta_2^2}}-(2-\frac{c^2}{\beta_2^2})^2\right]$$

$\beta_2 / c << 1$

$$\tan kH\sqrt{\frac{c^2}{\alpha_1^2}-1}\approx-\frac{\rho_2}{\rho_1}\frac{\sqrt{\frac{c^2}{\alpha_1^2}-1}}{\sqrt{1-\frac{c^2}{\alpha_2^2}}}\left[1-i4\sqrt{1-\frac{c^2}{\alpha_2^2}}\frac{\beta_2^3}{c^3}\right]$$

Data acquisition

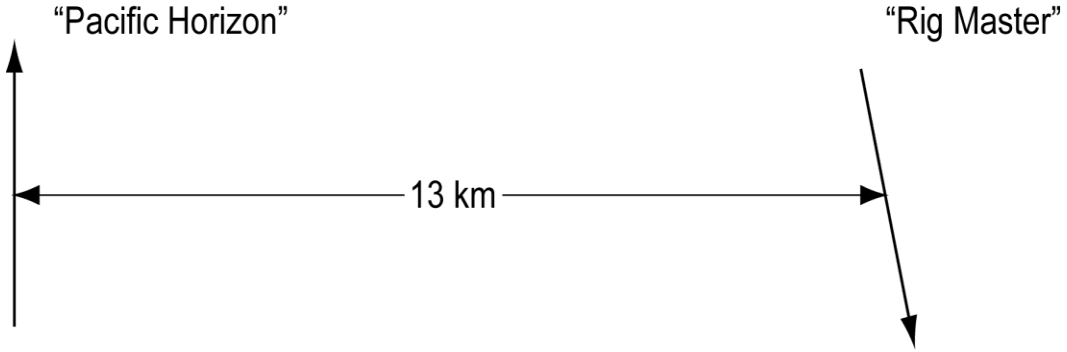

Data acquired by M/V Rig Master February 1989 in the Ekofisk area, North Sea. Part of the "Marine Seismic Noise" project performed by Seres in 1989.

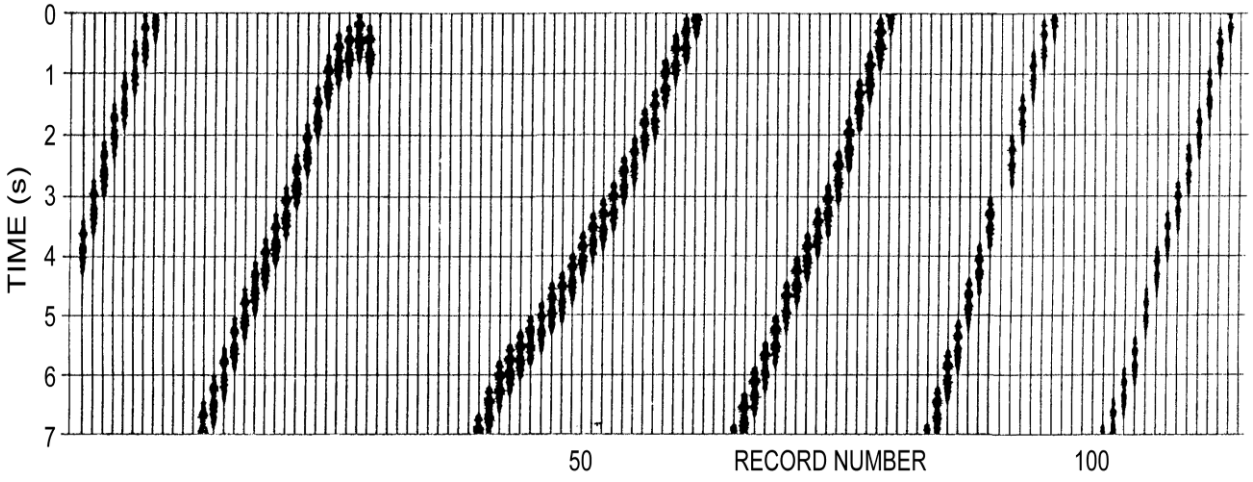

113 records of the mid-streamer trace

Ref.: Seismic interference noise recorded by M/V Rig Master, by M. Landrø and S. Vaage, 1989

Refraction wave => estimates of α_2

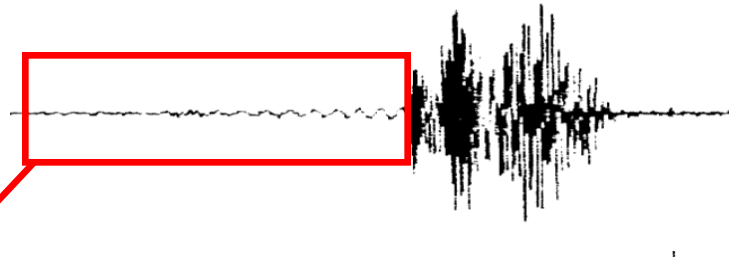

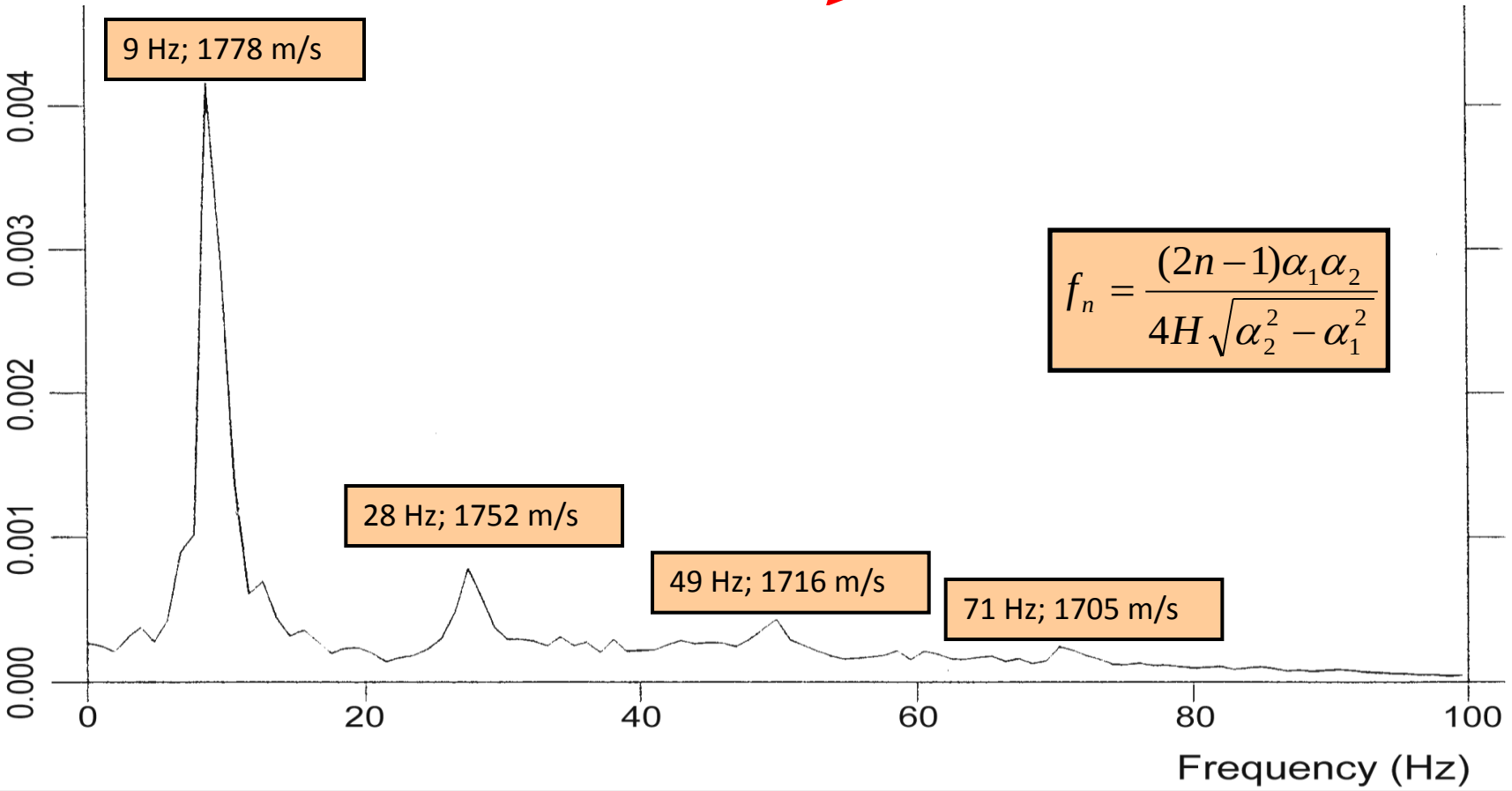

Low frequencies see ”deeper” into earth => velocity decrease with frequency

Comparing traveltimes

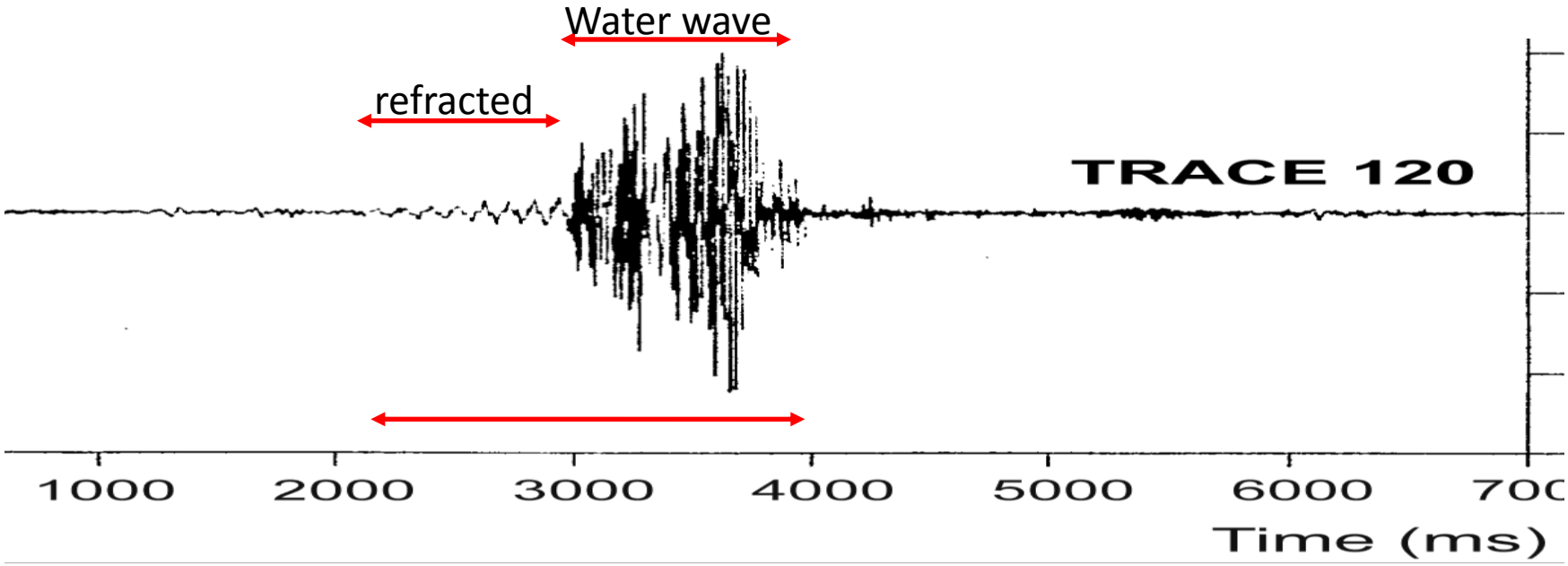

Direct wave thorugh water: $t_D = \frac{s}{\alpha_1}$

Arrival of critical reflections: $t_C = \frac{s\alpha_2}{\alpha_1^2}$

Duration of water wave: $\Delta t_W = \frac{s\alpha_2}{\alpha_1^2} - \frac{s}{\alpha_1} \approx 1.41s$

Refracted wave: $t_R = \frac{s}{\alpha_2} + \frac{2H\sqrt{\alpha_2^2 - \alpha_1^2}}{\alpha_1\alpha_2}$

Duration of interference noise: $\Delta t_{IN} = t_C - t_R = 2.6s$

Frequency spectrum of the signal 13 km away
~ 316 microbar – 70 m water depth

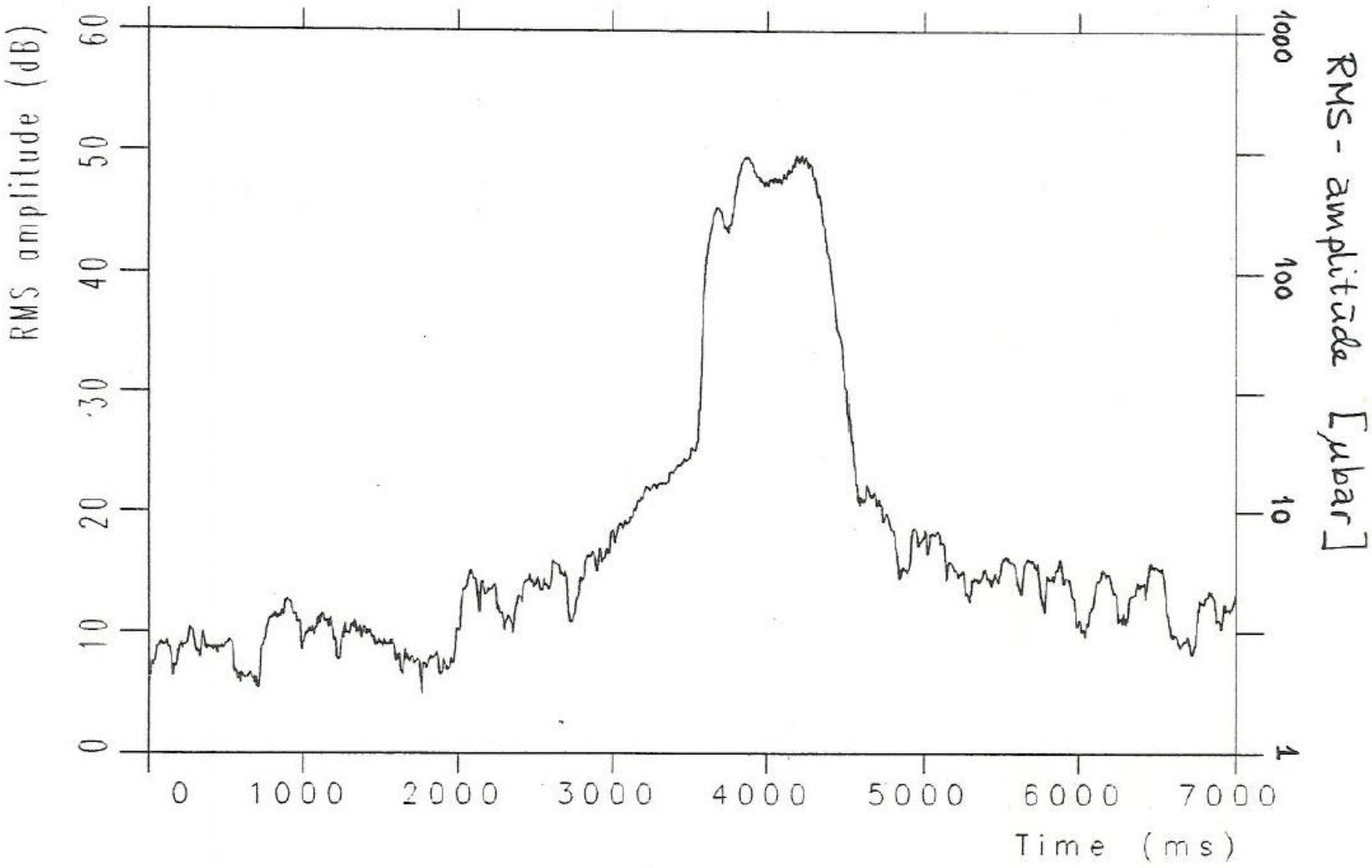

Simple raytracing considerations – water wave

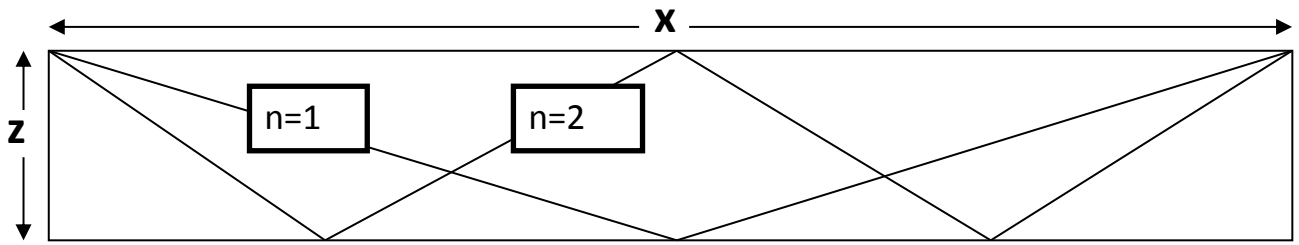

$$R_n = \sqrt{x^2 + 4n^2 z^2}$$

Characteristic frequency between two bounces:

$$f_n = \frac{1}{T_{n+2} - T_n} = \frac{\alpha_1}{R_{n+2} - R_n}$$

Assuming that x >> z:

$$f_n \approx \frac{\alpha_1 x}{8(n+1)z^2} \quad \text{and} \quad T_n = \frac{R_n}{\alpha_1}$$

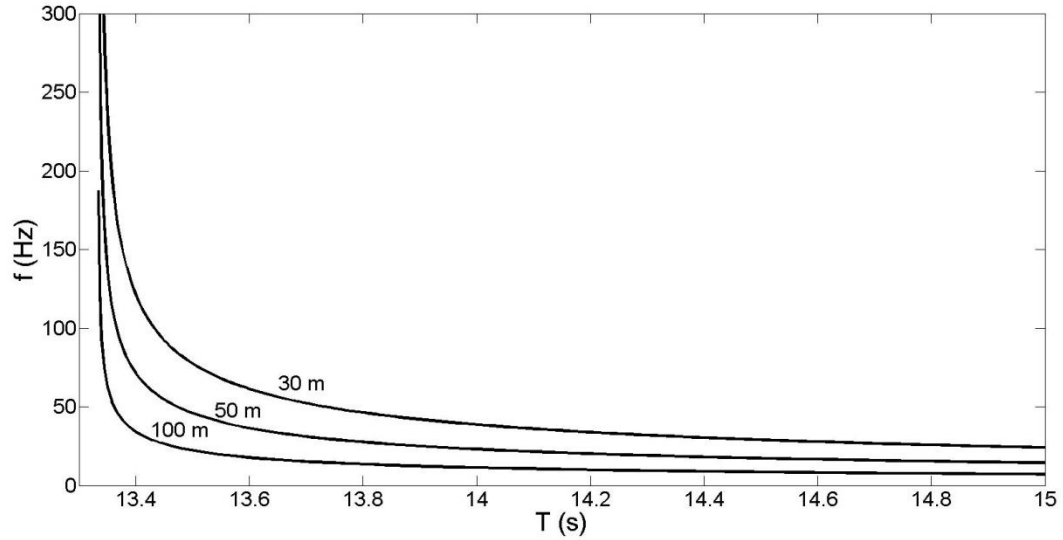

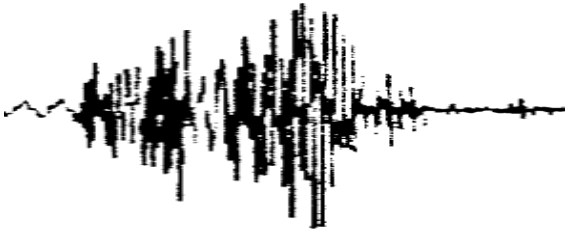

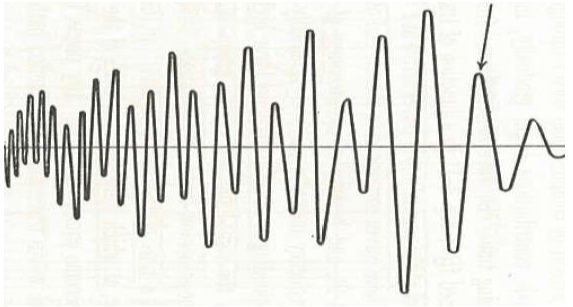

Frequency content of water wave decreases with increasing recording time

Observation of normal modes

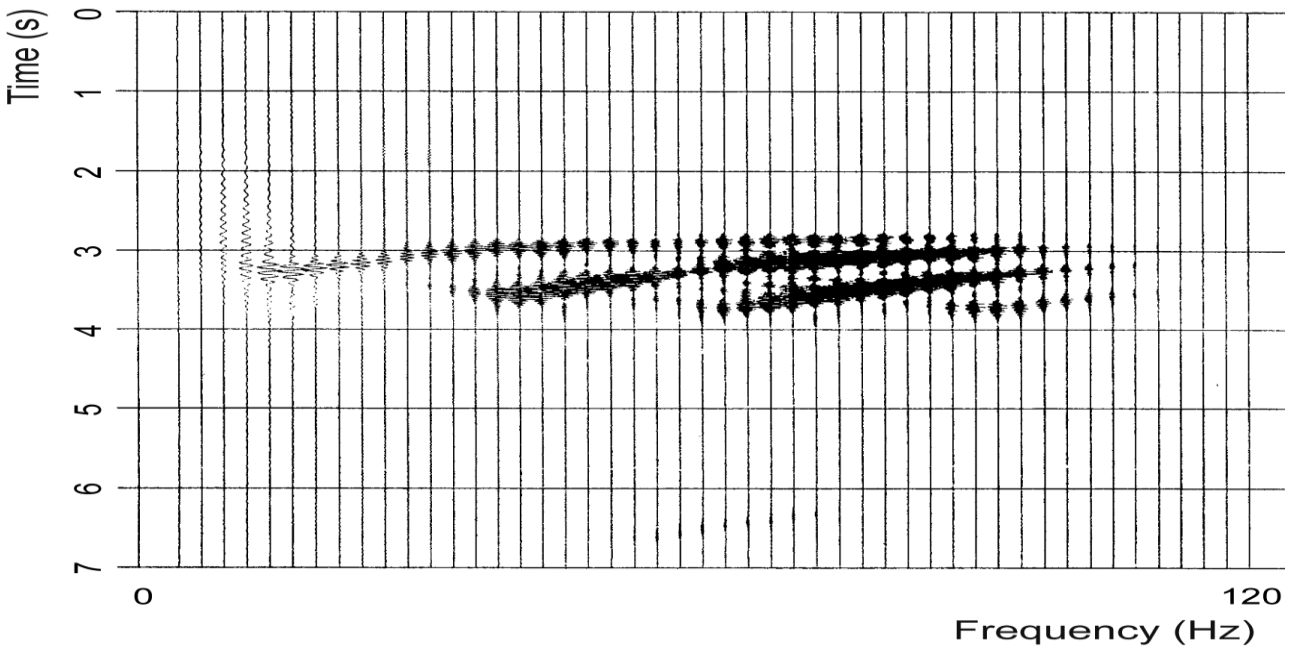

4 modes interpreted – assumping that the trends represent group velocity – hard to see phase velocity on this plot

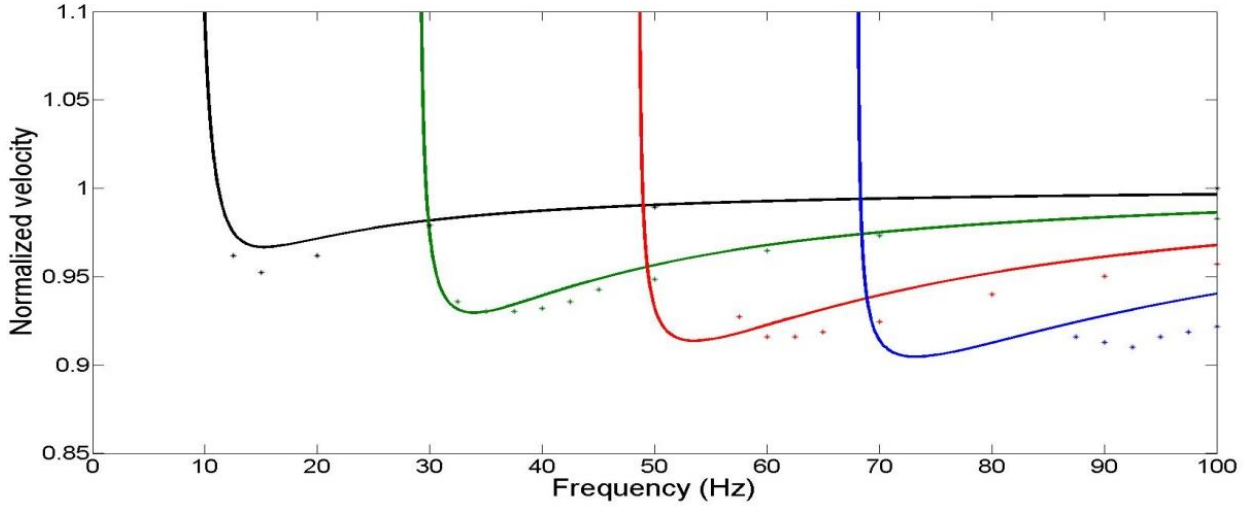

Modeling of 4 first modes assuming v2=1725 m/s and a density ratio of 1.8. Dots represent **group** velocity estimates from top figure

Effect of velocity change in layer 2 from 1700 m/s (solid) to 1800 m/s (dashed)

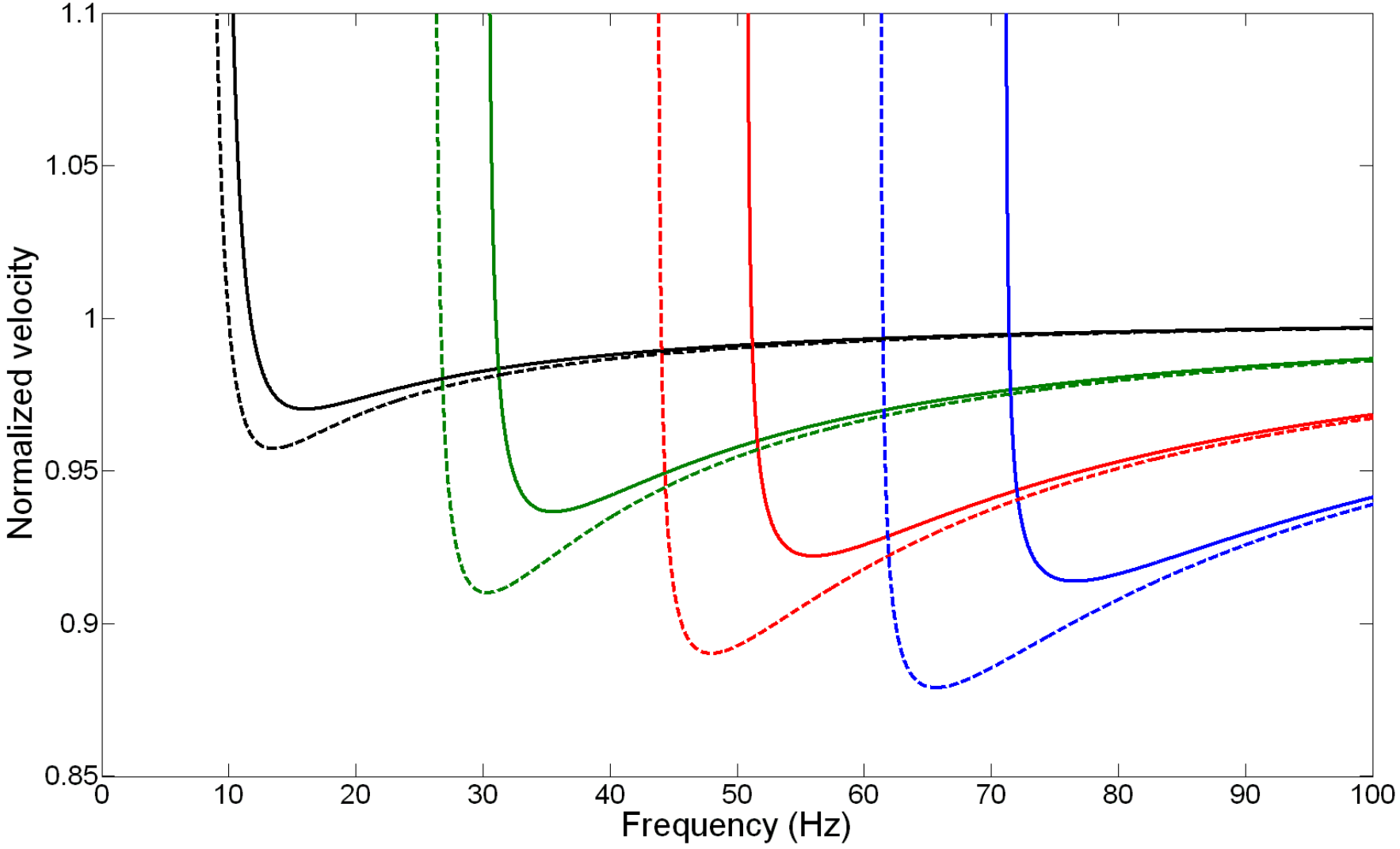

Effect of density change in layer 2 from 1.8 (solid) to 2.2 (dashed)

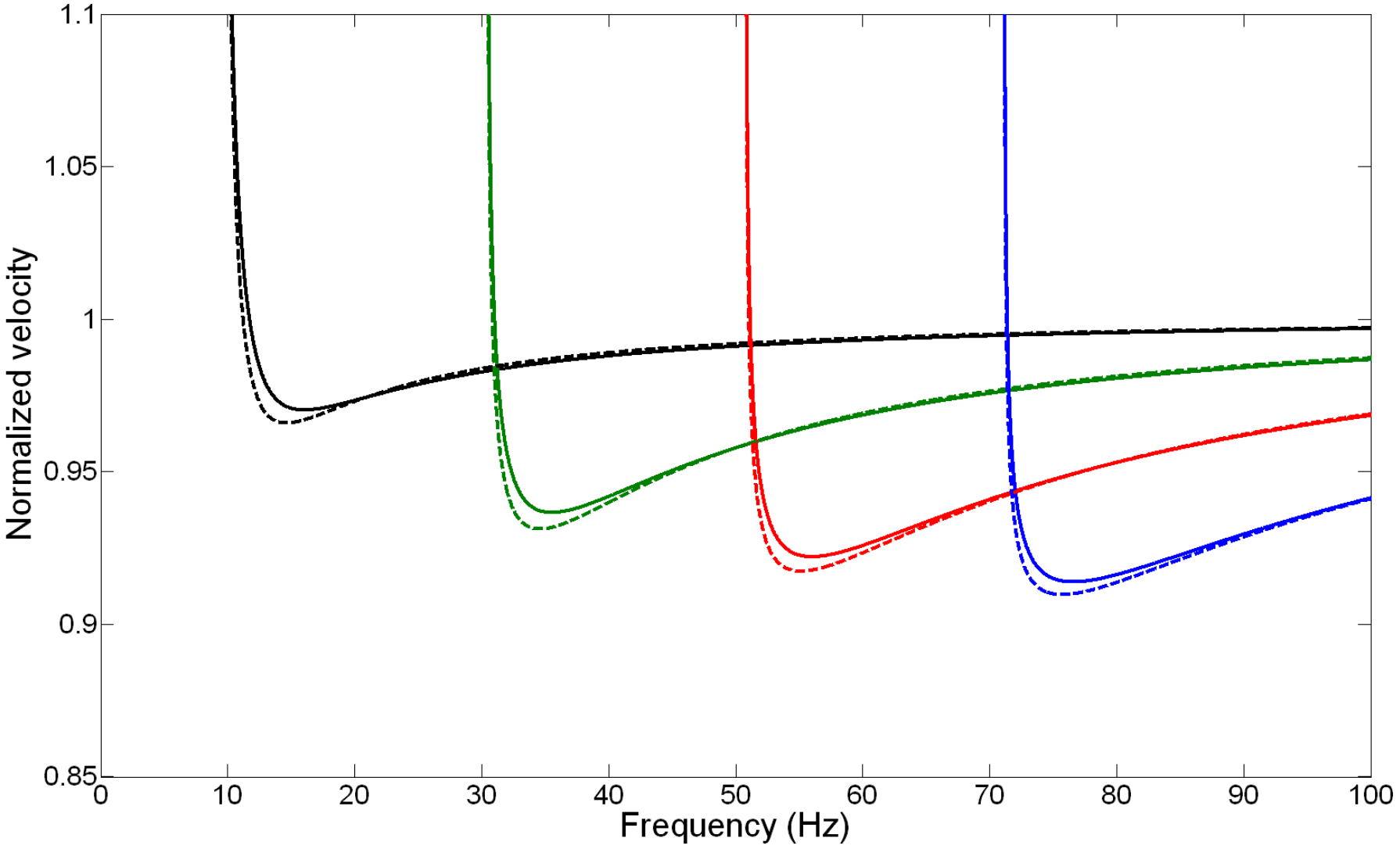

Effect of changing the water depth from 75 (solid) to 300 m (dashed)

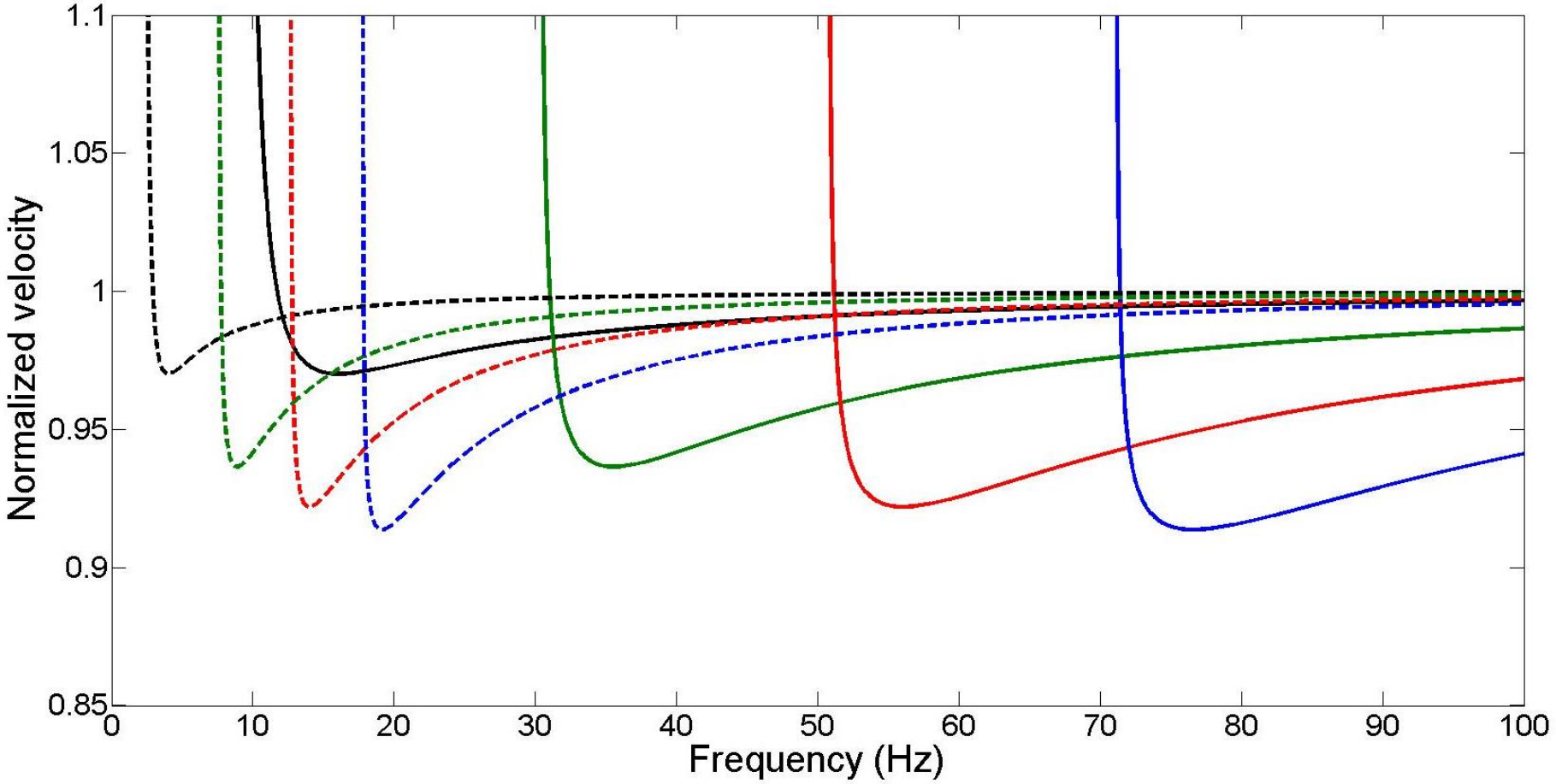

Valhall LoFS-data – Time-frequency plots of normal modes

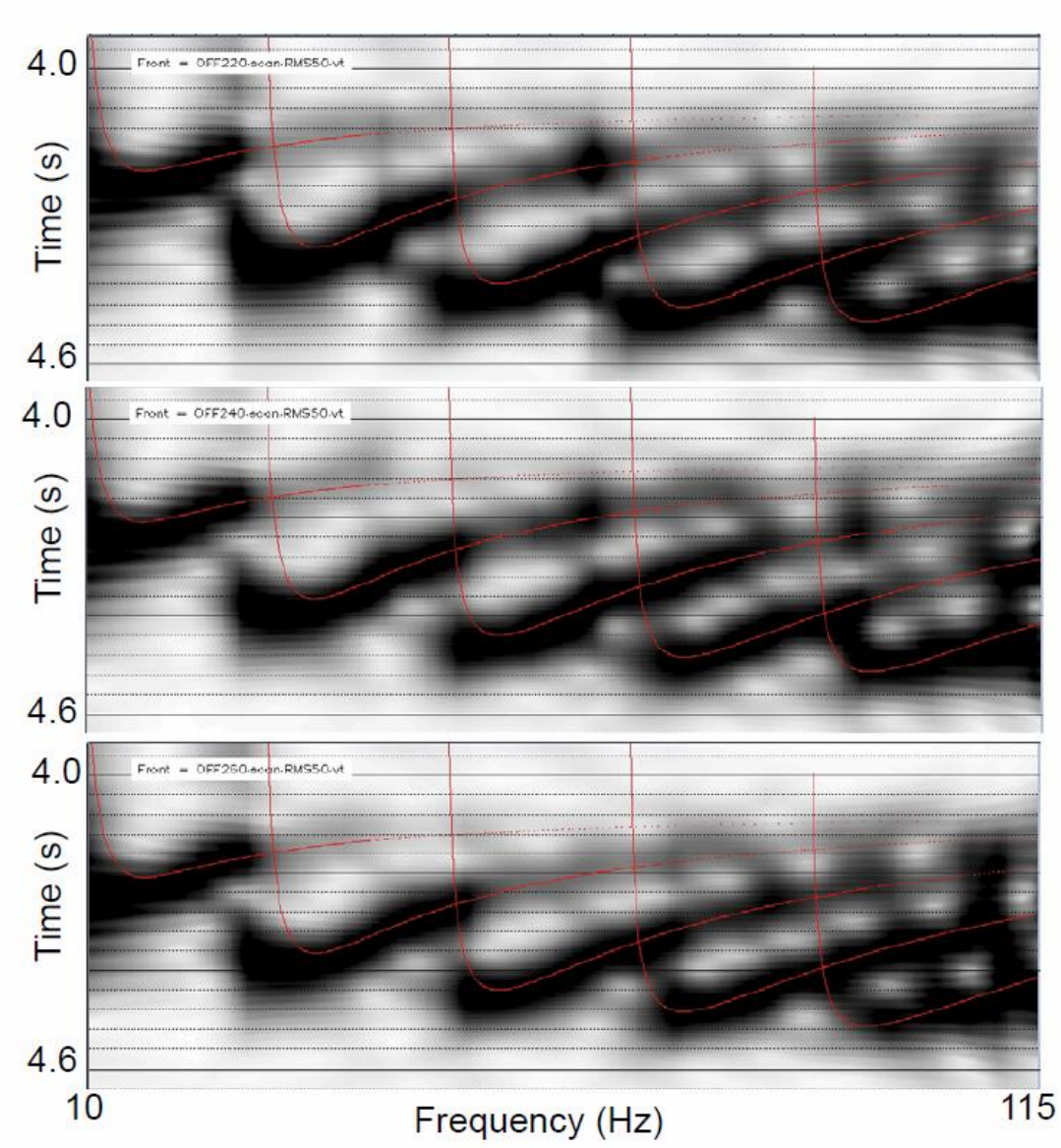

3 traces for a constant offset of 6 km, displaced by 1 km – notice minor shifts in the minima for the group velocity, indicating lateral velocity changes.

Red curves: Theoretical group velocity versus frequency assuming 80 m water depth, 1470 m/s water velocity, a density ratio of 1.6 and a velocity of 1700 m/s for the first layer below seabed.

Long arrays and beamsteering

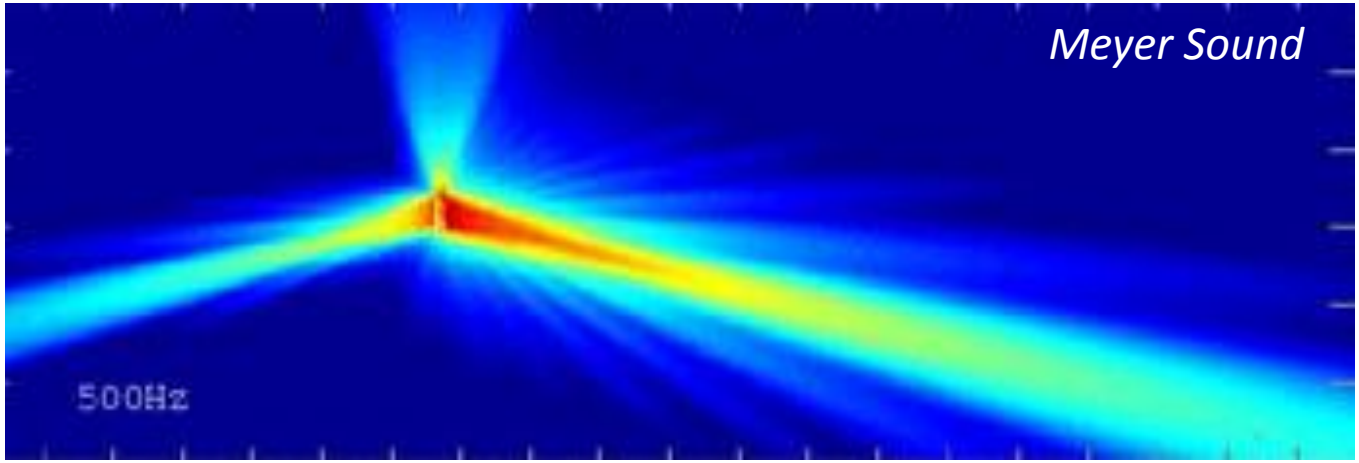

Acoustic measurements of amount of fish inside and outside the seismic area (from Løkkeborg's presentation)

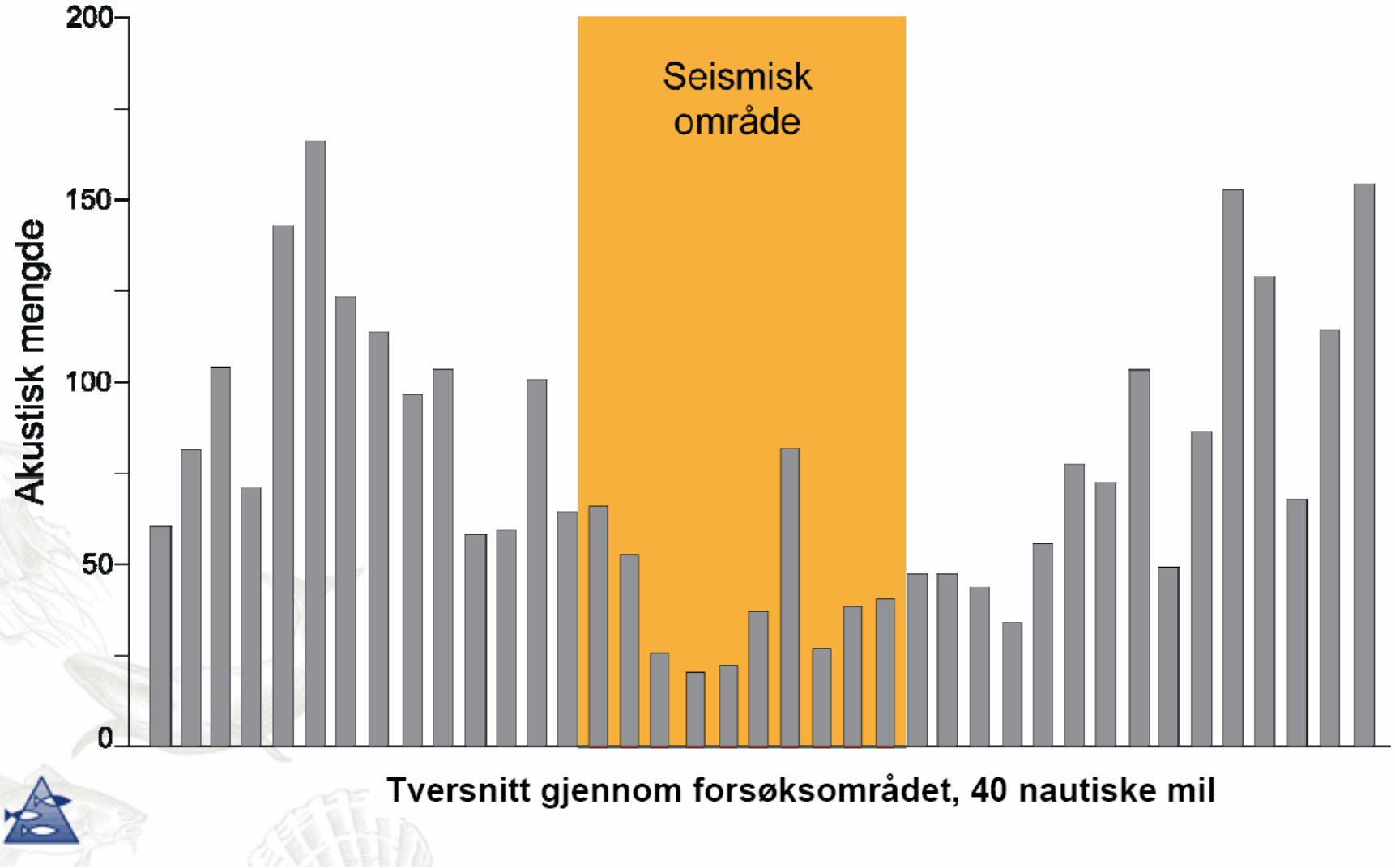

Source beamsteering – can it reduce this effect?

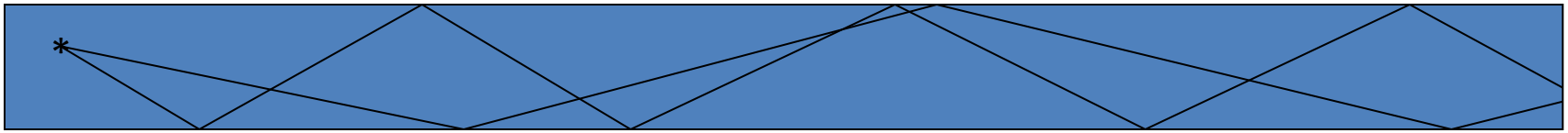

The seismic signal at long distances from the source is the harmonic modes being reflected within the water column layer (similar to the optic signal in a fiber optic cable). This means that the signal is emitted at high angles off the vertical.

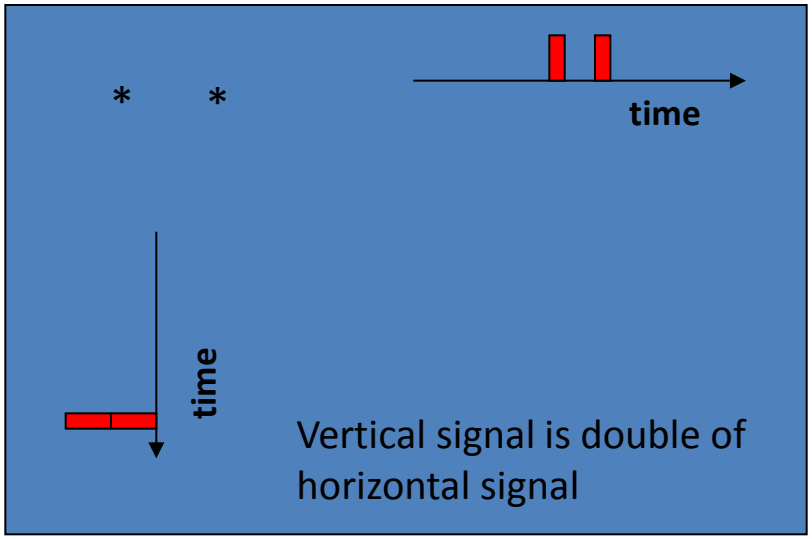

If we use two sources instead of one, the signal in the horizonal direction will consist of two peaks – however the vertical signal will add together constructively, corresponding to double amplitude in vertical direction compared to the horizontal direction – this is the basic idea behind source beamsteering.

For seismic purposes the main interest is the VERTICAL signal

A modeling example – 20 km away – with and without beamsteering

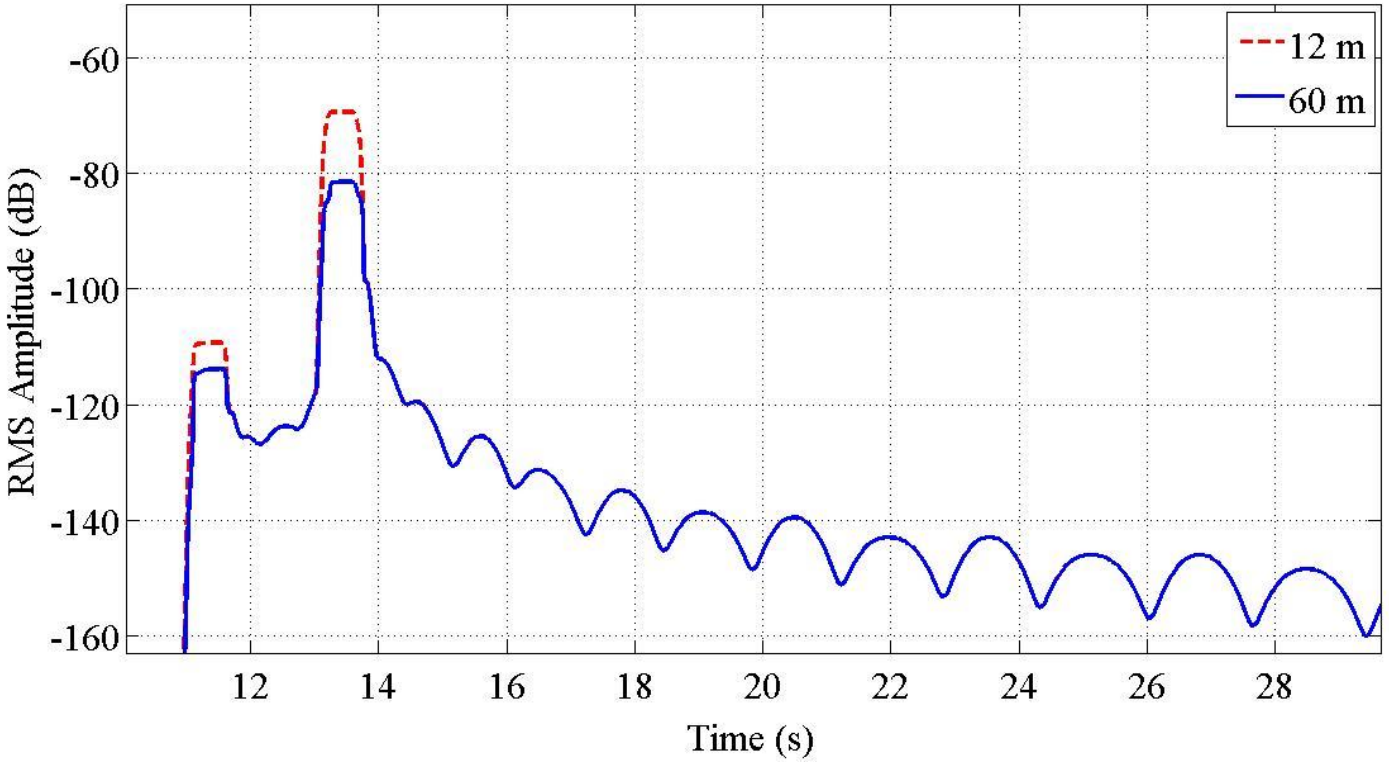

ref: H. Mehdi Zadeh and M. Landrø, 2009

The signal is reduced by a factor of 3 by beamsteering

Assuming a 1/r-decay curve:

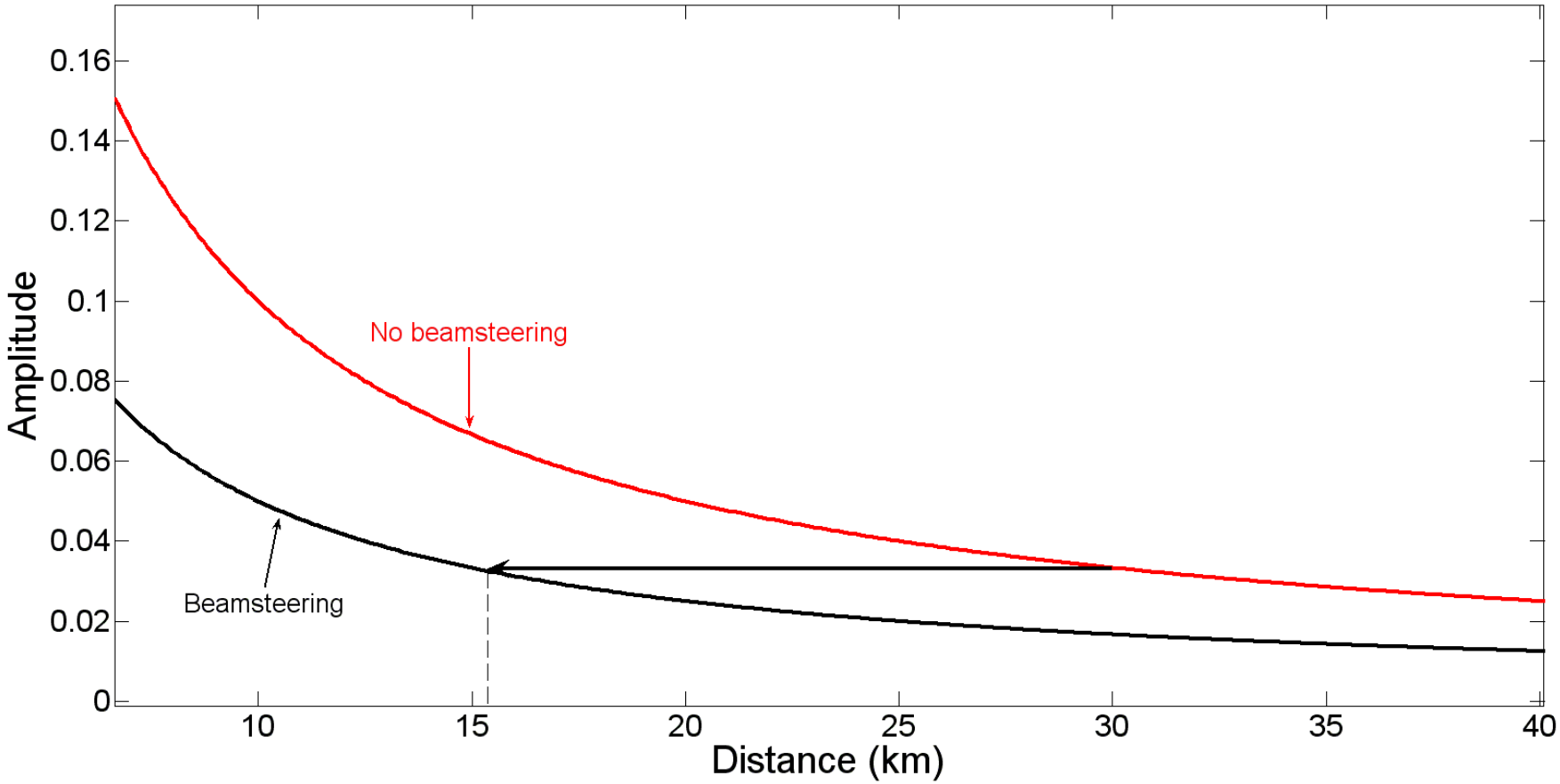

Critical radius reduced by a factor of 2

RMS amplitude versus offset – field data example

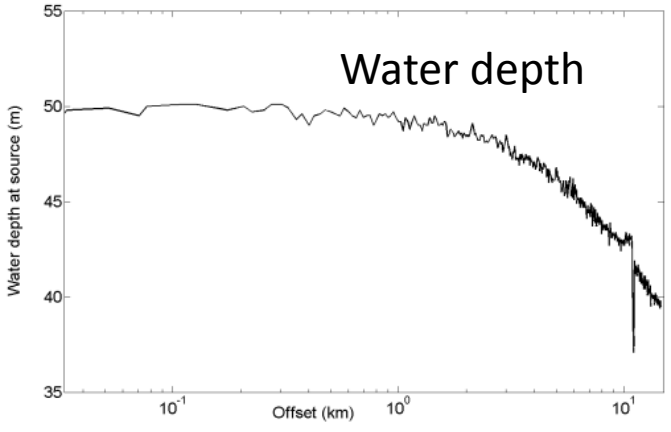

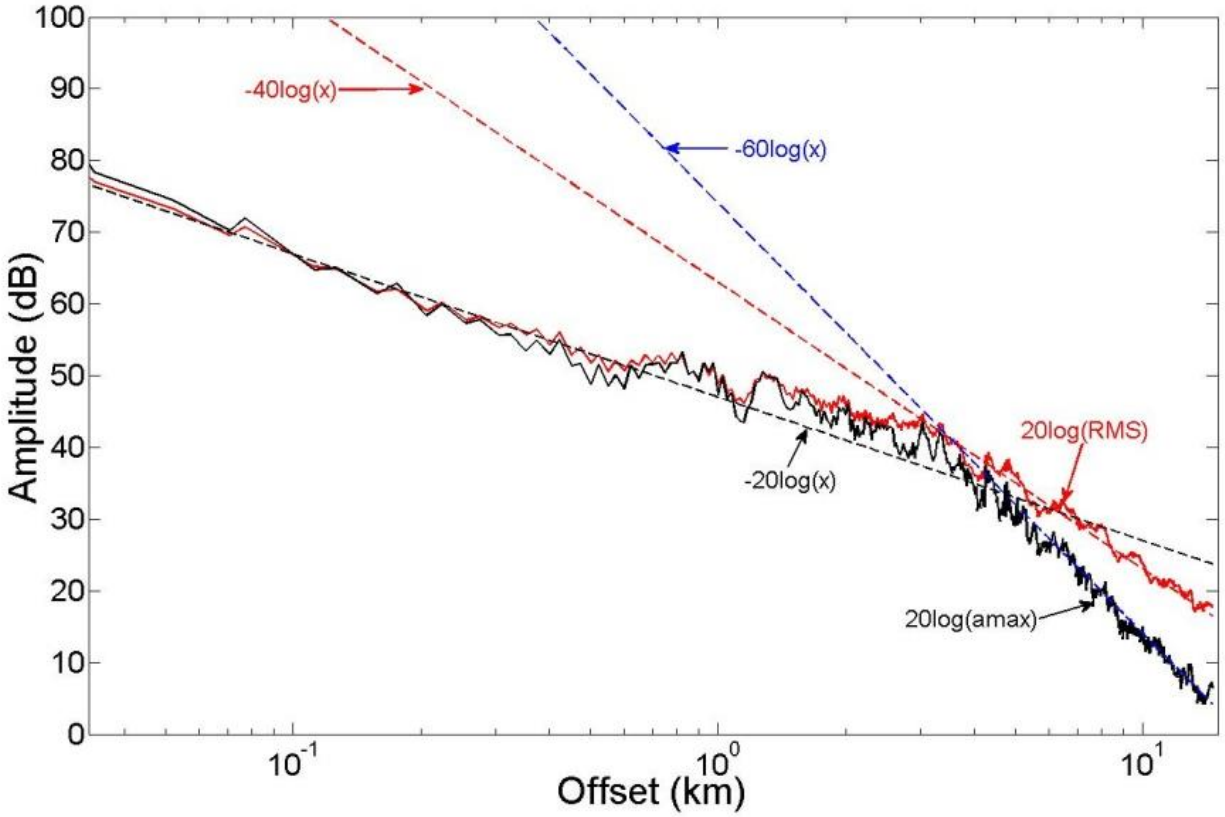

Strong attenuation for offsets larger than 4 km – 60 dB slope corresponds to $1/R^3$

$R < 4$ km : $1/R$

$R > 4$ km : $1/R^3$

Estimated reduction in the environmental disturbance zone area by 4 or more

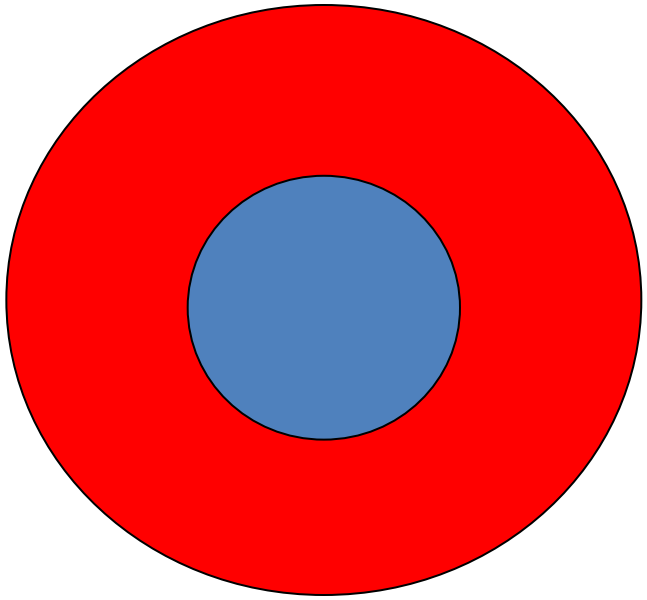

Challenges:

- **Needs experimental verification**
- **Need an areal source array configuration of 100 x 100 m**

Conclusions

- **Beamsteering is an old technique that is regurarly used**
- **Seismic applications were popular in the 1970-1980ies**
- **Present day source arrays are compact due to imaging purposes (want to have high angles to image steeply dipping subsruface interfaces**
- **Although we lack field measurements that demonstrate the efficiency of beamsteering it is very likely that it will reduce the ”environmental disturbance zone” significantly**